UNIVERSITY OF CALIFORNIA, MERCED

Sirtuin-1 Signaling Regulates Organismal Growth by Altering Feeding Behavior and Stem Cell Differentiation in Planarians.

A dissertation submitted in satisfaction of the requirements
for the degree Doctor of Philosophy

in

Quantitative and Systems Biology

By

Ben Ziman

Committee in Charge:

Professor Katrina Hoyer, Chair
Professor Fred Wolf, Member
Professor Aaron Hernday, Member
Professor Néstor J. Oviedo, Advisor

2019

The dissertation of Ben Ziman, titled, "*Sirtuin-1 Signaling Regulates Organismal Growth by Altering Feeding Behavior and Stem Cell Differentiation in Planarians*" is approved, and it is acceptable in quality and form for publication on microfilm and electronically:

_____

Aaron Hernday

_____

Fred Wolf

_____

Katrina Hoyer, Chair

_____

Nestor Oviedo, Advisor

University of California, Merced

2019

Table of contents

List of figures

List of Abbreviations

1. 4E-BP1- eIF-4E binding protein
2. ABL- Anterior branch length
3. AgRP- Agouti-related peptide
4. ALS- Acid labile subunit
5. A-MSH- alpha-melanocyte stimulating hormone
6. ANT2/3- ADP/ATP carrier proteins
7. AP- Anteroposterior
8. ARH- Arcuate nucleus of the hypothalamus
9. Atg- Autophagy related gene
10. Bcl2- B-cell lymphoma 2
11. BER- base excision repair
12. Brdu- Bromodeoxyuridine
13. CDK- Cyclin dependent kinases
14. CNS- Central nervous system
15. CSP1- Carbamoyl phosphate synthase 1
16. DAP1- Death associated protein 1
17. DIAP1- Drosophila inhibitor of apoptosis protein 1
18. Dj- Dugesia japonica
19. DMSO- Dimethyl sulfoxide
20. DSB- Double stand break
21. dsRNA- Double stranded RNA
22. EGFR1- Epidermal growth factor receptor 1
23. eIF2B- Eukaryotic initiation factor 2-B
24. FACS- Fluorescent activate cell sorting
25. FAO- Fatty acid oxidation
26. FGF- Fibroblast growth factor
27. FISH- Fluorescent in situ hybridization
28. FLI1- Friend leukemia integration 1 transcription factor
29. FoxO1- Forkhead transcription factor of class O-1
30. GDH- Glutamate dehydrogenase
31. GH- Growth hormone
32. GHRH- Growth hormone releasing hormone
33. GHRHR- Growth hormone releasing hormone receptor
34. GHS- Growth-hormone secretagogues
35. GHSR- Growth hormone secretagogue receptor
36. GSK3- Glycogen synthase kinase-3
37. GST1- Glutathione S-transferase 1
38. H3K- Histone 3 Lysine
39. H4K- Histone 4 Lysine
40. HIF1alpha- Hypoxia-inducible factor 1- alpha
41. HMGCS2- 3-hydroxy-3-methylglutaryl-CoA synthase 2
42. ICV- Intracerebroventricular injections
43. IDE- Insulin-degrading enzyme

44. IGF- Insulin growth factor
45. IGFBP- Insulin growth factor binding protein
46. IGFBPrP- IGFBP related proteins
47. IHC- Immunohistochemistry
48. IIS- Insulin/insulin growth factor signaling
49. ILP- Insulin-like peptide
50. ILR- Insulin-like receptor
51. IP- Intraperitoneal injections
52. JNK- Jun N-terminal kinase
53. MC4R- Melanocorin-4 receptor
54. MCD- Malonyl-CoA decarboxylase
55. miRNA- MicroRNA
56. mtDNA- Mitochondrial DNA
57. mTOR- mechanistic target of rapamycin
58. Mybbp1a- Myb-binding protein 1a
59. NA- Nicotinic acid
60. NAD- Nicotinamide adenine dinucleotide
61. NAM- Nicotinamide
62. NAMPT- Nicotinamide phosphoribosyltransferase
63. NGF- Nerve growth factor
64. NMNAT- Nicotinamide mononucleotide adenyltransferase
65. NPF- Neuropeptide F
66. NPY- Neuropeptide Y
67. Nrg1- Neuregulin 1
68. OGG1- 8-Oxoguanine-DNA glycosylase1
69. P27- CDK inhibitor 27
70. p70s6K- p70 ribosomal S6 kinase
71. PARP1- Poly ADP-ribose polymerase 1
72. PBL- Posterior branch length
73. PDGF- Platelet derived growth factor
74. PDHA1- Pyruvate dehydrogenase E1 alpha
75. PI3K- Phosphatidylinositol 3 kinase
76. Piwi- Smedwi-1
77. POMC- Pro-opiomelanocortin
78. PVH- Paraventricular nucleus of the hypothalamus
79. RESV- Reseveratrol
80. RhoA- Ras homolog gene family, member A
81. RNA- Ribonucleic acid
82. RNAi- RNA interference
83. ROS- Reactive oxygen species
84. SAV- Salvador
85. SEM- Standard error of the mean
86. Sir- Silent information regulator
87. Sirt1 – Sirtuin1
88. Smed- Schmidtea mediterranea

89. sNPF- Short neuropeptide F
90. SOD1- Superoxide dismutase [CuZn]
91. STACs- Sirtuin activating compounds
92. TNFalpha- Tumor necrosis factor alpha
93. Tpm1- Tropomyosin alpha-1
94. Tspan1- Tetraspanin 1
95. TUNEL- Terminal deoxynucleotidyl transferase (TdT) dUTP nick-end labeling
96. UPC2- Uncoupling protein 2
97. WISH- Whole mount in situ hybridization
98. WTS- Warts
99. YKI- Yorkie

Acknowledgements

I would like to take this opportunity to show my gratitude towards everyone who has helped me get through this program. I would like to thank Dr. Oviedo for his continuous support and guidance throughout my PhD program. He was there to encourage me when experiments did not work, and to celebrate when things went well. Your lab has crafted me to think critically and work independently. I would like to thank all of the Oviedo lab members, past and current. These people became my family, mentors, and great company. Their presence made my experience more enjoyable and I hope to continue these relationships.

I would also like to thank my committee members, who never gave up on me. They have been an incredible support system and continued to see that I progressed throughout the length of this program. Dr. Katrina Hoyer, thank you for pushing me to make deadlines, this has kept me on track for completing this program. Dr. Aaron Hernday, thank you for keeping me prepared to answer questions during committee meetings. Finally, a special thank you to my previous PI and mentor Dr. Fred Wolf. You helped guide me as an undergraduate and showed me how much I enjoyed research. Your support has stretched beyond undergrad and I am incredibly thankful to have had you as a committee member.

Finally, I would like to thank my family and girlfriend who have been there to support me unconditionally. My father, who has mentored me and pushed me to pursue higher education. My girlfriend Sonali, who has been there day in day out and never stopped believing in me. I wouldn't have made it this far without the encouragement from all of you.

CURRICULUM VITAE

Benjamin Ziman
Ph.D. Quantitative and Systems Biology
LinkedIn Profile

EDUCATION

University of California, Merced
Ph.D., Quantitative and Systems Biology 2014 - December 2019

- Work with the planarian model system to study stem cell proliferation, feeding behavior, and growth.
- Develop and conduct independent research directed at identifying the molecular mechanisms behind organismal growth.
- Identify post translational modifications through Sirtuin1 that regulate stem cell differentiation and food consumption in the adult body.
- Present my research at various conferences around the United States.
- Dissertation: Sirtuin-1 Signaling Regulates Organismal Growth by Altering Feeding Behavior and Stem Cell Differentiation in Planarians.
- Advisor: Nestor J. Oviedo

University of California, Merced
Bachelors of Science, Molecular and Cell Biology
2009 - 2013

- Graduated with Honors
- Academic Excellence Award, 2012
- Undergraduate Research: Identifying histone modification to ethanol exposure in the adult brain
  - Advisor: Fred Wolf, 2012-2013
- Volunteer Note-Taker, Disability Services, 2010

PUBLICATIONS

1. **Ziman, B**., Karabinis, P., Oviedo, N.J. (2019). Sirtuin-1 Signaling Regulates Organismal Growth by Altering Feeding Behavior and Stem Cell Differentiation in Planarians. Manuscript in preparation for resubmission
2. Davidian, D., Barghouth, P.B., LeGro, M., **Ziman, B.**, Rojas, S., Maciel, E.I., Pham, I., Escobar, A.L., Oviedo, N.J. (2019). Electric Stimulation Facilitates Rapid Stem Cell Repopulation by Enhancing Cellular Plasticity in Planaria. Manuscript under review.
3. **Ziman, B***., Barghouth, P.B*., Maciel, E.I*., Oviedo, N.J. (2019). TRAF Signaling is Required for Cell Survival and Differentiation. Manuscript in preparation. *equal contribution
4. Davidian, D., Karabinis, P., **Ziman, B**., Barghouth, P.B., Oviedo, N.J. (2019). Local Tissue Depolarization Acts as a Trigger to Initiate the Planarian Wound Response. Manuscript in preparation.

5. Barghouth, P.B., LeGro, M., **Ziman, B**., Oviedo, N.J. (2019). DNA damage underlies stem cells malignant transformation in planaria. Manuscript in preparation.

SKILLS

- Research methodologies: Extractions (RNA, DNA, Protein), Western blotting, qPCR, PCR, Immunohistochemistry, *In situ* hybridization, Hydrophobic interaction chromatography, Cell fractionation, Cell disassociation, Molecular cloning, Restriction digest, TUNEL, Reverse transcription, Gel extractions and ligations, Transformations, RNA interference, animal husbandry (Planarians and Drosophila)
- Authorized by the Nuclear Regulatory Commission to work with radioactive materials
- Microsoft Office Suite, Adobe Photoshop and Illustrator, Graphpad prism, Zotero, ImageJ, Image studio, Image lab, and R studio
- Operating Systems: Windows Vista, XP,8 and 10, MAC OSX
- Writing grants and presenting reports
- Supervising undergraduate research projects
- Excellent communication skills in a collaborative work environment

FELLOWSHIPS AND GRANTS

- 2019 Travel Grant, Graduate Division, University of California, Merced
- 2019 Graduate Summer Research Fellowship, University of California, Merced
- 2019 Travel Grant, Society for Developmental Biology
- 2019 Contribution Towards an awarded NIH R01 Research Grant titled: The Effect of Direct Current Stimulation in Adult Tissues, GM132753-01
- 2018 Graduate Summer Research Fellowship, University of California, Merced
- 2018 Travel Grant, Quantitative and Systems Biology, University of California, Merced

CONFERENCES

- 2019 Poster Presentation, Society for Developmental Biology International Conference, Boston, MA.
- 2018 Poster Presentation, International Planarian Meeting, Madison, WI
- 2015 Society for Developmental Biology Conference, Yosemite, CA.

Employment

University of California, Merced
Teaching Assistant, School of Natural Sciences
2014 - Present

- Instructed numerous undergraduate biology courses (Biological Math Modeling and Statistics, Embryos and Development Lab, Genetics, Introductory Biology, Molecular Cell Biology, Molecular Cell Biology Lab).
- Contributed towards developing syllabus and course materials.
- Evaluated laboratory write-ups, graded exams and administered all grades.
- Worked with faculty to help format classes and bring forth new ideas.

PROFESSIONAL MEMBERSHIPS

Society for Developmental Biology

2015 - Present

REFERENCES

- Nestor Oviedo, Molecular and Cell Biology, UC Merced; noviedo2@ucmerced.edu, (209) 658-2592 (PhD, Advisor)
- Fred Wolf, Molecular and Cell Biology, UC Merced; fwolf@ucmerced.edu, (415) 370-1132 (Committee Member and Undergraduate Advisor)
- Katrina Hoyer, Molecular and Cell Biology, UC Merced; khoyer2@ucmerced.edu, (209) 228-4229 (Committee Chair)
- Aaron Hernday, Molecular and Cell Biology, UC Merced; ahernday@ucmerced.edu, (Committee Member)
- Kamal Dulai, Molecular and Cell Biology, UC Merced; kdulai@ucmerced.edu, (209) 607-0304 (Instructor, worked alongside with for 4 years)
- Laura Beaster-Jones, Molecular and Cell Biology, UC Merced; lbeaster-jones@ucmerced.edu (Instructor, worked alongside with for 2 years)
- Leah Young-Chung, Biology/LES Staff Research Associate, UC Merced; lyoungchung@csustan.edu , 209-603-7210 (Instructional laboratory manager , worked alongside with for 5 years)

Abstract

Sirtuin-1 Signaling Regulates Organismal Growth by Altering Feeding Behavior and Stem Cell Differentiation in Planarians.

Ben Ziman
Ph.D. in Quantitative and Systems Biology
University of California, Merced
2019
Nestor, Oviedo, Advisor
Katrina Hoyer, Chair

Food consumption leads to an increase in body size in the planarian model *Schmidtea mediterranea*. How food consumption integrates with cell division at the organismal level remains unclear. Here we show that Sirtuin-1 signaling is evolutionarily conserved in planarians and specifically demonstrate that *Sirtuin-1* (Smed-*Sirt1*) regulates growth by impairing both feeding behavior and stem cell differentiation. Disruption of *Sirtuin-1* with either RNAi or pharmacological treatment leads to reduced animal growth. Conversely, activation of *Sirtuin1* with resveratrol accelerates growth. Differences in growth rates were associated with changes in the amount of time to locate food and overall consumption. Furthermore, *Smed-Sirt-1(RNAi)* animals displayed reduced cell death and increased stem cell proliferation accompanied by impaired differentiation of intestinal lineage progenitors that resulted in reduced branching of the gut. Altogether, our findings indicate Sirtuin-1 signaling is a crucial metabolic hub capable of controlling animal behavior, tissue renewal and morphogenesis of the adult intestine.

1.Introduction

1.1. The process of growth is a result of cellular size, proliferation, and survival

The difference in size between animals is determined by differences in either cell numbers, the size of cells, or a combination of both. Both intracellular and extracellular signaling is responsible for the number of cells, as well as the size of cells. In response to extracellular growth factors, cells increase their mass and duplicate their internal contents before dividing. This is not necessarily the case for all cells. Both myofibroblasts and hepatocytes have the ability possess more than one nuclei. Myofibroblasts can fuse together to form larger, multinucleated skeletal muscle fibers[1], while hepatocytes skip cytokinesis to become multinucleated[2]. However, most cells contain a single nuclei and their size is dependent on the careful coordination of signaling pathways, such as growth factor signaling.

Extracellular growth factors can activate intracellular signaling pathways which stimulate biosynthetic processes in the cell, such as protein synthesis. Biosynthetic processes enable macromolecules to be produced at a rate that exceeds degradation, supplying cells with the essential components to proliferate. Growth factors such as insulin growth factor (IGF) activate phosphatidylinositol (PI) 3 kinase (PI3K), known as the insulin/insulin growth factor signaling (IIS) pathway. IIS activates downstream AKT and mechanistic target of rapamycin (mTOR), leading to increased proliferation and cell survival, and increased protein synthesis respectively [3–8]. In Drosophila, IIS regulates size and proliferation[9]. Impaired PI3K signaling in fly larval imaginal discs results in fewer and smaller cell development[10,11]. Conversely, if PI3K is constitutively active or overexpressed in an imaginal disc, the organ grows bigger with more and larger cells[11,12]. Drosophila with impaired p70 ribosomal S6 kinase (p70s6K), a downstream target of mTOR, grow at a slower rate and are smaller in size[13,14]. IIS is one of the most established growth factors signaling pathways, whose function is conserved across species in regulating the size of cells, as well as organismal growth[15–17]. In addition to IIS, nerve growth factor (NGF) influences cell size. This can be seen in mice, where increasing NGF regulates post-mitotic sympathetic neuron size without increasing DNA content[18]. Overall cell size can contribute to the size of an animal, but the largest contribution is due to differences in total cell numbers [19].

Total cell numbers are maintained through a balance between cellular proliferation and cell death. Extracellular mitogens stimulate cell cycle progression by regulating cell division only when it is needed. This occurs through intracellular signaling pathways that promote cell cycle progression [20]. Cyclin dependent kinases (CDKs) are critical regulators for cell division. CDKs bind with cyclins to form complexes which can phosphorylate proteins required to activate different phases of the cell cycle at precise times.[21].

Concentration changes in mitogens are a big factor in determining the rate of cell cycle progression[22,23]. Both platelet derived growth factor (PDGF-AA) and fibroblast growth factor (FGF 4,8) are mitogens whose concentrations are known to regulate cellular proliferation. Mice with one or more copies of the PDGF-AA transgene have been shown to increase amounts of oligodendrocyte precursor cells[24]. In developing limb buds of chicks, increases in FGF 4,8 have been shown increase proliferation of mesodermal cells[25]. In the absence of mitogens, cells fail to enter the G1 phase of the cell cycle and instead enter a quiescent state known as G0[26]. Proliferation inhibitors can also inhibit cell cycle progression, usually arresting cells in G1[27]. As an organ grows, secreted inhibitory signals accumulate until a threshold is reached, at which point cellular proliferation stops, and the organ stops growing [28]. Here we present three examples of how disrupting inhibitory signals can lead to increased cellular proliferation and even enlargement of organ size. Myostatin is a protein produced by muscle cells to inhibit the formation of new muscle cells. In mice that completely lack myostatin, skeletal muscle is approximately three times the normal size, and contains more and bigger cells[29]. In *C. elegans,* Cul-1 is an E3 ubiquitin-protein ligase which helps cells exit the cell cycle during larval stages by degrading cell cycle promoters such as G1 cyclins[30]. The loss of Cul1 in *C*. *elegans* results in extra divisions of larval cell lineages, as these cells fail to exit the cell cycle and continue to proliferate.[31]. Lastly, CDK inhibitor 27 (P27) is thought to limit proliferation to ensure that precursor cells can exit from the cell cycle and terminally differentiate at the proper time[32].This can been seen in mice, where the absence of P27 results in organs being about 30% larger and possess more cells than normal[33–35]. Overall, growth factors and mitogens are required for cells to grow and divide, but for cells to avoid death, this requires adequate amounts of survival factors[36].

Survival factors regulate intracellular proteins that control apoptosis, including B-cell lymphoma 2 (Bcl2) family and inhibitors of apoptosis[37]. Apoptosis is a programmed cell death involving a cascade of cysteine proteases that become activated when cells fail to receive enough survival signal [38]. Apoptosis is necessary to balance out cellular proliferation in order to control the number of cells. For example, In the central nervous system (CNS) during development, oligodendrocytes are overproduced in rats. However, the limited amount of survival factors produced by axons will reduce the total number of oligodendrocytes[39]. Hippo signaling in Drosophila is required for normal tissue growth, by regulating Cyclin E control of cell proliferation, and survival factor drosophila inhibitor of apoptosis protein 1 (DIAP1). When hippo signaling becomes disrupted, cells become resistant to apoptosis and go through extra rounds of cell division[40,41]. The amount of survival factor also influences the size of an organ. Under normal conditions, organ apoptosis increases or decreases in response to the total cell mass being either too large or too small, respectively[36]. For example mice that

overexpress the survival factor Bcl2 in neurons have enlarged brains with more neurons, due to reduced cell death[42]. Lastly, the size of an animal can be influenced through changes in cell survival without altering cellular proliferation. Hydra maintains relatively constant levels of cellular proliferation regardless of the animal being fed or starved. In the absence of food, an increase in apoptosis counter balances cellular proliferation, and halts growth[43]. Taken together, cell survival plays a huge role in regulating growth and development, as does cellular growth and division.

1.2. Feeding behavior, growth hormone, and insulin signaling are the largest contributors that influence organismal growth

Environmental factors such as nutrition can play a role impacting linear growth, as animals that are not provided with adequate amounts of nutrients during development end up with smaller body compositions[44–47]. Under nutrient stress, Drosophila spend three to four times the amount of time to complete larval development and adult flies have overall reduced body size[46,48]. In humans, insufficient nutrients during pregnancy and within the first two years of life leads to reduced body stature, a condition known as childhood stunting[49,50]. Independent of food availability, the body has a network that determines hunger and fullness, a process known as feeding behavior.

Food intake is regulated by the CNS under the control of two major groups of neurons in the arcuate nucleus of the hypothalamus(ARH). Orexigenic, neuropeptide Y (NPY)/agouti-related peptide (AgRP) neurons that stimulate appetite, while pro-opiomelanocortin (POMC), anorexigenic neurons decrease appetite. Activation of POMC neurons decreases food consumption and body weight in response to melanocortin receptor signaling[51]. Stimulated POMC neurons release alpha-melanocyte stimulating hormone (A-MSH) which binds primarily to the melanocorin-4 receptor (MC4R) in the paraventricular nucleus of the hypothalamus (PVH). Binding of A-MSH to MC4R produces an anorexigenic or “full” effect[52]. Orexigenic effects of NPY/AgRP neurons are thought to be due to GABAergic neurotransmission, by inhibiting melanocortin signaling of anorexigenic neurons[53]. Ghrelin is a peptide hormone secreted by parietal cells in the stomach which drives hunger. Ghrelin induced hunger is a result of ghrelin binding to its receptor, growth hormone secretagogue receptor (GHSR) of NPY/AgRP cells in the ARC to inhibit POMC function[54–56]. Ghrelin administered into mice, via intracerebroventricular injections (ICV) into the CNS or intraperitoneal injections (IP) into the peripheral, will stimulate increased food intake[57]. NPY has been shown to have a greater orexigenic effect than AgRP, however both neuropeptides are essential to induce hunger[58]. Hunger can be driven in invertebrates that do not possess NPY, but contain orthologs called neuropeptide F (NPF) or short neuropeptide F (sNPF). NPF and sNPF are functionally and structurally similar to NPY except

for the replacement of tyrosine with phenylalanine in the C-terminus[59]. Ghrelin is not only an important regulator of feeding behavior but it can also function to regulate one of the most powerful growth controlling hormones.

Ghrelin's receptor GHSR can stimulate the release of growth hormone (GH) from the pituitary in response to synthetic molecules called growth-hormone secretagogues (GHS), as well as ghrelin itself[54]. Ghrelin injected either ICV or IP into rats was able to increase blood plasma levels of GH which was thought to be occurring at the hypothalamic level[57]. Under normal conditions, hypothalamic growth hormone releasing hormone (GHRH) binds to its receptor, growth hormone releasing hormone receptor (GHRHR) which in turn is responsible for the majority of GH release by the pituitary gland[60]. GH has been shown to play metabolic roles in increasing lipolysis, oxidation of free fatty acids, and protein metabolism[61]. However, the primary role of GH is concerned with growth, as individuals that are GH or GHRHR deficient fail to grow at a normal rate and become "dwarfs"[62]. GH exerts its growth effects by stimulating the production of IGF1, occurring mostly in the liver. IGF1 can stimulate biosynthetic processes leading to cell cycle progression and protein synthesis through IIS[63].

IIS is critical for growth and metabolic function across vertebrate and invertebrate species. In vertebrates, Insulin, IGF1, and IGF2 each have their own respective receptors, which can exert different downstream responses. As well, a hybrid Insulin/IGF1 receptor can act to bind more than one ligand. In invertebrates, there may be several insulin like peptides (ILPs) that mediate their effects through a single insulin receptor (ILR)[64].

In vertebrates, insulin is a hormone that is secreted by pancreatic beta cells and mainly counters the effects of glucose by binding to the insulin receptor. Insulin receptors downstream effects activate the AKT pathway, stimulating glycogen synthesis through the inactivation of glycogen synthase kinase-3 (GSK3)[65,66]. Insulin receptor signaling can also promote protein synthesis via GS3K inactivation leading to dephosphorylation of eukaryotic initiation factor 2-B (eIF2B) and mTOR activated promotion and inhibition p70s6K and eIF-4E binding protein (4E-BP1) respectively[67,68]. To a lesser extent, insulin can also stimulate a mitogenic effect by activating the Ras-MAPK pathway[69]. While insulin hormone signaling plays a more metabolic role, IGF1 receptor signaling plays more important roles in promoting organismal growth by stimulating protein synthesis, promoting cell survival, and initiating cellular proliferation[70,71]. The IGF2 (mannose-6 phosphate) receptor lacks known insulin signaling enzymatic activity in its cytoplasmic domain. It acts to regulate circulating levels of IGF2 by lysosomal degradation upon binding and internalization[72]. A hybrid insulin/IGF1 receptor can bind IGF1 with high affinity and insulin or IGF2 to a lesser extent[73]. Hybrid Insulin/IGF1 receptors act predominantly in an IGF signaling pathway manner, however they can also induce glucose uptake[74]. While some

vertebrate insulin receptors can serve multiple functions, the lack of multiple insulin receptors in invertebrates forces them to serve multiple roles.

Invertebrates express a single ILR but several ILPs can influence both metabolic and growth-factor like responses. The number of insulin-like peptides varies across species, for example, planarian possess only one ILP, whereas Drosophila contain eight ILPs, and *C.elegans* contain 38 ILPs. Across several species of invertebrates, IIS plays a critical role to regulate body size and growth[16,17,75]. Insulin signaling in invertebrates has also been correlated to lifespan, as reduced IIS has been shown to increase lifespan[76,77]. The regulation of ILPs has been mostly by influenced by nutrients, however additional components that are known to regulate IGFs in vertebrates might also play a role in invertebrates.

In addition to the activity of insulin receptors and their ligands, insulin growth factor binding proteins (IGFBPs) can act to regulate insulin growth factor signaling. In mammals a total of seven IGFBP's have been identified (IGFBP1-7) which bind to IGFs with high affinity. An additional nine IGFBP related proteins (IGFBPrP1-9) have also been identifies, however they bind to IGFs with relatively low affinity[78]. Three of the seven IGFBPs (IGFBP 3,5,7) require an additional component called an acid labile subunit (ALS), which form ternary complexes with IGFs [79–81]. Approximately 75-90% of all serum IGFs are found to be in complexes with IGFBP3 and ALS, about 10- 20% are bound in binary complexes (IGFBP 1,2,4,6), and only 1% remain free[81,82]. While IGFBPs can inhibit the actions of insulin growth factor signaling, they also serve dual functions to prolong the half-life of IGFs from about 10 minutes to 25 minutes in binary complexes, and up to 16 hours in ternary complexes[80,83] . ALS functions to maintain large amounts of circulating IGFs through the ternary complex it forms. Loss of ALS leads to IGFs and IGFBP3 being removed from circulation[84]. IGFBPs can be degraded by proteases and allow for IGFs to bind to receptors, providing a role in aiding insulin growth factor signaling[80]. IGFBPs exist in both vertebrates and invertebrates, however their role in invertebrates remains elusive.

1.3. Sirtuins are versatile metabolic regulators

Sirtuins are a group of highly conserved proteins which require nicotinamide adenine dinucleotide(NAD+) as a cofactor for their enzymatic function. Silent information regulator (sir) 2 was the first Sirtuin discovered in *Saccharomyces cerevisiae*, for its ability to silencing mating gene[85,86]. Sirtuins have been classified as a group of Class III histone deacetylases, targeting lysine residues on histones[87]. In recent years, Sirtuins have been found to do more than deacetylating histones, such as deacetylating non-histone proteins, possessing ADP ribosyltransferase activity, as well as transferring other chemical groups from the protein substrate to the ADP-ribose moiety of NAD+[88–90] (Figure 1). The number of Sirtuins vary across species. While there are seven mammalian Sirtuins, organisms such as *C. elegans* and

Drosophila melanogaster possess fewer orthologs [91,92]. These Sirtuins are localized to specific subcellular compartments which influences their functional roles, such as nuclear (Sirtuin-1,2,3,6,7), cytoplasmic (Sirtuin-1,2), and mitochondrial (Sirtuin-3,4,5)[87,93–97]. Regardless of their N-terminal localization signal, each Sirtuin possess a conserved Rossmann fold/NAD+ binding motif as well as a histidine residue for its catalytic activity[98].

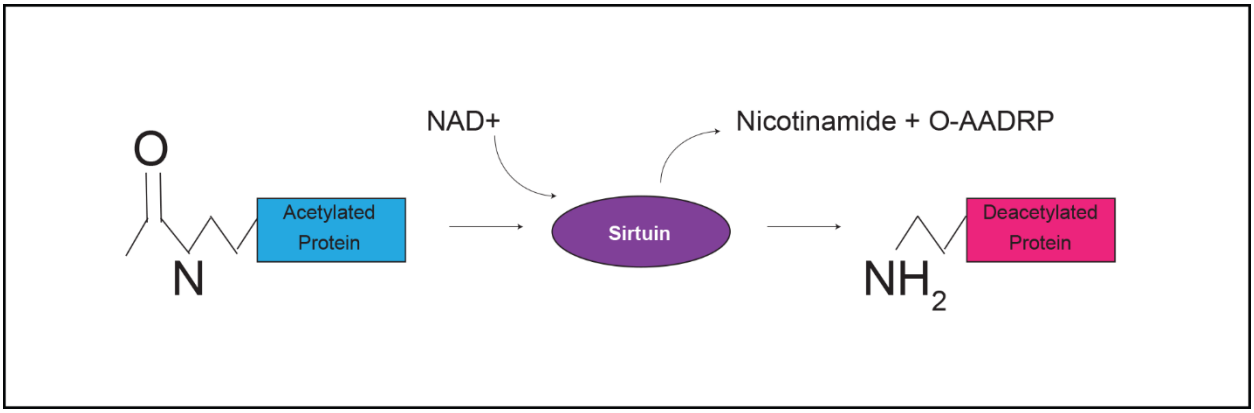

Figure 1. Mechanism of sirtuin deacetylation. Sirtuins enzymatically remove an acetyl group from lysine residues on protein substrates or histone tails. Sirtuins recognize and bind to lysine residues, as well as its coactivator NAD+. Once both are bound, NAD+ is hydrolyzed to produce Nicotinamide and the acetyl group from the lysine residue is removed and bound to the ADP ribose moiety of NAD+. This yields a deacetylated protein substrate or histone tail.

NAD functions in several energy production pathways such as fatty acid oxidation, glycolysis, and the tricarboxylic acid cycle[99]. Signaling processes that are NAD dependent require NAD to be cleaved resulting in mainly protein deacetylation and ADP-ribosylation[100]. Due to the relatively short half-life of NAD (15 minutes to 15 hours) across different tissues, NAD is constantly being re-synthesized[101]. In mammals, the NAD salvage pathway produces the majority of NAD. This pathway recycles nicotinamide (NAM), a by-product of NAD cleavage to produce new NAD through an intricate coordination of enzymes. Nicotinamide phosphoribosyltransferase (NAMPT) converts NAM into nicotinamide mononucleotide (NMN). The next step requires nicotinamide mononucleotide adenyltransferase (NMNAT) for the adenylation of NMN to form NAD[99–107]. Three isozymes of NMNAT(NMNAT1-3) are localized to subcellular compartments such as nuclear (NMNAT1), mitochondria (NMNAT2), and cytosolic (NMNAT3), where they overlap with NAD-dependent reactions[100,107].NAD can also be produced de novo via tryptophan catabolism, as well as through the Preiss-Handler pathway using nicotinic acid (NA) as a precursor[99–101,104–107]. NAD Precursor NAM has been used as supplements for over 80 years to help improve metabolic function as well as other diseases[100,106,108]. However, NAM at higher doses leads to inhibition of NAD consuming enzymes, such as Sirtuins[100,103,109,110]. NAM has been proposed to bind to the location where NAD conformational changes

and cleavage occurs in Sirtuins, thereby preventing hydrolysis of NAD and inhibiting Sirtuins function[103].

Due to the nature of Sirtuins requiring NAD for their enzymatic activity, Sirtuins have been linked to metabolic function. Of the seven mammalian Sirtuins, Sirtuins (1-3) have been the most studied, with Sirtuin-1 as the most well known[111–114]. Over the past 35 years since the first discovery of the mammalian Sirtuin-1 orthologue Sir2*,* over 8000 Sirtuin-1 articles have been published. More than 1100 articles have been published in just the last year alone. Despite Sirtuin1 being the center of attention, all Sirtuins are being investigated for their novel metabolic functions. Below are key finding for each of the seven mammalian Sirtuins.

Sirtuin-7 has been the least studied of the seven mammalian Sirtuins. Sirtuin-7 has been shown to function mostly as a deacetylase, within the context of tumor formation. Sirtuin-7 has been identified to regulate chromatin formation by deacetylating H3K18, leading to enhanced tumor formation[115]. MicroRNA (miRNA) miR-125a-5p and miR-125b suppression of Sirtuin-7 was found to inhibit human hepatocellular carcinoma tumor growth in human patients by causing cell cycle arrest, possibly through regulation of p53[116,117]. The functions of Sirtuin-7 also extend out to preserving heart function by preventing apoptosis and inflammation[118]. Despite Sirtuin-7 being the least studied Sirtuin, it has become a power tool towards therapeutic approaches.

Sirtuin-6 can target proteins or histones through several different mechanisms. Sirtuin-6 has been reported to possess mono-ADP-ribosylation function[88]. This is a reversible protein modification in which an ADP ribose moiety is transferred onto a specific target, which can allow for activation/ inactivation of protein substrates[119].Mono-ADP ribosylation of lysine 521 on poly ADP-ribose polymerase 1 (PARP1) by Sirtuin-6 can activate and stimulate Double Stand Break (DSB) repair in response to oxidative stress[120]. Sirtuin-6 can stimulation secretion of tumor necrosis factor alpha (TNFalpha) by the removal of fatty acyl groups modifications to lysine residues 19&20, important for inflammatory responses[121]. Sirtuin-6 can also function as a histone deacetylase by targeting H3K9 at the hypoxia-inducible factor 1-alpha (HIF1alpha) target gene promoters, regulating glucose homeostasis[122]. This was observed in Sirtuin-6 deficient mice that had reduce glucose intake leading to lethal hypoglycemia[95,122]. The diverse functions of Sirtuin-6 offer a wide range of regulation from DNA integrity, to inflammation, and glucose homeostasis.

Sirtuin-5 shows very little deacetylase function, and acts rather as a modifier of negatively charged groups on lysine residues[123]. Sirtuin-5 can catalyze the removal of malonyl, succinyl, and glutaryl -CoA lysine modifications[124–126]. Loss of Sirtuin-5 in mice leads to increase levels of carbamoyl phosphate synthase 1(CSP1), an important mitochondrial enzyme for the urea cycle[124,127]. The changes in CSP1 were shown to be through

deacetylation[127], however more recently succinylation of lysine1291[124] , as well as eight candidate lysine glutarylation[126] sites show to be greater regulators for CSP1. Sirtuin-5 also acts to prevent oxidative stress induced cell death. In lung tumor cells, desuccinylation of K123 of CuZn superoxide dismutase (SOD1) by Sirtuin-5, activates SOD1 leading to decreased reactive oxygen species (ROS) and increased growth[128]. As well, overexpression of Sirtuin-5 was shown to increase levels of pro-survival Bcl-Xl in cardiomyocytes exposed to hydrogen peroxide, aiding to prevent oxidative stress induced cell death[129]. Sirtuin-5 plays an important role in the mitochondria regulating the urea cycle and promoting cell survival.

Sirtuin-4 is a mitochondrial Sirtuin whose functions also extend beyond just deacetylation[98,130,131]. Sirtuin-4 has been primarily shown to regulate insulin secretion. Sirtuin-4 in pancreatic beta cells can impair insulin secretion through ADP-ribosyltransferase activity by targeting glutamate dehydrogenase (GDH)[132], ADP/ATP carrier proteins (ANT2/3), and insulin-degrading enzyme (IDE)[133]. Sirtuin-4 was also shown to regulate insulin secretion by removing acyl moieties on leucine oxidation intermediates, methylglutaryl, hydroxymethylglutaryl, and 3-methylgluataconyl [134]. As well, Sirtuin-4 has the ability to repress fatty acid oxidation (FAO) in muscle cells by deacetylating malonyl-CoA decarboxylase (MCD) , leading to increased malonyl CoA, which inhibits FAO and stimulates fat synthesis[135,136]. Sirtuin-4 as a regulator of insulin secretion, has potential to be a therapeutic target for type 2 diabetic patients.

Sirtuin-3 is another mitochondrial Sirtuin which acts with robust deacetylation functions[137,138]. Sirtuin-3 has been shown to deacetylate pyruvate dehydrogenase E1 alpha (PDHA1) at lysine 321 stimulating oxidative phosphorylation[139]. Sirtuin-3 can increase key tone bodies production of beta hydroxybutyrate in hepatic beta cells by deacetylating and activating transcription of mitochondrial 3-hydroxy-3-methylglutaryl-CoA synthase 2 (HMGCS2)[140]. Skeletal muscle cells from Sirtuin-3 deficient animals show elevated ROS levels which can lead to insulin resistance via jun N-terminal kinase (JNK)[141]. Sirtuin-3 also plays an important role in oxidative damage on mitochondrial DNA (mtDNA). Deacetylation of 8-oxoguanine-DNA glycosylase1 (OGG1), a DNA repair enzyme by Sirtuin-3 prevents stress induced apoptosis by enhancing base excision repair (BER) of mtDNA[142]. Sirtuin-3 is the most well studied mitochondrial Sirtuin, possessing an array of functions.

Sirtuin-2 is classically a cytoplasmic Sirtuin, however it has also shown to act in the nucleus, deacetylating H4K16 during the G2-M transition of the cell cycle[143,144]. In the CNS, Sirtuin-2 has shown to play important roles in the differentiation of oligodendrocytes [145,146]. Adipocyte differentiation has shown to be regulated through Sirtuin-2 interaction with forkhead transcription factor of class O (FoxO1), whose acetylation status leads to terminal differentiation

of adipocytes[147,148]. Sirtuin-2 has also been identified as a positive regulator of AKT, enhancing insulin signaling[149]. Sirtuin-2 has important role in cell cycle and differentiation but its deacetylation function can also extend to insulin signaling.

Sirtuin-1 has an extensive list of histone and non-histone protein targets[150]. Sirtuin-1 has been shown in the two cell stage of embryos to be highly expressed, indicating importance for embryogenesis[151]. Sirtuin-1 in pancreatic beta cells helps secrete insulin in response to glucose by repressing uncoupling protein (UPC2)[152]. Sirtuin-1 plays important roles in regulating IGF signaling, impacting growth in Sirtuin-1 null mice[153–155]. Sirtuin-1 can also regulate peptides that influence food intake such as ghrelin signaling[156–159]. Sirtuin-1 acts as a critical regulator of growth and development, as well as a regulator of insulin signaling among several other metabolic functions not listed here.

Small molecule Sirtuin-activating compounds (STACs) have been identified to enhance Sirtuin function[160]. One of the first STACs to be identified is the polyphenol Resveratrol (RESV). Resveratrol speeds up the rate of Sirtuin-1 enzymatic function by lowering the substrate binding activity (Km)[107,161]. Resveratrol has been shown to enhance Sirtuin-1 dependent lifespan extension in various organisms[162]. RESV has been used in various clinical trials and has shown to improve insulin sensitivity and lowered blood glucose levels in human patients with type 2 diabetes[163–166]. The use of Resveratrol has become increasingly popular, over the past two decades. As a result, this compound is widely available to the general population.

Studying Sirtuins can be challenging, in which knockout models can lead to developmental defect and early death. Knockout of Sirtuin-7 caused 59% decreased lifespan in mice[118]. Sirtuin-6 knockout mice are smaller in size and with severe metabolic defects. They have impaired DNA repair, leading to premature death at 4 weeks of age[95]. As well, Sirtuin-1 knockout mice present developmental defects and most do not make it to adulthood[153–155]. Loss of Sirtuin-1 in other models such as yeast, Drosophila, and *C. elegans* has also been shown to reduced lifespan[167–169]. As a result, studying Sirtuins in the adult body becomes a challenge, mostly tissue specific knockouts are favored as a consequence.

1.4. The planarian model *Schmidtea mediterranea*

The planarian *Schmidtea mediterranea*, has been used as a model to circumvent early death associated with loss of function in the adult body[170]. Planarians are triploblastic flatworms, expressing bilateral symmetry, and belonging to the Platyhelminthes phylum[171–173]. The planarian *Schmidtea mediterranea* has two strains based off chromosomal translocation leading to either sexual or asexual reproducing animals[174]. The sexual strain are hermaphrodites, that cross-fertilized to produce cocoons, which develop into

juveniles, and then mature into adults. The asexual strain, and to a lesser extent the sexual strains, can reproduce through a process known as fissioning. During fissioning, planarians attaches their posterior end to a surface and stretch their anterior end until they break into two fragments. Each fragment will then regenerate into fully functional adult animal[174–178]. The underlying mechanisms that determine when fissioning occurs remain mostly unknown, however body size and population density seem to be driving factors.

The planarian body plan is not as elaborate compared to more complex organisms. The CNS consists of a bi-lobed, cephalic ganglia, two ventral nerve cords that are interconnected by commissural neurons, as well as sensory receptors (photoreceptors, chemosensing receptors, and rheoreceptors). Visualization is made possible by pigment cells that form the optic cup with the aid of photoreceptors [171,172,175,179]. They contain an excretory systems which consists of a protonephridia network that allows for fluids to be exchanged[180]. Their movement is made possible through cilia on their dorsal side, allowing them to glide across surfaces in water[181]. Feeding takes place through their pharynx, which serves dual purpose as both a mouth and anus. The pharynx is connected to the gastrovascular system. The gastrovascular consisting of one anterior and two posterior gut branches, each containing sub-branches. The lumen of the gut contains intestinal phagocytes which absorb food particles for digestion and goblet cells that release digestive enzymes[182]. All of the intermediate space between the CNS and gut is known as the mesenchyme. The mesenchyme contains a population of resident adult pluripotent stem cells known as neoblasts[171,172,183].

Neoblasts are the only dividing cells in the body, making up roughly 25% of the cell population, and can be depleted using sub-lethal gamma irradiation[171]. Neoblasts are a heterogeneous population which give rise to all the cell types of the body with different degrees of potency [171,184–191]. Clonogenic neoblasts have the highest level of potency, capable of rescuing a neoblast depleted host after irradiation[188,191,192]. As a result, neoblasts allow for high rates of cellular turnover and tissue homeostasis.

Neoblasts enable planarians to have a robust regenerative capacity. A small fragment of an animal (1/279), has the capacity to regenerate into a new fully functional organism[193,194]. In response to injury, a generic wound response is triggered, requiring careful coordination of cellular proliferation and cell death[187,195]. As a result, a mass of undifferentiated cells forms a blastema at the wound site, where these cells differentiate, and completely regenerate the missing tissue[171]. This unique feature of regeneration has been the one of the main focuses for the planarian model with an ever growing wealth of literature[172,184–186,195–199,199–217]. With the aid of stem cell marker Piwi, neoblasts can be separated from differentiating and terminally

differentiated cells via fluorescent activate cell sorting (FACS)[218–221]**.** Single cell RNA sequencing can be used in unison with established genomes to identify transcripts that are critical for regeneration and cellular turnover[191,217,222–226,226,227,227–230].

The planarian also has the unique ability to respond to nutrient availability by either increasing or decreasing body size while maintaining complete proportionality in only a matter of weeks.[171,231] This coordination is due to balancing proliferating cells with dying cells, while maintaining a constant ratio of different cell types[232,233]. The body size is influenced by the total number of cells in the planarian, rather than the size of the cells[234,231,235].The ability to consume nutrients is another factor for regulating organismal size in planarians[16,170,217].

The planarian possesses chemoreceptors which are able to sense nutrients[217]. A network of neuropeptides has been shown to regulate the capacity to consume food, as well as the requirement for the pharynx to extend out for feeding[236]. The process for how these neuropeptides regulate feeding behavior remains elusive. IIS is the only established metabolic regulator of growth in planarians[16,170,237,238]. While loss of IIS prevented animals from growing at a normal rate after being fed, no data was provided stating if these animals consumed less food than control animals. Therefore, metabolic regulation of size in planarians remains mostly unknown with regards to feeding behavior.

Loss of metabolic regulators in other models can lead to severe developmental defects and early death[15,17,153–155,239–243]. Asexual planarians remain as adults throughout their life and are essentially immortal, as they do not age[244]. This is thought to be contributed to the regeneration of telomeres through indirect mTOR signaling[245]. Studying Sirtuins in the planarian model offers the ability to explore how Sirtuins function in the adult body without premature death that occurs in other models[95,118,153–155]. The small size of planarians and a wide range of molecular tools offers the advantage to study biological function in whole animals. We can study proliferating stem cells, gene expression, and protein expression, by using bromodeoxyuridine (Brdu), in situ hybridization, and immunohistochemistry (IHC) respectively[182,246–252]. Due to the aquatic nature of planarian, manipulations with pharmacological compounds can be easily performed[253]. RNA interference (RNAi) through methods of soaking, feeding, or injecting is effective for loss of function studies[254–257]. Recent updates to genomes with the aid of single cell RNA sequencing has provided the opportunity to study novel genes with insight to its expression levels in different cell populations, anatomical expression, as well changes in expression due to stimulation such as irradiation and amputation[222–227]. Overall, we present the planarian as an ideal model for studying Sirtuin function and its role in regulating organismal growth and feeding behavior. This is due to fact that Sirtuin functionality can be easily

manipulated and Sirtuins influence of systemic stem cell function and tissue renewal can directly impact body size.

2. Materials and Methods

2.1 Materials

2.1.1. Organisms

Planarians:
The planarians used in these experiments were the *Schmidtea mediterranea* CIW4 and *Dugesia Japonica* SSP. Cultures were maintained as previously described[258].

Bacterial strains:
Two types of bacterial strains were used in experiments. NEB5-alpha competent E. *coli* (High Efficiency), a derivative of the popular DH5α sourced from New England Biolabs (cat# C2987H). This was used for cloning and sub cloning for plasmids pCR-Topo and pBluescript.

2.1.2. Selection of primers and cloning vectors

Plasmids:
TOPO-TA Cloning Vector, pCR was used for the initial cloning, Invitrogen (cat# 450030). pBlueScript II SK (+) was used as the final vector for cloning, Agilent (cat# 212205).

Primers:
Primers were identified and designed using both Primer3 (http://bioinfo.ut.ee/primer3-0.4.0/) and NCBI Primer BLAST (https://www.ncbi.nlm.nih.gov/tools/primer-blast/). Primers in the form of custom oligonucleotides were obtained from Thermofisher and Eurofins MWG Operon, Part of Thermofisher scientific. Primers listed below are for both cloning (bolded) and qPCR. All primers were diluted in MilliQ Water to 40pM. All primers were tested with PCR using cDNA, prior to being used in experiments.

List of primers used in this study:

Name	5' Forward Primer	5' Reverse Primer
Sirtuin1(BMZA1/BMZA2)	**CATGGATCATTTGCATCAGC**	**TCCTCAGTCGCTTCATCAGA**
Sirtuin2(BMZB10/BMZC1)	**GCAGAAAAGAGCTCCAATCCC**	**AGGCAAAGATTCGCCAAACA**
Sirtuin3(BMZC8/BMZC9)	**CCGGAGCTGGCATAAGTTGT**	**TTAAAACCCGAGGAGTGCCG**
Sirtuin4(BMZC6/BMZC7)	**AGTTGTAACAGGAGCTGGAGT**	**TGTTCCCAAACACAACAGACC**
Sirtuin5(BMZB4/BMZB5)	**TTTGGAAAACCCGTCTCTTG**	**CGAAGCAGGGCCTCTAATAA**

Sirtuin6(BMZB6/BMZB7)	**AAAATGTGGTGCACCTGAGA**	**CAGTGAAGTTCCAAGGCACA**
DJSirt1	**ATTTCAGTCCCTTGTGGGGTG**	**ACGCTTCCTGGTCCTTTTCTT**
Sirtuin1	TGCATCAGCTACTTGCATGAGA	TCGACTTCGTCTGAATTTCCA
Sirtuin2	GGCCATTGCTTATCTTGCGAA	TCCGGCTTAACTAAACCATTGC
Sirtuin3	AGCTGTGTTCGTTGTGGTGA	TCAGGTTTAACGATTCCTCGACA
Sirtuin4	ACAGGAGCTGGAGTTTCTACA	GCGAGCCCAATATCGTTGTC
Sirtuin5	GCGTCCAAATGTTGTCTGGT	GACCGGTTGAACGATTCCAG
Sirtuin6	GCAGGTATCAGTACGGGTGT	CCGCAGCTTCTAACGCATTT
Nrg-1	CCAATGCCAGGCTGAAGGATA	TTTGCTTCGTCGGATTTTTCAAC
EGFR1	TGTTTGCGATTGATCGGTGT	TGCTATCTGTTCGGCCCATT
1020HH	CTGACGGGACCAGTTTGGAA	CCATCTGATACCGCCTTTCA
NP2Pre(npp2)	GACTCAAAAGCAGCCGTCAG	TTTGCCTATCAGTCCACGCC
SecPepPro19	ATCGTGCTCCTTGCGTCATT	TTCCCCAGGAATCAGGCATT
NPPre(npp4)	ACCAGCTGACCGATGATTCG	CGCGCCTTTTACCGAACCTA
EYE53-2	CGTCGCACATAAAACGAGCG	TCATCCCATGCGTCTGGAAC
NP22Pre(npp22)	GTCTCGTGTTGATTGCCAGC	TATTTGGCCCGCTTTCCCAA
SecPepPro15	ACTGTAGGTTTATTCCACGTCA	TCTTTTGTCAAACAGGATCGGA
SecPepPro5	TGCGTGGTTTTCGTATTCGC	TCCCCATGCGCAGTATTCTC
SecPepPro8	TCTGGCTGTTTGTGCTTTTGA	GGCAAACCCTGACCCAAATG
SecPepPro16	TGTCAGTTACGAGGAGCTTTCC	TCGAACTGACCCTTGCCAAT
NPY1	TAGAACCACCGGCAAAACCA	CTTGGTCGACCTACTATGGCA
NPY2	TCTGCGATGGAAGATGACACA	TGGACGGCCGGCAATTAAA
NPY3	CTGCAAACAAAGACGAGCTTGA	GTCTCGGTGGAATTTCTGACG
NPY4	AAGTTTTGTTGTGCTCCCCG	ACTTTCCGCTTGACCTCCTT

NPY5	TGCAATGTGGCTAAGTGGGA	TCTTGCCATATCGTGGACGC
NPY6	TCAACTTTCTCGTCGGACCC	GCCAAATCTGGGTCTTCCGT
NPY7	CCAGGACTCCTATCGCTGGTA	GCGAAAGGGGTACAGAGGATT
NPY8	ACTTGCAATCAGAAAAGGCCG	TTGCCAAATCTTGGTCTTCCT
NPY9	TCAGCTTAACGCTCTGTGTGA	TCGGACGAGAACTCAATGCAA
NPY10	TCAGTGGTACGACAAAAGAGAT	ACCATATCTCGGTCTTCCAGC
Smedwi1	TTTATCGTGACGGTGTTGGA	TTGGATTAGCCCCATCTTTG
TSPAN1	TGCTGCGGACGAATCAGTTAT	ATGCAGCCGGTGTTCCAAT
BCL2	TGGTAGAAGCTCAAGACCGTG	ACTCTGGACCACCGTATACAA
ILP1	CTAAGACACTTTTTCGCCAATCG	TTTGTAAATCGGGTGCATTATGTTA
ILR1	TGGAAACCAGAACCAAGGAG	CATGACTCCATGCACTTGTCA
ALS	TCGATTCATAAACCTTTCGCACA	TCCCTAAACGTCTGAAAGCGA
IGFBP3	CATTTTGGTGTCCTCCATGCG	TCTCTCCTTCTTGAAGCCCAC
IGFBP5	CCGCCCTGTTTCCAACAAGA	TCGTGACGCATCTCAAACCG
IGFBP7	AACTCTGGCAGTTGTTTCTGC	TCTTCCAATCCGCAAACCTCA
AKT	GAGAACTGAAACCGGAACCA	CCCAAATGTTCCTTTGCCTA
mTOR	AACTCGCGGAACTTGAAGAA	TTGATTTGGTGTCAGGACCA
FoxA	TGCCAAGCCTCCATACAGTT	ATCGAATTCTGCCATCGCTGT
Rab13	TTTCCGTAAAGCTGACGGTGT	CAGTACCCTCTTCAACGCCA
GATA456	GCAATGCTTGCGGCTTGTAT	TGATTCTGAAGACGGCACCT
FRK	CGGCTTTGGTTGCCGTAAAA	TTGGGTCGTCTGTGCAAACT
ODC1	CAAAGTATTGGCCGCAAGCAA	TTCGCTTACGCTCTGAGTTC
GST1	TGTTGCACGAAAACATGGGT	TTATCCCGACCAGAGGTTGC
ASCL1	AAAACGGGTGGAACAGGTCA	TCAATCGCGACTCTCAAAGTT

POU2/3	TCGGGTTAGCCCTCGGTAAT	TCGGCTTCTTGCAACCACTT
LLGL1	GCTCATGTCGAATTACCCGC	TCTTCTTGCGCTACTGCGAT
ATOH8	CTTACCAGAGAACGCCGAGT	AATAACCAGGCACAGCATGGC
ATG2B	GGCCGATAAGGAACCGCATT	ATTGGATCCGTCGAAGCAGA
ATG3	TTCTTAACGGCCAACCAGGA	GGACTTCCATTGTCACGGTT
ATG5	AGAGGATTGCTCATTCAGGCT	CCAACAGCTTTGTTGGCTTCA
ATG7	ACTACAGGAGCAACATCACCA	TTCTTAACGGCCAACCAGGA
ATG10	GAGCCGAGGATGACAAAGGA	ATGCATCGAGAAACAGGGCA
ATG12	AGCAGCTGGAGATGCTCCTAT	ATCGGTGTCGAGTGATGGTG
BECN1	AAAGGGCAAGGATGCTCGAT	AAAGAGGCACTCACCAACCA
ATG8	CCAAACATTTCCTGGGACGC	AGCATGGTGACAATGTCGAG
DAP1	TCCTGGCGTGGAAATTGATGA	ACAGGTTTCGTTGGCTTGCT
ZFP-1	ACTCATCCAGTACAGCCAGTTT	TTGATTCGTGGGTACTGGACT
mex3	CCCTACACCACCATTCCAACA	TGTGAAAAGTGACGCGGAGT
FLI-1	TCTGCATCAGGAAGCATACCA	GGCTGCTGCGTGTTGAAATA
TATABoxBP	GCAGCGAGAAAGTTTGCCAG	TGTAGCAAACTGGGTGTGTGA

2.1.3. Antibodies, enzymes, and reagents

Antibodies

Name	Host	Dilution	Source	Cat #
Anti-beta Tubulin (E7)	Mouse	1:10000	Developmental Studies Hybridoma Bank	AB2315513
Anti-Caspase3	Rabbit	1:500	Abcam	Ab13847
Anti-digoxigenin-AP	Sheep	1:2000	Rcohe	11093274910

Anti-digoxigenin-POD	Sheep	1:2000	Roche	11093274910
Anti-phosphorylated histone H3 (ser10)	Rabbit	1:500	Millipore Sigma	05817RI
HRP Goat Anti-Mouse	Goat	1:3000	Invitrogen	G21040
HRP Goat Anti-Rabbit	Goat	1:500	Millipore Sigma	112-348-MI
IRDye 680RD goat-anti-mouse IgG	Goat	1:10000	LI-COR	925-68070
IRDye 800RD goat-anti-rabbit IgG	Goat	1:2000	LI-COR	925-32211

Enzymes

Name	Source	Cat #
Not1-HF	New England Biolabs	R3189S
Polymerase(1U/uL)dnTPack	Roche	4738225001
Powerup SYBR Master Mix	ThermoFisher	D2425372
Proteinase K (20mg/mL)	Invitrogen	25530-049
Pst1	New England Biolabs	R0140S
RiboLock RNase Inhibitor	ThermoFisher	FEREO0382
RQ1 RNase-Free DNase	Promega	PR-M6101
T3 RNA Polymerase	New England Biolabs	M0378S
T4 DNA Ligase(1U/uL)	Invitrogen	15224017
T7 RNA Polymerase	ThermoFisher	FEREP0111
Verso cDNA synthesis kit	Thermo Scientific	AB1453A

Uncategorized Reagents

Name	Source	Cat #
10X Dig RNA Labeling Mix	Sigma-Aldrich	11277073910
10X Fluorescein RNA Labeling Mix	Sigma-Aldrich	11685619910
10X RIPA Buffer	Cell Signaling Technology	9806S
2.0mL Locking Lid Micro Centrifuge Tube	Fisher	14-666-315
20X SSC	Fisher	PRV4261
2-Mercaptoethanol	Fisher	034461-100

4-Iodophenylboronic acid (4-IPBA)	Sigma-Aldrich	471933-5G
6X Loading dye,Orange-G/ Blue	Bioworld	10570025-1 (700822)
96 well plates, round bottom	Fisher	07-200-704
Acrylamide,30%	GenDEPOT	50-101-5462
Agarose	Fisher	BP1356-100
Ammonium acetate	Fisher	A637-500
Ammonium Persulfate (APS)	BioRad	1610700
ApopTag Red In Situ Apoptosis Detection Kit	Millipore	S7165
Bacto typtone	Fisher	BD 211705
Bacto yeast extract	Fisher	BD 212750
BCIP/NBT	Sigma-Aldrich	B5655-25TAB
Boric Acid	Fisher	A73-1
Bovine Serum Albummin (BSA)	Sigma-Aldrich	A2153
Bradford Reagent	VWR	E530-1L
Bromophenol Blue Solution, 0.04%	Fisher	SI12-500
Carbenicillin	Fisher	BP2648-1
Casein	Sigma-Aldrich	B6429
Chloroform	Fisher	606-4
Chloroform (Approx. 0.75% Ethanol as Preservative/HPLC),	Fisher	C606-4
cOmplete mini tablet	Roche	4693159001
Deionized Formamide	Millipore	S4117
Dextran Sulfate	Sigma-Aldrich	D8906-100G
Dimethyl Sulfoxide (DMSO)	Millipore	MMX14577
DTT	Sigma-Aldrich	D5545-5G
Erioglaucine disodium salt dye	Sigma-Aldrich	861146-5G
Ethanol, 200 proof (EtOH)	Acros organics	AC61509-5000
Ethidium Bromide (1%)	Fisher	BP1302-10
Ethyl Alcohol Denatured	Fisher	A407-4
Ethylenediaminetetraacetic acid	Sigma-Aldrich	E9884-500G
exACTGene DNA Ladder 1kb plus	Fisher	BP2579-100
Ficoll 400	Sigma-Aldrich	F2637

Formaldehyde solution, 36%	Sigma-Aldrich	F8775-500ML
Formamide	Fisher	BP227-500
Glass Disruptor Beads(0.5mm)	Chemglass	CLS-1835-BG5
Glycerol	Acros organics	AC41098-5000
Glycine	VWR	97063-736
Halt Phosphatase Inhibitor Cocktail	ThermoFisher	1862495
Heparin	Sigma-Aldrich	H3393
High-Quality Ribonucleoside Triphosphates	Promega	P1221
Horse Serum	Fisher	SH3007403
Hydrochloric Acid (HCl)	Fisher	A144-500
Hydrogen Peroxide, 30% (H_2O_2)	Millipore	HX0635-3
Imidazole	Sigma-Aldrich	I5513-5G
Isopropanol	Fisher	A516-500
Isopropyl-β-D-thiogalactopyranoside (IPTG)	Fisher	BP1755-1
Kanamycin Sulfate	Fisher	BP906-5
LB Agar	Fisher	51343180
Lithium Chloride	Fisher	L121-500
Luminata Forte Western HRP Substrate, 100mL	MilliporeSigma	WBLUF0100
Magnesium Chloride, anhydrous ($MgCl_2$)	Sigma-Aldrich	M8266-100G
Maleic Acid	Sigma-Aldrich	M0375
Methanol (MeOH)	Fisher	A454-1
MicroAmp 96-Well Reaction plate, 0.1mL	ThermoFisher	43-469-07
MicroAmp Optical Adhesive Film Kit	ThermoFisher	43-136-63
N-Acetyl-L-(+)-cysteine (NAC)	Fisher	O1049-25
NEB2.1	New England Biolabs	B7202S
Nicotinamide	Acros Organics	128271000
Nonfat Dry Milk	Walmart	9278117
Nunc Biobanking and Cell Culture Cryogenic Tubes	Fisher	12-565-167N
PageRuler Protein Ladder	ThermoFisher	26616
Paraformaldehyde, 16%	Fisher	50-980-487
Pellet Pestle Cordless Motor	Fisher	12-141-361

Petri Dishes Specialty (Deep Dish)	Fisher	FB0875711
Phenol Chloroform	Fisher	BP17521-100
Phenylmethanesulfonyl Fluoride (PMSF)	Sigma-Aldrich	78830-1G
Polyvinyl Alcohol (PVA)	Sigma-Aldrich	P8136
Polyvinylpyrrolidone	Sigma-Aldrich	PVP40
Potassium Chloride	Sigma-Aldrich	P9541-500G
Potassium phosphate monobasic (KH_2PO_4)	Sigma-Aldrich	P5379
QIAprep Spin Miniprep Kit	Qiagen	27104
QIAquick Gel Extraction Kit	Qiagen	28704
Resveratrol	TCI America	R0071-1G
Rnase Free Disposable Pellet Pestles	Fisher	12-141-364
Round-Bottom Polypropylene Tubes	Falcon	14-959-11B
Sodium Azide (NaN_3)	Fisher	AC19038-0050
Sodium Chloride (NaCl)	Fisher	BP358-1
Sodium Dodecyl Sulfate (SDS) Powder	Sigma-Aldrich	L4390
Sodium Dodecyl Sulfate 20% (SDS)	Fisher	BP1311-200
Sodium Phosphate dibasic(Na_2HPO_4)	Sigma-Aldrich	S3264
Sterile 100mm x 15mm Polystrene Petri Dish	Fisher	FB0875712
Tergitol, NP40	Sigma-Aldrich	NP40S-100ML
Tetramethylenediamine (TEMED)	BioRad	1610800
Tris Base	Fisher	T393-500
Triton X-100	Sigma-Aldrich	T8787
TRIzol	Invitrogen	15596026
Tween-20	Fisher	BP337-500
Yeast RNA	Roche	10109223001

2.1.4. General Solutions and buffers

General solutions

0.05%PBSTx (1L)	10X PBS Triton-X 100 MilliQ Water	100mL 0.5mL 895mL
0.1%PBSTx (1L),pH 7.4	10X PBS Triton-X 100	100mL 1mL

	MilliQ Water	899mL
0.3%PBSTx (1L)	10X PBS Triton-X 100 MilliQ Water	100mL 3mL 897mL
10X PBS, pH 7.0 (1L)	NaCl KCl Na_2HPO_4 KH_2PO_4 MilliQ Water	80g 2g 14.4g 2.4g up to 1L
1X PBS (1L)	10X PBS MilliQ Water	100mL 900mL
2XYT Media,pH 7.0 (1L)	Bacto typtone Bacto yeast extract NaCl MilliQ Water	16g 27.5g 5g up to 1L
5X TBE(1L)	Tris Base Boric Acid EDTA (0.5M,pH 8)	54g 27.5g 20mL
Agar Plates (0.5L)	Bacto typtone Bacto yeast extract NaCl LB Agar MilliQ Water	5g 2.5g 5g 7.5g up to 0.5L
Gelvatol	PVA Gylcerol 0.2M Tris, pH8.5 10% Sodium Azide MilliQ Water	21g 42mL 106mL 10uL 52mL

NAC fixation solutions

4% Formalin (10mL)	Formaldehyde (36%) 0.3%PBSTx	1.1mL 8.9mL
5% NAC (10mL)	NAC 1X PBS	0.5g up to 10mL
Reduction Solution (10mL)	1M DTT Tergitol 20% SDS 10X PBS MilliQ Water	500uL 100uL 250uL 1mL up to 10mL

Formamide fixation solutions

5.7% HCl (10mL)	HCl	570uL

	MilliQ Water 10mL	up to
Formamide Fix (10mL)	Formamide H_2O_2 0.05% PBSTx	300uL 2mL up to 10mL

dsRNA solutions

Stop Solution(50mL)	10M ammonium acetate EDTA 0.2471 g 20% SDS MilliQ Water 10mL	5mL 0.5mL up to

Whole mount in situ hybridization (WISH) solutions

Proteinase K (10mL)	Proteinase K (20mg/mL) 20% SDS 10XPBS MilliQ Water 10mL	1uL 50uL 1mL up to
4% Formalin (10mL)	Formaldehyde (36%) 0.3%PBSTx	1.1mL 8.9mL
4% Paraformaldehyde (10mL)	Paraformaldehyde (16%) 0.3%PBSTx 10mL	2.5mL up to
50X Denhardts (1L)	Ficoll 400 Polyvinylpyrrolidone BSA MilliQ Water 1L	10g 10mL 10g up to
AP Buffer (20mL)	1M Tris pH9.5 1M $MgCl_2$ 5M NaCl MilliQ Water 20mL	2mL 1mL 400uL up to
AP Buffer(5% PVA) (10mL)	1M Tris pH9.5 1M $MgCl_2$ 5M NaCl 10% PVA MilliQ Water 10mL	1mL 0.5mL 200uL 5mL up to
MABT (1L),pH 7.5	Maleic Acid NaCl Tween-20	11.6g 8.76g 1mL

	MilliQ Water up to 1L
MABTB (10mL)	Heat Inactivated Horse Serum 1mL BSA 0.1g MABT up to 10mL
Pre Hybe (10mL)	Deionized Formamide 5mL 20X SSC 2.5mL 20% SDS 0.5mL 50X Denhardts 200uL Heparin(10mg/mL) 100uL 10% Triton-X 100 50uL 10% Tween-20 50uL 1M DTT 50uL Yeast RNA 10mg MilliQ Water up to 10mL
Ultra Hybe (10mL)	Deionized Formamide 5mL 20X SSC 2.5mL 20% SDS 0.5mL 50X Denhardts 200uL Heparin(10mg/mL) 100uL 10% Triton-X 100 50uL 10% Tween-20 50uL 1M DTT 50uL Yeast RNA 10mg 50% Dextran Sulfate 0.5mL MilliQ Water up to 10mL
Wash Hybe (50mL)	Deionized Formamide 25mL 20X SSC 12.5mL 50X Denhardts 1mL MilliQ Water up to 50mL

Fluorescent in situ hybridization (FISH) solutions

Proteinase K (10mL)	Proteinase K (20mg/mL) 1uL 20% SDS 50uL 0.1% PBSTx up to 10mL
4% Formalin (10mL)	Formaldehyde (36%) 1.1mL 0.1%PBSTx 8.9mL
Blocking Solution (10mL)	10X Casein 0.5mL Heat Inactivated Horse Serum 0.5mL

	0.1%PBSTx 10mL	up to
FITC Tyramide solution (10mL)	Tyramide Buffer 4IPBA 30% H_2O_2 FITC	10mL 10uL 1uL 10uL
Hybe (50mL)	Deionized Formamide 20X SSC 20% Tween-20 Yeast RNA 50% Dextran Sulfate MilliQ Water 50mL	25mL 12.5mL 2.5mL 50mg 5mL up to
Pre Hybe (50mL)	Deionized Formamide 20X SSC 20% Tween-20 Yeast RNA MilliQ Water 50mL	25mL 12.5mL 2.5mL 50mg up to
Tyramide Buffer (500mL), pH8.5	NaCl Boric Acid MilliQ Water 500mL	58.44g 3.09g up to

Bleaching solutions

FISH (10mL)	20X SSC Formamide 30% H_2O_2 MilliQ Water 10mL	250uL 0.5mL 400uL up to
Immunohistochemistry (10mL)	30% H_2O_2 0.05%PBSTx	2mL 8mL
TUNEL (10mL)	30% H_2O_2 1XPBS	2mL 8mL
WISH (10mL)	30% H_2O_2 100% MeOH	2mL 8mL

IHC solutions

FITC PBSTI (5mL)	FITC PBSTI 5mL	5uL up to
PBSTI (50mL)	1M Imidazole 0.05% PBSTx 50mL	500uL up to

PBSTxB (50mL)	BSA 0.05% PBSTx 50mL	0.25g up to

Protein extraction solutions

1X RIPA Buffer (1mL)	MilliQ Water 10X RIPA Buffer 1mM DTT Protease Inhibitor cocktail 100mM PMSF Phosphatase Inhibitor	720uL 100uL 10uL 150uL 10uL 10uL
6X Laemmli Buffer, pH 6.8 (25mL)	Tris base SDS Glycerol 2-Mercaptoethanol Bromophenol blue MilliQ Water 25mL	1.47g 1.5g 1.2mL 2.25mL 7.5mg up to
Protease Inhibitor cocktail (1.5mL)	cOmplete mini tablet MilliQ Water	1 1.5mL

Acrylamide gels/western blot solutions

10X Running Buffer (1L)	Tris Base Glycine 20% SDS MilliQ Water 1L	30.3g 144g 50mL up to
10X Transfer Buffer (1L)	Tris Base Glycine MilliQ Water 1L	30.3g 144g up to
1X Running Buffer (1L)	10X Running Buffer MilliQ Water	100mL 900mL
1X Transfer Buffer (1L)	10X Running Buffer MeOH MilliQ Water	100mL 100mL 800mL
Blocking for 1° Antibodies (10mL)	BSA TBS-T 10mL	0.5g up to
Blocking for 2° Antibodies (10mL)	Nonfat Dry Milk TBS-T/SDS 10mL	0.5g up to
TBS-T (1L)	1M Tris, pH7.4 5M NaCl Tween-20	50mL 30mL 1mL

	MilliQ Water 1L	up to
TBS-T/SDS (1L)	1M Tris, pH7.4 5M NaCl Tween-20 20% SDS 0.5mL MilliQ Water 1L	50mL 30mL 2mL up to

TUNEL solutions

10% NAC (10mL)	NAC 1X PBS 10mL	1g up to
1X PBS/SDS (10mL) 1% SDS	20% SDS 0.5mL 1X PBS 9.5mL	
4% Formalin (10mL)	Formaldehyde (36%) 1.1mL 0.3%PBSTx 8.9mL	
Rhodamine Antibody Solution (130uL) 53% Blocking solution, 47% Anti-Digoxigenin	Blocking Solution Anti-Digoxigenin	68uL 62uL
Stop Solution (250uL) 2.86% Stop Buffer, 97.14% Water	Stop Buffer 7.14uL MilliQ Water 242.86uL	
TUNEL Mix (TdT Enzyme) (110uL) 70% Reaction Buffer, 30% TdT Enzyme	Reaction Buffer TdT Enzyme	77uL 33uL

Feeding dye assay solutions

Erioglaucine dye liver 0.2% Erioglaucine disodium salt dye	Erioglaucine dye 10uL Liver paste 500uL	

2.2. Methods

2.2.1. Planarian husbandry

All planarians were maintained in colonies with 1x Montjuic salts. Animals were fed once a week with a diet consisting of beef liver paste. Experiments required that animals were starved for at least one week unless otherwise noted.

2.2.2. Identification of homologs and phylogenetic analysis

Sirtuins were identified by blasting human Sirtuin protein sequences into available genomic resources for Schmidtea mediterranea and Dugesia japonica[222,225]. Identified sequences went through a six-frame translation using the Pfam protein domain database (http://pfam.xfam.org/) and domain conservation was confirmed using both UNIPROT (https://www.uniprot.org) and PROSITE(https://prosite.expasy.org/) . The sequences were further validated by blastn and blastp in NCBI (http://blast.ncbi.nlm.nih.gov/Blast.cgi) . The confirmed sequences were aligned by CLUSTALW using sequences obtained using HomoloGene (www.ncbi.nlm.nih.gov/homologene). Presentation of protein alignment was done using SeaView software (http://doua.prabi.fr/software/seaview). Color scheme for amino acids denotes categories (Blue=hydrophobic, Red= Positive charge, Magenta= Negative charge, Green= Polar, Pink= Cysteines, Orange= Glycines, Yellow= Prolines, Cyan= Aromatic, White= unconserved). A predictive phylogenetic tree was built using MEGA7 software(www.megasoftware.net).

2.2.3. Single-cell sequencing data

Sirtuin gene expression analysis was obtained via the planaria single-cell database curtesy of the Reddien Lab at the Whitehead Institute for Biomedical Research (https://radiant.wi.mit.edu/app/)[226] and https://digiworm.wi.mit.edu/[227].

2.2.4. RNAi Experiments

The synthesis of dsRNA was performed as previously described[259]. Microinjections were performed following the schedules (Figures 4A, C, E, 6A).

2.2.5. Behavioral feeding assay

A custom-made dish containing 10 lanes approximately 1Cm by 10 Cm were filled half way with planarian water. In the middle of each lane two drops of liver paste, 10μL each was placed. Video recording began prior to the addition of animals. Individual animals were placed into each end of the lane for all lanes, 2 animals total per lane. Lanes 1-5 contained the control group and lanes 6-10 contained the experimental group. Animals were fed for 1 hour and then removed from lanes. The amount of time to begin feeding was quantified as the time in seconds, which the animal extended their pharynx

out onto liver and ingesting it from the time the animal was placed into the lane.

2.2.6. Feeding dye assay

Surface Area measurements were taken for all animals prior feeding. Animals were fed liver paste containing 0.2% Erioglaucine disodium salt dye overnight. Prior to homogenization, dishes containing animals were cleaned and animals were placed into 2mL centrifuge tubes with 1.5mL of 1X PBS and a small amount of glass beads. Samples were homogenized using a Bead Ruptor homogenizer for 30 seconds. Samples were centrifuged at 20,817 g for 1 minute. 1mL of supernatant was used to measure activity at a 620nm absorbance. Food consumption was measured by taking the absorbance reading for the sample and dividing it by the surface area (mm^2) of the individual animals in each group. These values were normalized and measured in fold change between groups.

2.2.7. Liver stimulation assay

Homogenized liver paste (50uL) was added to 50mL of planarian water and repeatedly vortexed. The water settled for 10 minutes at room temperature. Using a serological pipette, 40mL of the 0.1% liver water was taken, avoiding anything that sank to the bottom of the tube and was transferred to clean dishes. Animals that underwent stimulation were carefully transferred to these dishes containing 0.1% liver water for 30 mins. Non-stimulated, control animals were transferred to clean dishes containing 40mL of planarian water. Following this incubation period, animals were removed, and placed into TRIzol for RNA Extractions.

2.2.8. Whole mount immunofluorescence

Animals were killed in 5.7% 12N HCl solution for 10 minutes on ice. Animals were washed twice with 0.05% PBSTx on ice and then fixed in 3% formamide, 6% H_2O_2 in 0.05% PBSTx for 30 minutes at room temperature. Fixation was removed and worms were bleached overnight in solution containing 6% H_2O_2 in 0.05% PBSTx. Primary antibody, anti-H3P was used at 1:500. Secondary antibody HRP-conjugated Goat anti-rabbit was used at 1:1000. Neoblasts were counted and normalized to the area (mm^2) using ImageJ.

2.2.9. Quantitative real-time PCR

Quantitative real-time PCR (qPCR) was performed as previously described [238,260]. TATA box binding protein domain were used as an internal control. Each individual experiment consisted of triplicates per condition and experiments were independently repeated twice. RNA was extracted from intact animals (≥20 per condition) and converted to cDNA using the Verso

cDNA synthesis kit. Gene expression was shown as fold change in comparison to the control group.

2.2.10. Whole mount *in situ* hybridization

Riboprobes for *in situ* hybridization were synthesized using T3 or T7 polymerases and digoxigenin labeled ribonucleotide mix using specific PCR templates as previously described [246]. WISH and FISH was performed as previously described [247].

2.2.11. Protein extraction

Animals were placed into 2mL centrifuge tubes with 250μL of 1X RIPA Buffer and a small amount of glass beads. 1X RIPA buffer contained protease inhibitors: Complete Mini Protease Inhibitor Cocktail, 1mM PMSF;1mM DTT. Samples were homogenized using a Bead Ruptor homogenizer for 20 seconds. Samples were incubated on ice for 30 minutes and then centrifuged at 20,817 g for 20 minutes at 4°C. The supernatant was transferred to a new tube and placed on ice. A 10μL aliquot of the supernatant was set aside to measure protein concentration using a Bradford protein assay. The remaining supernatant was mixed with equal volumes of 2X Laemmli buffer (4%SDS, 10%-mercaptoethanol, 20% glycerol, 0.004% bromophenol blue, 0.125M Tris-HCl) and incubated at 94°C for 10 minutes to denature and reduce. Protein lysates were stored at -20°C.

2.2.12. Western blot

Protein lysate aliquots of 20μg were heated at 94°C for 5 minutes and loaded into a 15% SDS-PAGE gel along with a molecular weight marker. Samples were transferred to a 1 minute methanol-activated PVDF membrane overnight at 30V in 1X Tris-glycine transfer buffer [25mM Tris base, 192mM glycine,20%(v/v) methanol] at 4°C. The membrane was blocked with 5% BSA for 2 hours and incubated in the primary antibodies overnight at 4°C on a rocker. Primary antibodies: anti-beta-tubulin E7 (1:10000), anti-caspase (1:500). The membrane was washed four times for 20 minutes prior to the addition of the secondary antibodies: IRDye 800RD goat-anti-rabbit IgG antibody (1:2000) for anti-caspase, IRDye 680RD goat-anti-mouse IgG antibody (1:10000) for anti-beta-tubulin E7. Blots were imaged using a Li-COR 9120 Odyssey Infrared Imaging System. Band quantification was performed by taking band intensities and computing the area under the curve, using ImageJ. Cleaved Caspase activity was normalized to beta-tubulin.

2.2.13. TUNEL

Tunnel assay was performed as previously described [187].

2.2.14. Pharmacological treatment

All pharmacological treatments were performed via animal soaking. Drugs were diluted into 50mL of planarian water and administered every other day for the length of the experiment. All NAM experiments were performed at a 100uM concentration with the control group receiving planarian water alone, unless otherwise noted. All RESV experiments were performed at a 20uM concentration with the control group receiving planarian water containing 0.04% dimethyl sulfoxide (DMSO), unless otherwise noted. All animals were soaked in drugs 5 days prior to assays, unless otherwise noted.

2.2.15. Growth and degrowth experiments

Intact animals were used for all growth and degrowth experiments. During growth experiments, animals approximately 2mm in length were fed liver paste once a week, as noted by feeding schedules (Figures 4E,5E,6A). Animals were approximately 8mm in length for all degrowth experiments and were starved for the entirety of the time course. Live images were taken either every 5 days for RNAi experiments or every week for drug soaking experiments. Changes in the size of the animals were normalized to the initial day imaged, and represented as fold change.

2.2.16. Imaging and data processing

All live images were taken using a Nikon AZ-100 multizoom microscope and NIS Elements AR 3.2 software. Surface area measurements were calculated using ImageJ and the difference in animal size was determined as fold change in reference to control group at each time point. Band quantification was performed by using band intensities and computing the area under the curve, using ImageJ. Cleaved caspase activity was normalized to beta-tubulin. Neoblasts were counted and normalized by area size (mm^2) using ImageJ.

2.2.17. Statistical analysis

One-way ANOVA, Two-way ANOVA, or T-test statistics were performed and data is shown as the mean ± standard error of the mean (SEM) or fold change ± SEM, as noted in each figure. All statistics were performed by pooling samples together for analysis. One-way ANOVA were performed using multiple comparisons to compare the mean of each column with the mean of a control column. Two-way ANOVA were performed within each row with compared columns (simple effects within rows), and compared each cell mean with the control cell mean on that row. One-way ANOVA and Two-way ANOVA's did not use matching or pairing data in rows, data was assumed as Gaussian distribution, and a Dunnett's test was used to correct for multiple comparisons. Statistical analysis was performed using Prism7, Graphpad software Inc. (http://www.graphpad.com).

3. Results

3.1. Sirtuin-1 is evolutionarily conserved and ubiquitously expressed in the planarian *Schmidtea mediterranea*

Sirtuins are a group of NAD+ regulated deacetylase enzymes that are highly conserved from yeast to humans[91,261]. In the genome of *Schmidtea mediterranea* [228], we identified six out of seven mammalian Sirtuin homologs, *Smed-Sirt-1-6*. *Smed-Sirt-1* showed the highest molecular similarity to its human counterpart, with a 60% identity in the SIRTUIN domain (Figure 2A). Sirtuin-1 is also evolutionarily conserved across species, with the planarian *Schmidtea mediterranea* Sirtuin-1 being most closely related to *Caenorhabditis elegans* and *Saccharomyces cerevisiae* (Figure 2B).

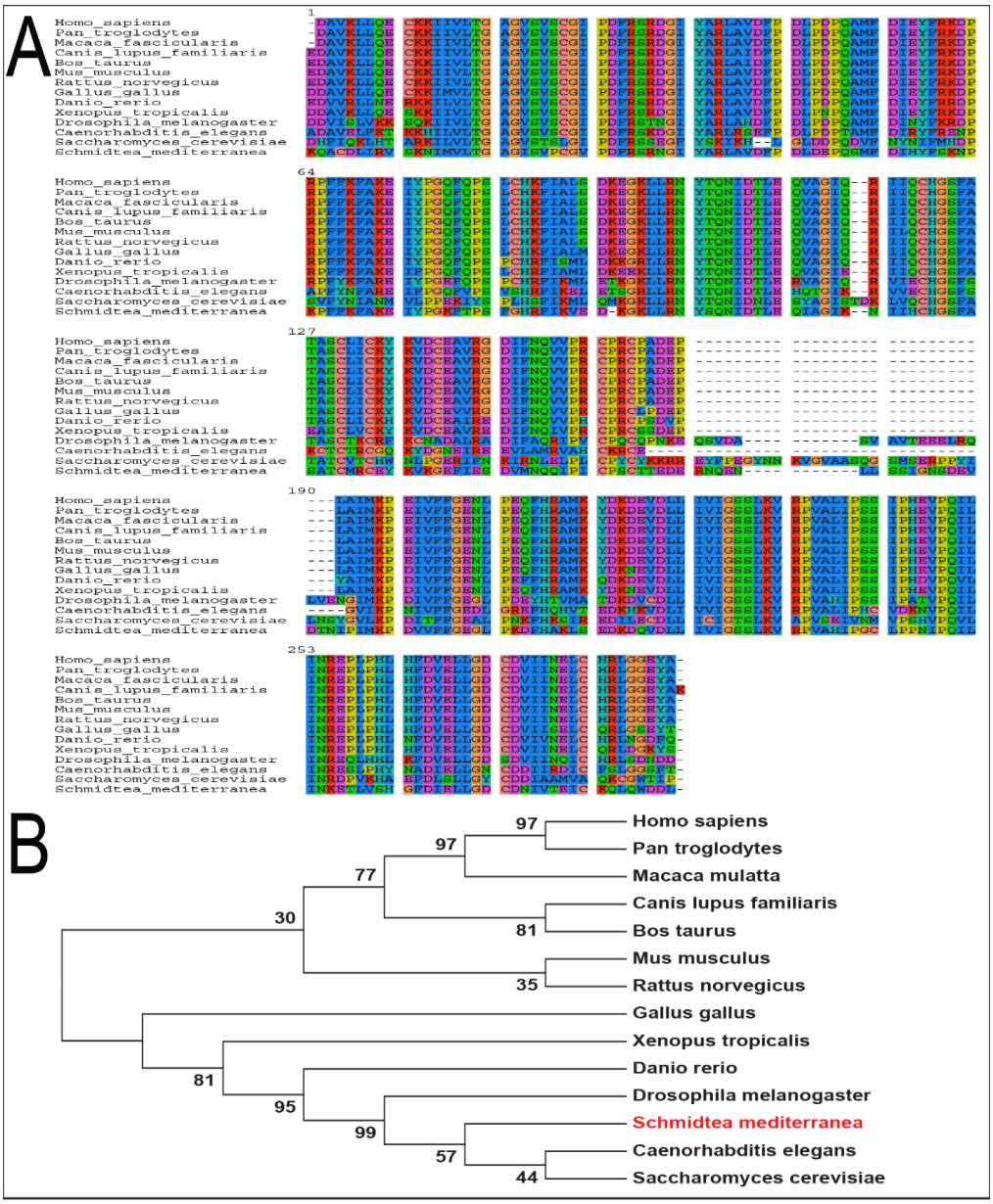

Figure 2. Sirtuin-1 is highly conserved in the planarian *Schmidtea mediterranea*. A) Protein alignment of planarian Sirtuin-1 and other various species. Human and planarian Sirtuin-1 protein sequences are 60% identical. Colors of amino acids represent the group to which they belong (see methods 2.2.2 for more information). **B)** Phylogenetic tree of Sirtuin-1 across various phyla. Numbers represent branch support through bootstrap replications.

The spatial expression of *Smed-Sirt-1* was determined by WISH. The signal appears ubiquitously expressed, but it is enriched in the prepharyngeal area (Figure 3A). This finding was validated *in silico* by analyzing the expression of *Smed-Sirt-1* along the planarian anteroposterior (AP) axis[228,262] (Figure 3B). We also extended the analysis at the single cell resolution[227] and confirmed *Smed-Sirt-1* expression is scattered among different cell types and not restricted to specific clusters (Figure 3C). Altogether, our results reveal *Smed-Sirt-1* is evolutionarily conserved in planarians and its expression pattern is broadly detected across the planarian body.

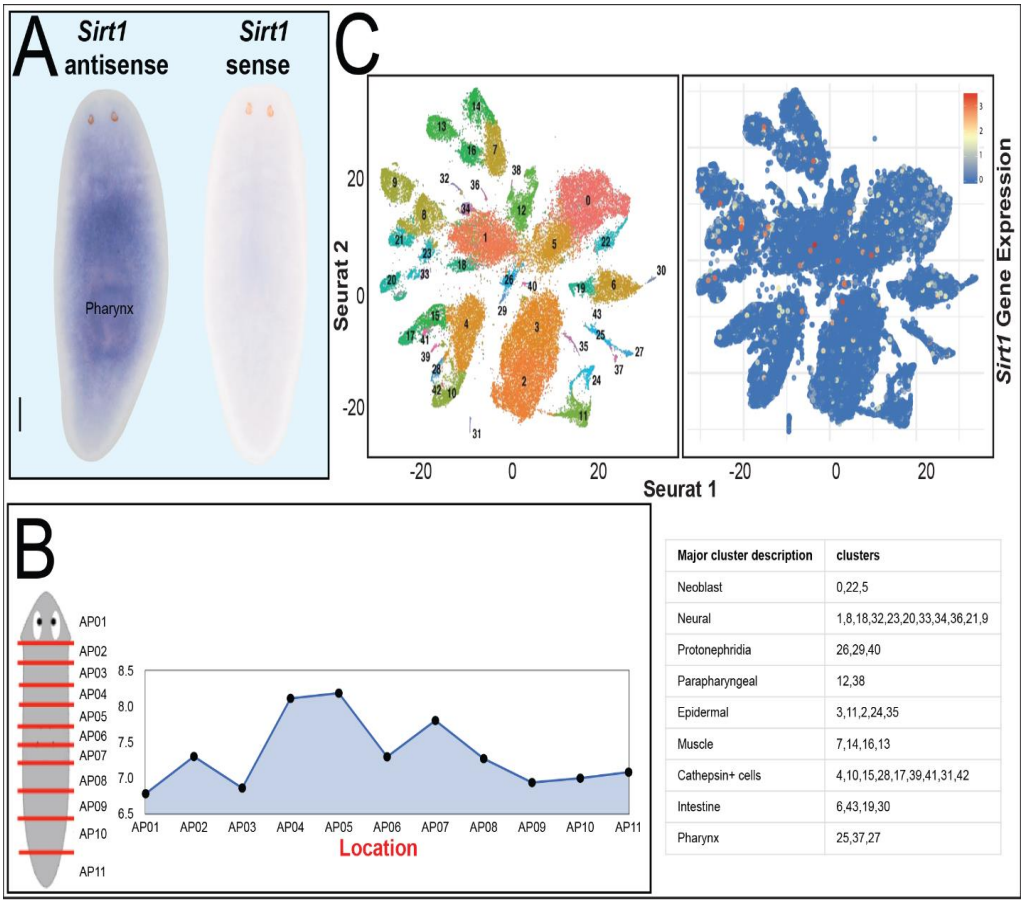

Figure 3. *Smed-Sirt-1* is ubiquitously expressed along the planarian anteroposterior (AP) axis. **A)** Whole mount in situ hybridization using both sense and antisense probes against *Smed-Sirt-1*. Gene expression is diffused throughout the body, but it is enriched in the pre-pharyngeal area. **B)** Predicted gene expression pattern distributed along the AP axis from single cell RNA sequencing analysis, obtained from PlanMine (http://planmine.mpicbg.de/planmine/begin.do) [228,262]. Changes in gene expression is represented by the Y axis. **C)** t-SNE plot of single cells displaying *Smed-*

Sirt-1 expression among major clusters of neoblasts and differentiated cells. Gene expression levels are based on the scale bar top right (red is high, and blue is low). The single cell gene expression was obtained from the cell type transcriptome atlas database, provided by the Reddien Lab at the Whitehead Institute for Biomedical Research (https://digiworm.wi.mit.edu/)[227].

3.2. Sirtuin-1 is required for organismal growth in the planarian *Schmidtea mediterranea*

To functionally characterize the role of Sirtuins in planarians, we performed individual RNAi of *Smed-Sirt-1-6.* We developed an RNAi strategy based on multiple microinjections with dsRNA over ten days, and animals were fixed 15 days after the first injection (Figure 4A). We confirmed the protocol was effective in knocking down the gene expression for two weeks without noticeable abnormalities (Figure 4B).

Sirtuin function is linked to regulation of metabolism; therefore, we analyzed how nutrient availability impacted animal size over time. First, we prolonged the RNAi protocol for three weeks in the absence of nutrients and evaluated the effects in the reduction of animal size (Figure 4C). These experiments indicated that disturbing *Smed-Sirt-1-6* function did not alter surface area relative to control starved animals, indicating that each gene alone does not play an important role in the reduction in size “degrowth” (Figure 4D). Second, animals subjected to RNAi were exposed to nutrients and their growth was evaluated for almost two months. This protocol alternates six feedings with RNAi for each individual *Smed-Sirt-1-6* and was effective in keeping the expression down for about two months (Figure 4E, F). The analysis shows that control and *Smed-Sirt-2-6(RNAi)* animals increased in size at a similar rate, whereas animals subjected to *Smed-Sirt-1(RNAi)* displayed a 30% reduction in growth (Figure 4G, H). Based on these observations, we concluded that *Smed-Sirt-1* is required for animal growth when nutrients are available. Therefore, we focused our attention on *Smed-Sirt-1*.

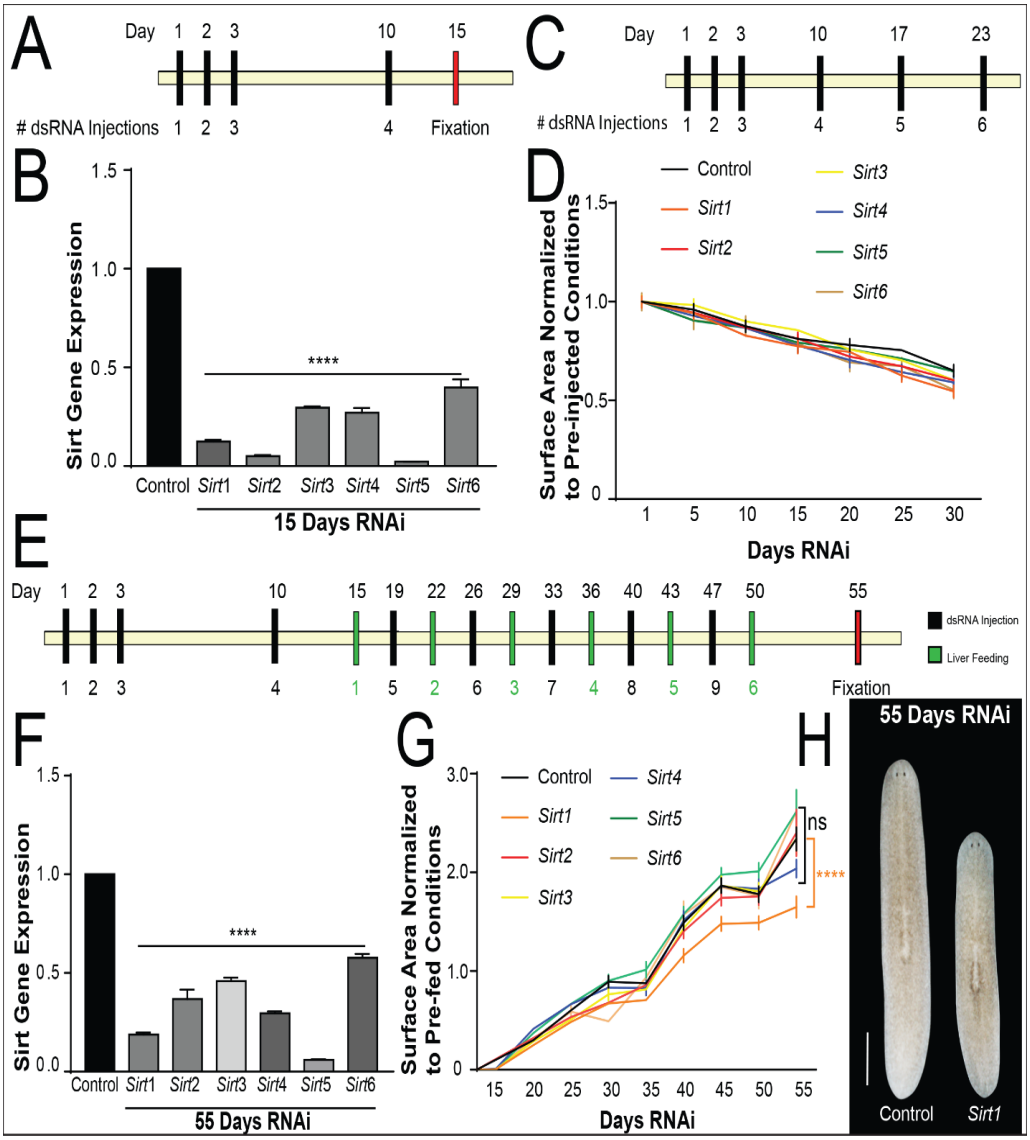

Figure 4. *Smed-Sirt-1* regulates planarian growth. **A)** RNAi schedule based on micro injections with dsRNA to perform knockdown of *Smed-Sirt-1-6*. All control animals were injected with water. Black bars represent injections and the red bar represents fixation. **B)** Gene expression levels of *Smed-Sirt-1-6*, in *Smed-Sirt-1-6* (*RNAi*) animals 15 days after the 1stinjection. Gene expression is represented in fold change normalized to control. Data was obtained with an N=20 from at least 2 individual experiments; ****p< 0.0001; one-way ANOVA. **C)** RNAi schedule of individual Sirtuins for animals subjected to one month of starvation. Black bars represent injections with *Smed-Sirt-1-6* dsRNA. **D)** Changes in surface area (fold change) over the RNAi degrowth schedule, normalized to pre-injected conditions. Data was obtained with an N=20 from at least 2 individual experiments; two-way ANOVA. **E)** RNAi growth schedule, which combines micro injections with *Smed-Sirt-1-6* dsRNA (black bars) alternated with liver feeding (green bars). The red bar represents fixation. **F)** Gene expression levels of *Smed-Sirt-1-6*, in Sirtuin RNAi animals 55 days after the 1st injection. Data was obtained with an N=20 from at least 2 individual experiments; ****p< 0.0001; one-way ANOVA **G)** Changes in surface area over the RNAi growth schedule. Changes in the surface area are represented as fold change, normalized to pre-fed conditions at 15 days post first injection. Data was obtained with at least an N=30 from at least 3 individual experiments; **p<0.01;

***p<0.001; ****p<0.0001; two-way ANOVA. **H)** Representative images of control and *Smed-Sirt-1(RNAi)* animals 55 days after the 1st injection. Scale bar = 1mm.

3.3. Sirtuin-1 can be regulated through pharmacological administration

The activity of Sirtuin proteins can be modulated by treatment with pharmacological compounds[100,103,107,109,110,161]. Specifically, planarians were treated with RESV a known Sirtuin-1 enhancing compound, or NAM a Sirtuin inhibitor. First, we determined the concentration in which RESV, and NAM did not lead to any macroscopic or behavioral defects. This was achieved by diluting RESV in DMSO and NAM directly in the water where planarians live. Concentrations that were shown to be sub-lethal with the first few days did not lead to death beyond the time course (Figure 5A, B). Following this strategy, we determined that treating animals with concentrations greater than 20uM RESV occasionally lead to anterior tissue loss known as head regression (Figure 5C). Treatment with NAM with concentrations above 100uM affected planarian locomotion manifested by inching movements and lack of motility. Therefore, we chose to treat planarians with RESV (20uM) and NAM (100uM) as these concentrations do not produce evident toxicity.

Next, we evaluated the response to degrowth and growth in animals exposed to treatment with RESV and NAM. Under these protocols, drugs were replaced every other day over the length of the entire experiment. In the absence of nutrients, RESV and NAM treatment did not affect planarian "degrowth" (Figure 5D). The growth protocol allowed animals to be fed once a week starting five days after the first drug exposure (Figure 5E). These experiments revealed that worms treated with RESV grew 37% more than the respective control (DMSO treated). Conversely, planarians exposed to NAM displayed about 40% reduced growth (Figure 5F, G). These results demonstrate that it is possible to pharmacologically modulate planarian growth in the presence of nutrients by targeting Sirtuin1 signaling. Importantly, neither RESV or NAM appear to regulate changes in body size in the absence of nutrients, consistent with the results obtained after *Smed-Sirt-1(RNAi)*.

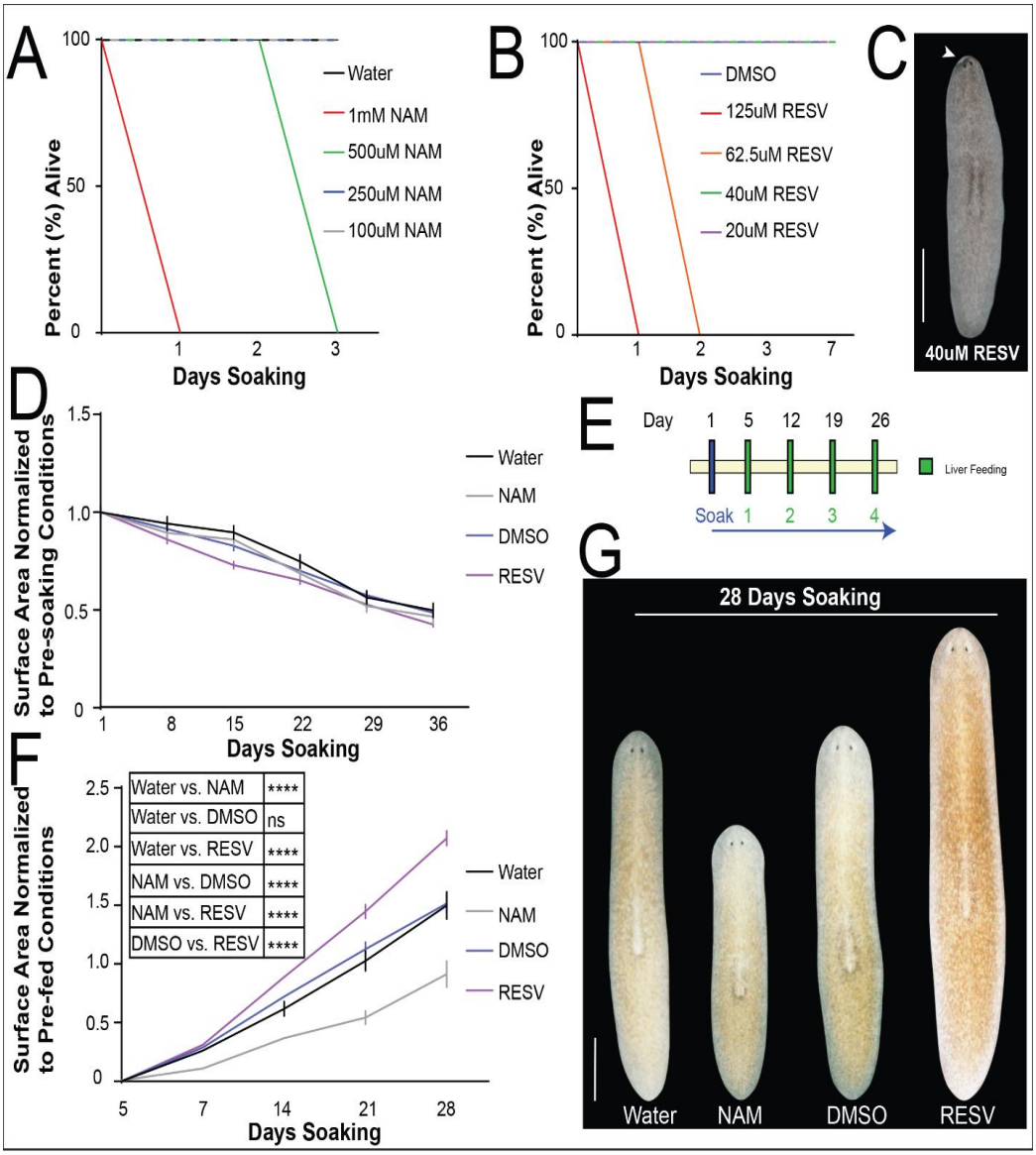

Figure 5. Pharmacological regulation of Sirtuin-1 signaling. A, B) Survival graphs of various concentrations of inhibitor, NAM (**A)** and enhancer, RESV (**B**). Data was obtained using 5 animals per concentration. **C)** Representation of toxic effects seen in 40uM RESV soaked animal. Location of head regression is indicated with white arrow. Scale bar =1mm. **D)** Changes in surface area over the pharmacological degrowth schedule. Drugs were replenished every other day into their water. Changes in the surface area is represented as fold change, normalized to pre-soaked conditions. Data was obtained with an N=20 from 2 individual experiments; two-way ANOVA. **E)** Schematic representation of feeding and treatment with pharmacological compounds. Animals were soaked with either inhibitor, NAM (100μM), or enhancer, RESV (20μM). Drugs were replenished every other day and animals were fed once a week. Blue bar represents the initial soaking and green bars represent feedings with liver paste. **F)** Changes in surface area over the pharmacological growth schedule. Changes in the surface area is represented as fold change, normalized to pre-fed conditions, 5 days after the first soaking. Data was obtained with at least an N=30 from at least 3 individual experiments; ****p<0.0001; two-way ANOVA. Displayed statistics was provided for only 28 days post

1st soaking (right). **G)** Representative images of control (Water and DMSO), NAM, and RESV treated animals 28 days after the 1st soaking. Scale bar = 1mm.

We devised a protocol combining treatments with *Smed-Sirt-1(RNAi)* in the presence of nutrients (Figure 6A). We found that NAM treated animals in combination with *Smed-Sirt-1(RNAi)* also led to a similar size reduction as seen with NAM treatment alone (Figure 6B). These results suggested that either method to impair *Smed-Sirt-1* function proved effective, as NAM soaked animals showed similar growth pattern observed in *Smed-Sirt-1(RNAi)* animals. However, NAD is required for various cellular functions and is not limited to being just a cofactor for Sirtuins[106]. Therefore, it is not surprising that using NAM treatment, a more serve effect is seen than *Smed-Sirt-1(RNAi)* alone.

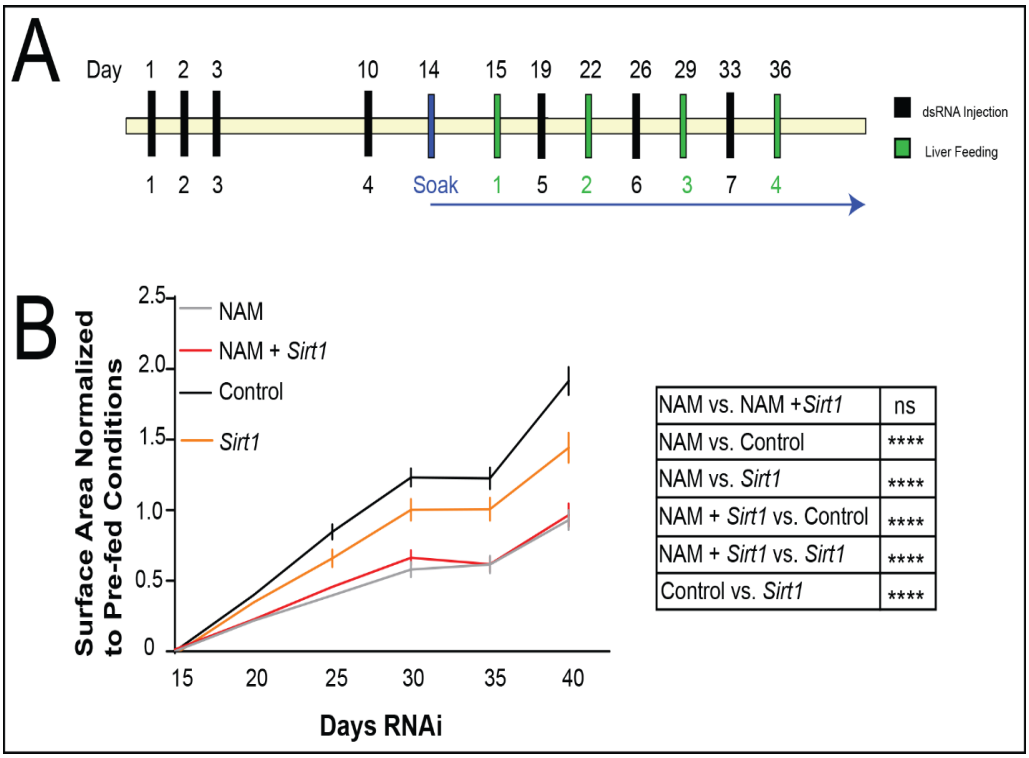

Figure 6. NAM, a Sirtuin inhibitor resembles *Smed-Sirt-1 RNAi*. A) Pharmacological RNAi growth schedule. Animals were injected with dsRNA and then introduced to NAM 24 hours prior to the first feeding. Drugs were replenished every other day into their water and animals were fed/injected once a week. Black bars represent injections, blue bar represents the initial soaking, and green bars represent feedings. **B)** Changes in surface area over the pharmacological RNAi growth schedule. Changes in the surface area is represented as fold change, normalized to pre-fed conditions, 15 days after the first injection. Data was obtained with at least an N=25 from 3 individual experiments; ****p<0.0001; two-way ANOVA. Statistics shown for surface area at 40 days post 1st soaking.

3.4. Resveratrol is a Sirtuin-1 enhancer in the planarian *Schmidtea mediterranea*

To assess whether RESV requires *Smed-Sirt-1* for its effects in growth in the presence of nutrients, we simultaneously treated animals with RESV and inhibited *Smed-Sirt-1* function with either RNAi or NAM. We found that RESV treatment did not lead to increased growth when *Smed-Sirt-1* was downregulated (Figure 7A). Furthermore, inhibiting *Smed-Sirt-1* function with NAM demonstrated that RESV failed to enhance growth (Figure 7B). Our findings suggest that RESV induced animal growth proceeds through *Smed-Sirt-1* enhancement.

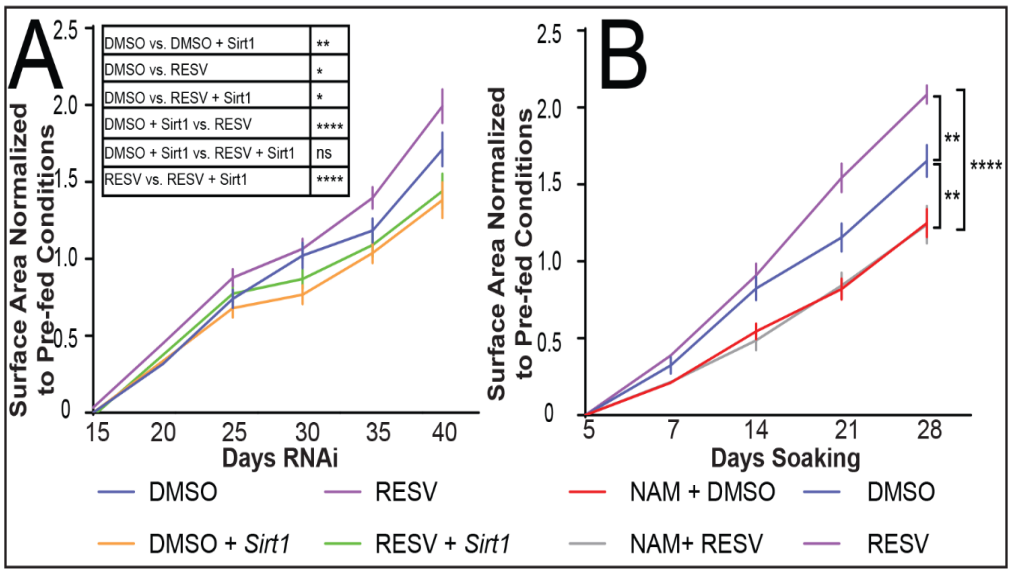

Figure 7. RESV, an enhancer of sirtuin-1, is *Smed-Sirt-1* specific. **A)** Changes in surface area over the pharmacological RNAi growth schedule (Figure 6A) using RESV and *Smed-Sirt-1(RNAi)*. Changes in the surface area is represented as fold change, normalized to pre-fed conditions, 15 days after the first injection. Data was obtained with at least an N=25 from 3 individual experiments; *p<0.05; **p<0.01; ****p<0.0001; two-way ANOVA. Displayed statistics was provided for 40 days post 1st soaking. **B)** Changes in surface area over the dual pharmacological treatment integrated with growth schedule. Changes in the surface area is represented as fold change, normalized to pre-fed conditions, 5 days after the first soaking. Data was obtained with an N=20 from 2 individual experiments; **p<0.01; ****p<0.0001; two-way ANOVA. Displayed statistics was provided for only 28 days post 1st soaking

3.5. Sirtuin-1 regulates feeding behavior in the planarian *Schmidtea mediterranea*

To address potential mechanisms involved in *Smed-Sirt-1* regulation of animal size, we evaluated feeding behavior. Specifically, we implemented an experimental strategy that allowed us to consider the time it takes to begin feeding and the overall food consumption. First, we designed a chamber to individually track the time each worm spent to find food and begin feeding as evidenced by protrusion of the pharynx and continuous contact with the food source. This setup was effective in tracking up to 20 worms in each individual experiment (Figure 8A). Briefly, animals were placed at similar distance from

the source of food and time it took to locate food and begin feeding was visually recorded. Animals subjected to *Smed-Sirt-1* inhibition by either RNAi or treatment with NAM took 50% longer to locate food and begin feeding (Figure 8B, C). Conversely, RESV treated animals were 37% faster to begin feeding (Figure 8D). These results demonstrate that inhibition and enhancement of *Smed-Sirt-1* signaling affects the timing to begin feeding in planarians.

Since the time it takes to locate food does not necessarily imply the amount of food ingested, we implemented an additional assay to estimate food consumption. We mixed a known amount of planarian food (liver paste) with a non-toxic dye commonly used in Drosophila behavioral experiments (0.2% Erioglaucine disodium salt)[263,264]. The mix was offered overnight, animals were then homogenized and the absorbance readings in a spectrophotometer were used to determine the relative amounts of food being consumed (Figure 8E). Because differences in planarian size may be a reflection of the amount of food ingested, we built a standard curve considering the size of the animal. As expected, we found that the food consumption was proportional to the animal size (Figure 8F, G). Using this assay, we identified that *Smed-Sirt-1(RNAi)* and NAM treated animals consumed less food than control animals (12% and 35%, respectively) (Figure 8H, I). On the other hand, RESV soaked animals consumed about 16% more food than the DMSO treated control group (Figure 8J). Altogether, our findings suggest *Smed-Sirt-1* signaling influences feeding behavior in planarians (i.e. time to begin feeding and the amount of food intake).

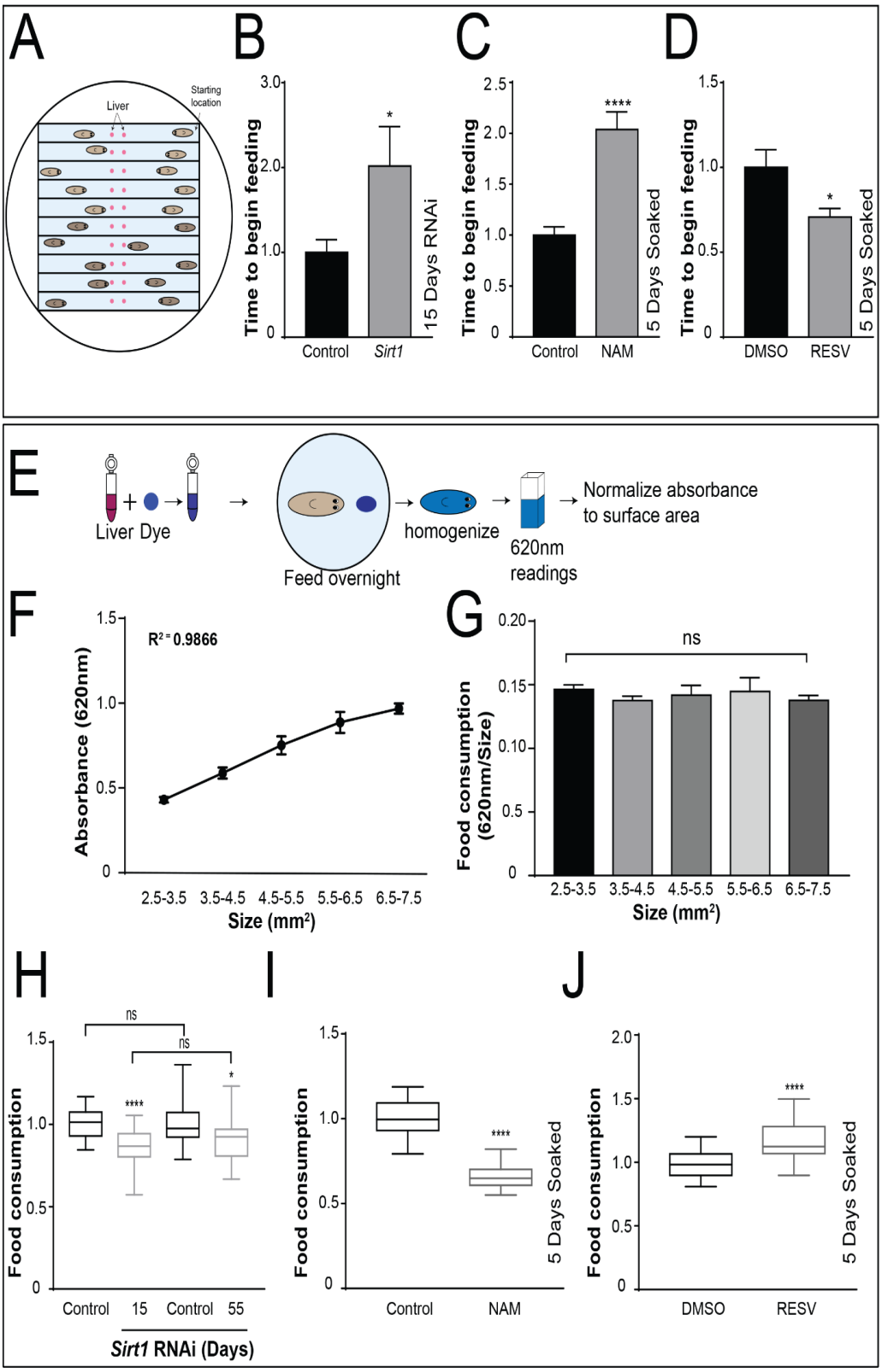

Figure 8. *Smed-Sirt-1* signaling influences feeding behavior. A) Schematic representation of feeding assay. Briefly, individual channels were made with plastic resin (total of 10) in a petri dish and small amounts of liver (pink dots) were placed in the

middle of each channel. Animals were placed at the end of the lane and video recording captured the amount of time to reach food and begin feeding. **B-D)** The total length of time to reach food and begin feeding is represented as fold change. *Smed-Sirt-1(RNAi)* animals used in this assay were 15 days post 1stinjection (**B)**. Pharmacologically soaked animals used were 5 days after the 1st soaking (**C**, **D**). Data was obtained with at least an N=25 from 3 individual experiments; *p<0.05; ****p<0.0001; Unpaired t test. **E)** Schematic representation of dye feeding assay. A small quantity of dye was added to liver which was fed to animals. Animals were homogenized and absorbance readings at 620nm were measured and normalized to the pre-fed surface area of the animals. **F, G)** Standard curve using animals of various sizes (mm^2) and the respective absorbance after feeding dyed food. Data was obtained with an N=30 from 3 individual experiments. **H)** Changes in food consumption among *Smed-Sirt-1(RNAi)* animals. Food consumption was measured at 15 days (left) or 55 days after the 1stinjection. Data was obtained with at least an N=30 from at least 3 individual experiments; *p<0.05; ****p<0.0001; one-way ANOVA. **I, J)** Changes in food consumption among pharmacologically soaked animals. Animals were soaked with either NAM or RESV for 5 days prior to feeding. Data was obtained with at least an N=25 from 3 individual experiments; ****p<0.0001; Unpaired t test.

3.6. Sirtuin-1 regulates genes that are upregulated in response to liver stimulation

To gain insights about the underlying molecular mechanisms affected by *Smed-Sirt-1* signaling in planarians, we performed a gene expression analysis of markers commonly associated with neural signaling and feeding behavior[16,217,236,265]. Planarians are able to sense food through chemosensory signal mediated by the nervous system. Thus, we explored possible mechanisms underlying the chemosensory response associated with the *Smed-Sirt-1* signaling in planarians. This prompted us to devise an assay in which planarians can sense food without physically ingesting it to avoid intestinal distention that is known to activate metabolic pathways. The assay was intended to stimulate chemosensory response by placing planarians in water containing highly diluted liver (0.1%) for 30 minutes. This was considered the stimulated group, and as a control, we used a similar condition without liver (baseline group) (Figure 9A). The experiments were carried out using starving animals either control or subjected to 15 days of *Smed-Sirt-1(RNAi)*. A panel of neural genes predicted to be associated with feeding behavior were analyzed for changes in gene expression using qPCR. Changes in gene expression were first compared within each group (control or *Smed-Sirt-1(RNAi)*) between baseline and stimulated conditions. Changes in gene expression upon stimulation was then compared between the control and *Smed-Sirt-1(RNAi)* group.

The results show that upon chemosensory stimulation most genes in the control group were upregulated (15/27), while only few genes were downregulated (4 out of 27). Conversely, animals subjected to *Smed-Sirt-1(RNAi)* displayed extensive downregulation (14/27) under the same circumstances (Figure 9B). Interestingly, about half of the genes that were upregulated in the control group upon stimulation were found to be

downregulated in *Smed-Sirt-1(RNAi)* animals (Figure 9C). The results imply *Smed-Sirt-1* signaling regulates the expression of genes associated with chemosensory stimulation.

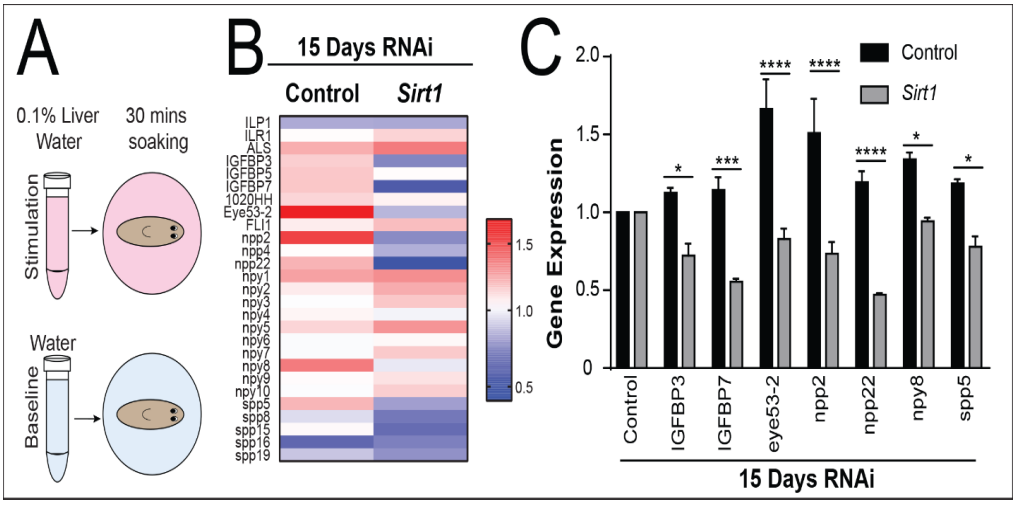

Figure 9. *Smed-Sirt-1* alters the genetic response to feeding stimulation. A) Schematic representation of liver stimulation assay. Animals were placed into either 40mL of planarian water (baseline) or 40mL of planarian water containing 0.1% liver (stimulated) for 30 minutes prior to RNA extractions. **B)** Heat map representing genes expression levels of transcripts normally associated with feeding response in control and *Smed-Sirt-1(RNAi)* animals. The reference scale bar for gene expression denotes higher expression in red and lower in blue. **C)** Difference in gene expression between control and the experimental group upon feeding stimulation assay. Data was obtained with an N=20 from 2 individual experiments; *p<0.05; ***p< 0.001; ****p<0.0001; Two-way ANOVA.

3.7. Loss of Sirtuin-1 leads to increased mitotic activity and decreased cell death

The number of cells rather than their size determines organismal dimension in planarian[231,233,235,266]. The planarian size is maintained by a constant renewal of tissues that relies on a fine balance between cell proliferation and death[184]. Based on this premise, we evaluated cell division and cell death to determine how *Smed-Sirt-1* signaling affects organismal growth at the cellular level. First, we analyzed mitotic events throughout the animal using immunostaining with the phosphorylated histone 3 (H3P) antibody (Figure 10A). Intriguingly, *Smed-Sirt-1(RNAi)* animals had an average of 37% more dividing cells than the control group. About 27% increase in cell division in the experimental group was observed as early as 15 days post-RNAi (Figure 10B). During this stage, animals are starving and the overall size is similar between both the control and experimental groups. The increase in cell division in the *Smed-Sirt-1(RNAi)* animals was greater after the 55-day period (48%) when they are markedly smaller than the control group (Figure 10A, B). In response to nutrients, planarians undergo a “mitotic burst” of dividing cells occurring 6,12,24 hours after being fed[267,268].

The rapid influx of dividing cells significantly influences the total number of cells in the body, thus leading to changes in body mass. Unexpectedly, *Smed-Sirt-1(RNAi)* animals displayed an even larger mitotic burst after feeding (Figure 10C). These results suggest *Smed-Sirt-1* signaling regulates cell division, which is restricted to a subpopulation of neoblasts.

We further expanded the analysis by measuring levels of gene expression of the pan-neoblast marker *smedwi-1 (Piwi)* and the recently identified marker for the clonogenic neoblast *tetraspanin-1 (Tspan-1)* that labels the Nb2 subclass[191,218]. We found about 28% overexpression for both *Piwi* and *Tspan-1* over the observational period (Figure 10D, E). Our findings demonstrate that *Smed-Sirt-1* signaling regulates cellular division and the expression of neoblast markers.

Next, we evaluate whether *Smed-Sirt-1* signaling regulate the rate of dying cells. The apoptotic maker caspase-3 is cleaved in the final stages leading to induced programmed cell death. We found a significant reduction in cleaved caspase-3 activity at 15 and 55 day *Smed-Sirt-1(RNAi)* (87% and 32%, respectively) (Figure 10F-H). We further confirmed the reduction in cell death in the experimental group at day 15 post RNAi by using TUNEL (Figure 10I). To explore other means of cell loss, we evaluated autophagy by measuring levels of gene expression for critical autophagosome formation markers (*Atg 5,8,12*)[269,270]and the planarian autophagy marker, *DAP1* [271]. We identified that *Smed-Sirt-1(RNAi)* animals had about 20% lower expression in autophagy markers *Atg8* and *DAP1* when compared to control (Figure 10J, K). To further validate these findings, we analyzed pro survival levels in cells, and found the expression of *Bcl2* to be upregulated by 32% in *Smed-Sirt-1(RNAi)* animals 15 days after RNAi (Figure 10L). Taken together, the results suggest that *Smed-Sirt-1* is required to maintain the balance between cell division and cell death during adult tissue turnover.

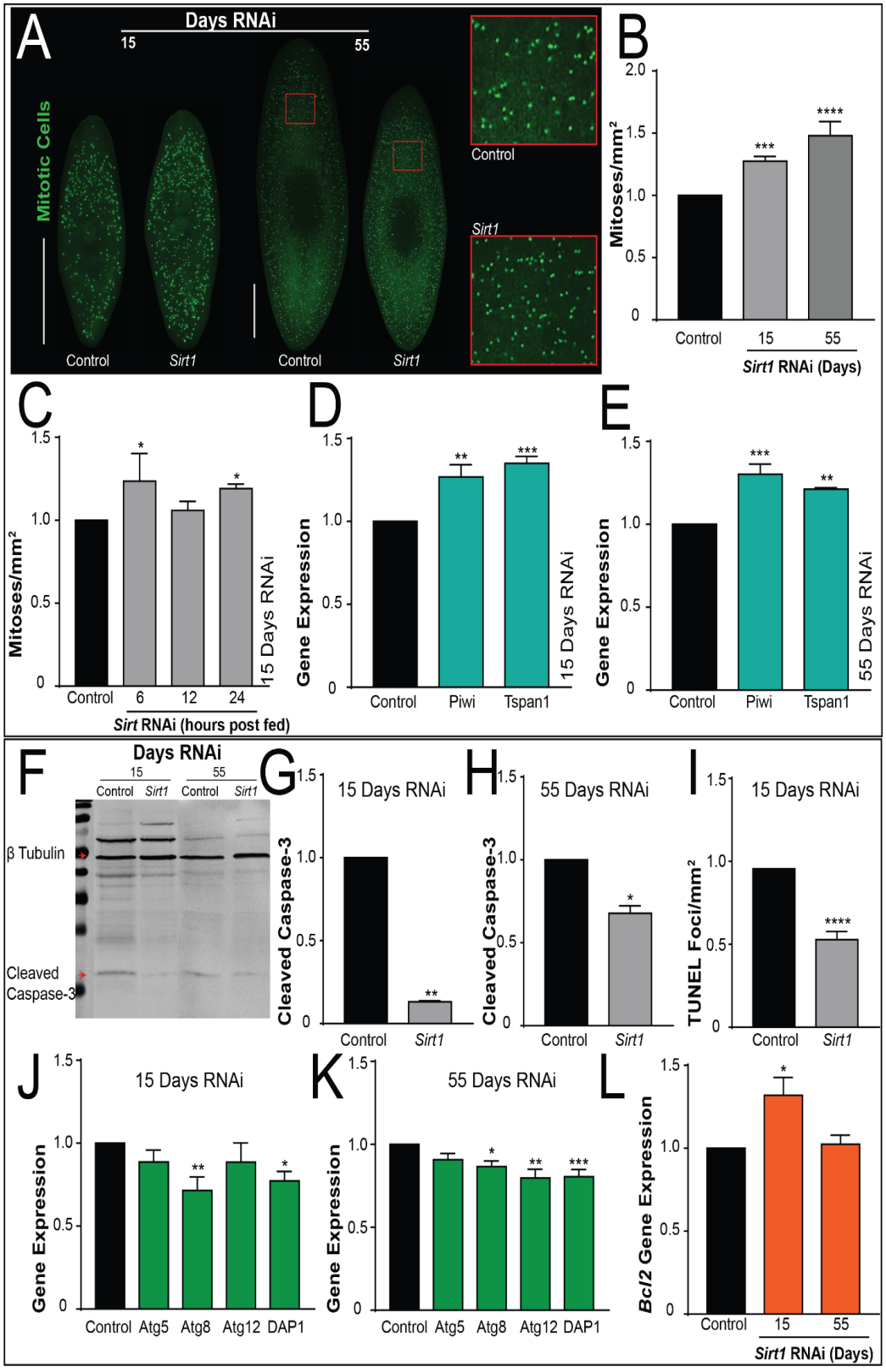

Figure 10. *Smed-Sirt-1* regulates the balance between proliferation and dying cells. **A)** Whole mount immunohistochemistry using phospho-histone H3 (serine10) (H3P) antibody at 15- and 55-days RNAi. Insets represent magnified areas within red squares.

Scale bar = 1mm. **B)** Number of mitoses at 15- and 55-days RNAi, represented as fold change. Data was obtained with at least an N=20 from at least 3 individual experiments; ***p<0.001; ****p<0.0001; Unpaired t test. **C)** Number of mitoses at the given length of time post feeding in animals 15 days after the 1stinjection, represented as fold change. Data was obtained with an N=10 from 1 individual experiments; *p<0.05; one-way ANOVA. **D, E)** Gene expression levels of neoblast markers, in *Smed-Sirt-1(RNAi)* animals 15- and 55-days after the 1stinjection. Gene expression is represented in fold change normalized to control. Data was obtained with an N=20 from 2 individual experiments; **p<0.01; ***p< 0.001;****p<0.0001; one-way ANOVA. **F-H)** Western-blot and subsequent quantification for Cleaved Caspase-3 in control and *Smed-Sirt-1(RNAi)* animals 15 days(left) and 55 days after the 1stinjection. Beta tubulin was used as an internal control. Data was obtained with at least an N=30 from at least 2 individual experiments; *p<0.05;**p<0.01; unpaired t test. **I)** TUNEL foci in animals 15 days after the 1stinjection. Data was obtained with at least an N=25 from 3 individual experiments; ****p<0.0001; Unpaired t test. **J, K)** Gene expression levels of autophagy markers, in *Smed-Sirt-1(RNAi)* animals 15 and 55 days after the 1stinjection. Data was obtained with an N=20 from 2 individual experiments; *p<0.05;**p<0.01;***p<0.001; one-way ANOVA. **L)** Gene expression levels of BCL2, in *Smed-Sirt-1(RNAi)* animals 15 and 55 days after the 1stinjection. Data was obtained with an N=20 from 2 individual experiments; *p<0.05; one-way ANOVA.

3.8. Sirtuin-1 is required for gut differentiation and intestinal branch morphology

The results demonstrate that *Smed-Sirt-1(RNAi)* animals grow smaller despite excessive cellular proliferation, and lower levels of cell death. Next, we asked whether cellular differentiation was also part of the cellular imbalance. We considered a range of markers linked to terminal differentiation of distinct cell populations in the intestine, excretory, muscle, and epithelial cells[191,272]. The results evidenced an initial reduction in the expression of markers associated with the gut and parapharyngeal cells that was extended to other cell types as the phenotype progresses (Figure 11A, B). In addition, we found *Smed-Sirt-1(RNAi)* animals display about 30% decrease in the expression of putative cytoskeletal regulators, *(Tpm1)* and *(RhoA)* (Figure 11C, D), which are critical regulators of gut branching formation[273].

To address the possibility that reduced expression of the intestinal differentiation markers may affect the gut architecture, we used FISH with the intestinal marker *Smed-inx-9* [204]. This approach allowed us to appreciate with detail gut morphology, while using the main branch length as a reference to quantify sub-branches within the anterior and posterior regions (ABL/PBL) (Figure 11E)[182,274]. Our results show that *Smed-Sirt-1(RNAi)* animals had fewer 3^{ary} intestinal branches (Figure 11E, G). We also observed that the internal sub-branches “internal branches” in the PBL were missing or severely reduced in early and late phases of the phenotype (Figure 11E, G). These results suggest that *Smed-Sirt-1* is required for differentiation of intestinal cells and for maintaining proper morphology of the planarian digestive system.

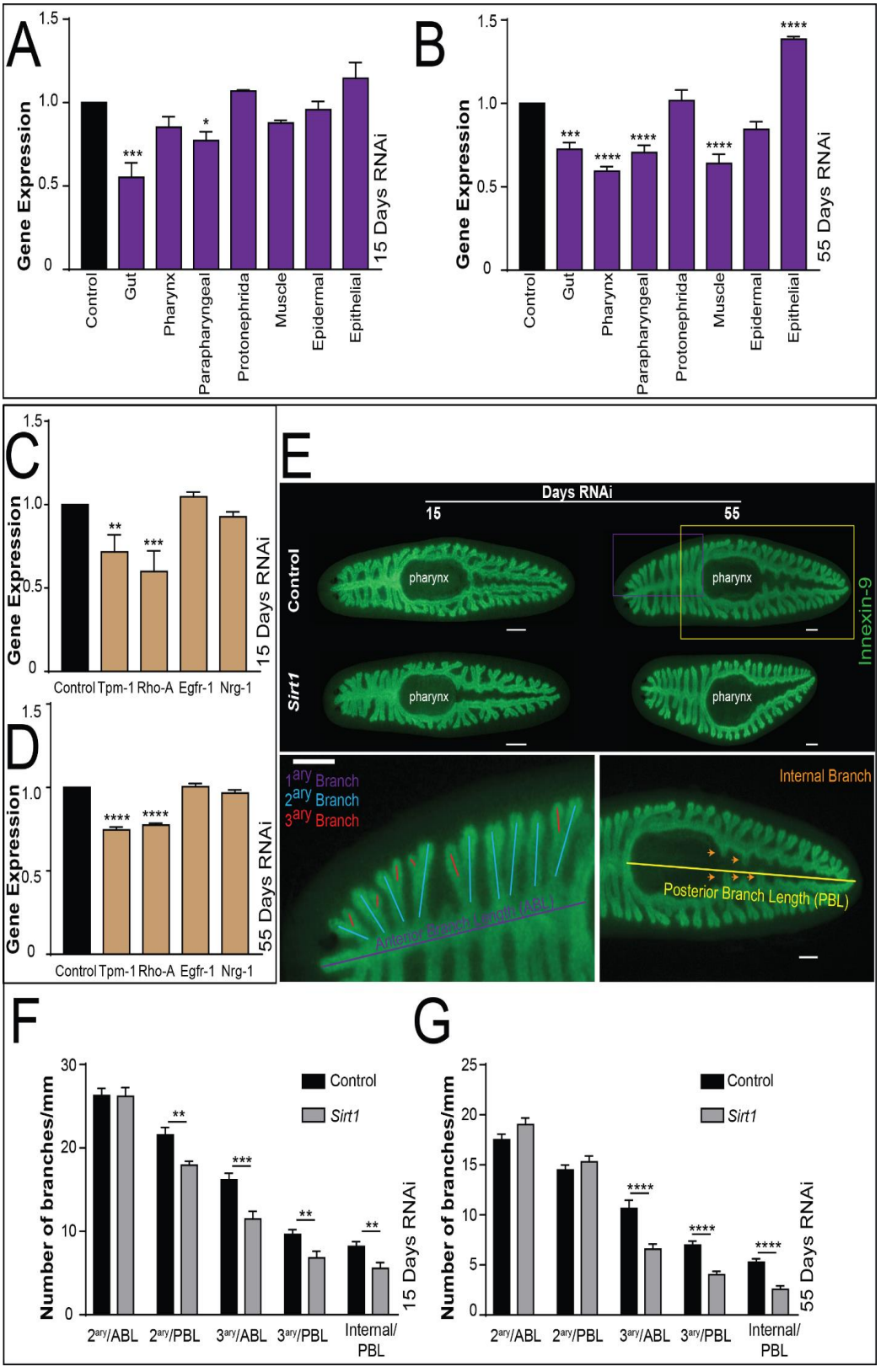
A
Gene Expression
15 Days RNAi
Control
Gut
Pharynx
Parapharyngeal
Protonephrida
Muscle
Epidermal
Epithelial
B
55 Days RNAi
C
Control Tpm-1 Rho-A Egfr-1 Nrg-1
D
E
Days RNAi
15
55
Control
Sirt1
pharynx
Innexin-9
1ary Branch
2ary Branch
3ary Branch
Anterior Branch Length (ABL)
Internal Branch
Posterior Branch Length (PBL)
F
G
Number of branches/mm
Control
Sirt1
2ary/ABL
2ary/PBL
3ary/ABL
3ary/PBL
Internal/ PBL

Figure 11. *Smed-Sirt-1* is required to maintain gut morphology. A, B) Gene expression levels of differentiation markers, in *Smed-Sirt-1(RNAi)* animals. Gene expression is represented in fold change normalized to control. Data was obtained with an N=20 from 2 individual experiments; *p<0.05; ***p<0.001; ****p<0.0001; one-way ANOVA. **C, D)** Gene expression levels of markers critical for gut branching, in *Smed-Sirt-1(RNAi)* animals. Gene expression is represented in fold change normalized to control. Data was obtained with an N=20 from 2 individual experiments; **p<0.01; ***p<0.001; ****p<0.0001; one-way ANOVA. **E)** Fluorescent *In Situ* Hybridization (FISH) expression of gut marker *Smed-inx-9* in control and *Smed-Sirt-1(RNAi)* animals. Magnified anterior portion of animal in purple box (bottom left panel) and posterior portion of animal in yellow box (bottom right panel) display branches and branch lengths used for quantification. Scale bar = 200um. **F, G)** Quantification of branches per length (mm) in control and *Smed-Sirt-1(RNAi)* animals. Data was obtained with at least an N=20 from at least 2 individual experiments; **p<0.01; ***p<0.001; ****p<0.0001; two-way ANOVA

3.9. Sirtuin-1 might influence growth through disrupted insulin signaling components

In invertebrates, IIS through ILPs, plays major roles in regulating growth during development[17,241,242]. IIS and its downstream components AKT and TOR are known regulators of growth in the planarian model[16,170,237,238,275]. We found that animals subjected to *Smed-Sirt-1(RNAi)* display an important reduction in insulin signaling components, particularly *IGFBP3* and *IGFBP5*. We also detected a 26% and 29% reduction in *ALS* and *ILP1* during the early and late phases of the phenotype respectively (Figure 12). These results suggest that *Smed-Sirt-1* may interfere with insulin signaling components that are required for growth in the planarian.

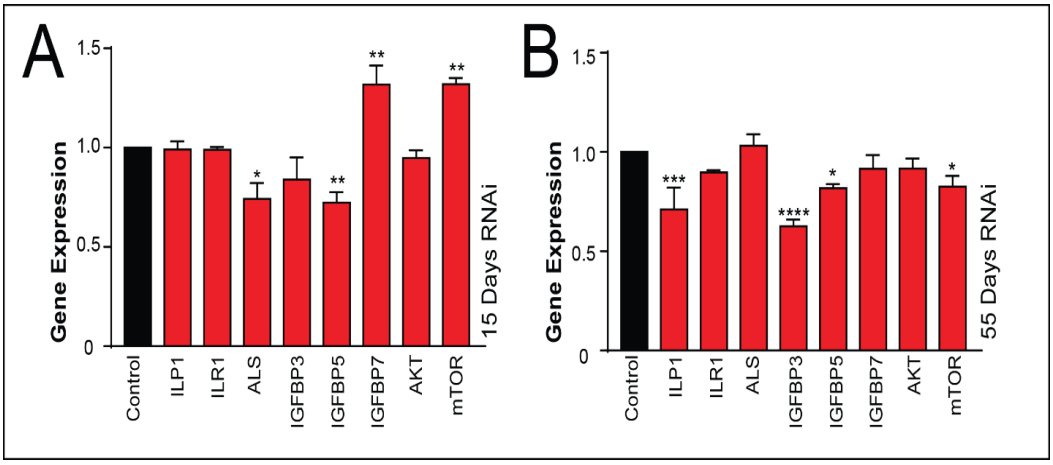

Figure 12. *Smed-Sirt-1* might influence growth through disrupted insulin signaling components. **A, B)** Gene expression levels of Insulin signaling components and downstream markers in *Smed-Sirt-1 (RNAi)* animals. Data was obtained with an N=20 from 2 individual experiments; *p<0.05; **p<0.01; ***p<0.001****p<0.0001; one-way ANOVA.

3.10. Sirtuin-1 does not impair the growth rate of missing tissue in response to injury

Based on previous results indicating that *Smed-Sirt-1* is required to maintain the balance between cell division and cell death, we wanted to understand if this impaired coordination would impact regeneration. Both controls and *Smed-Sirt-1(RNAi)* animals were amputated in anterior and posterior regions and the regenerating fragments were evaluated over 7 days (Figure 13A). The results demonstrate both control and the experimental group developed blastemas with equal dynamics and size and were indistinguishable, suggesting Sirtuin1 function is more relevant in the context of animal growth (Figure 13B, C). The data suggest *Smed-Sirt-1* is required to maintain the balance between cell division and cell death during adult tissue turnover.

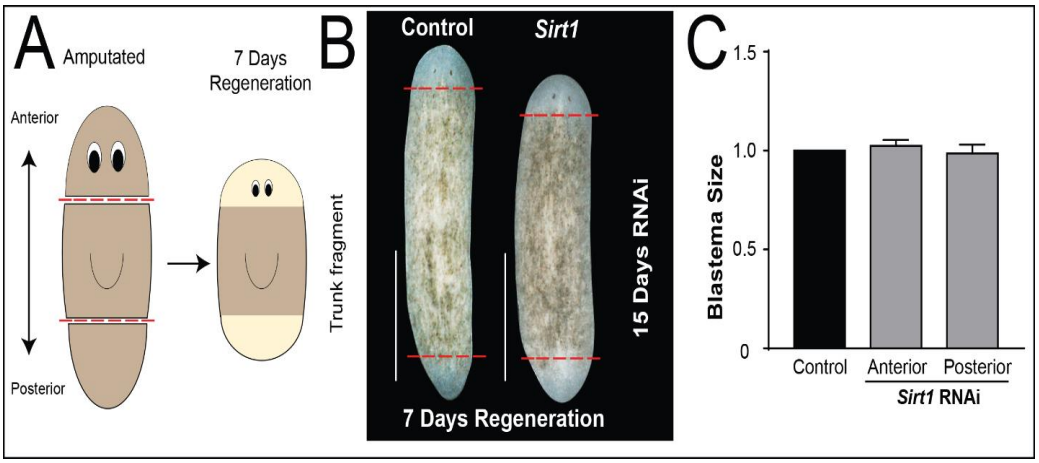

Figure 13. *Smed-Sirt-1* does not impair the growth rate of missing tissue in response to injury. **A)** Schematic of regeneration experiment. Animals were amputated both anterior and posterior to the pharynx (red dashed lines), and allowed 7 days to fully regenerate. **B)** Representation of control and *Smed-Sirt-1 (RNAi)* trunk fragments 7 days post amputation. Newly regenerated tissue (blastemas) is shown (red dashed lines). Scale bar = 1mm. **C)** Quantification of anterior and posterior blastemal size represented as fold change in 7 day regenerated trunk fragments. Data was obtained with an N=20 from 2 individual experiments; one-way ANOVA.

3.11. Sirtuin-1 function is conserved among the planarian model *Dugesia japonica*

The planarian model *Dugesia japonica (Dj)* is widely used as an alternative or in addition to the *Schmidtea mediterranea* planarian model. The *Dugesia japonica* model has been more widely used for classifying neuropeptides, which were translated from *Dugesia japonica* into *Schmidtea mediterranea* in this current study[236]. We wanted to understand if Sirtuin-1 function remained the same in the *Dugesia japonica* model, as this model could help to validate neuropeptide analysis in *Smed-Sirt-1 (RNAi)* animals. As expected, we found that Sirtuin-1 function with respect to the regulation of growth was conserved in *Dugesia japonica* as *Dj-Sirt-1 (RNAi)* animals grew at a 35% slower rate than control animals (Figure 14A-B). We also validated these results using the same pharmacological approach, however *Dugesia*

japonica appeared to be more sensitive to these drugs, and therefore concentrations on RESV and NAM were adjusted 5µM and 50µM respectively. These experiments revealed that animals treated with RESV grew 16% more than the respective control (DMSO treated). Conversely, animals exposed to NAM displayed about 40% reduced growth (Figure 14C-D). Overall, we find Sirtuin-1 to be a regulator of growth in not one, but two different planarian species.

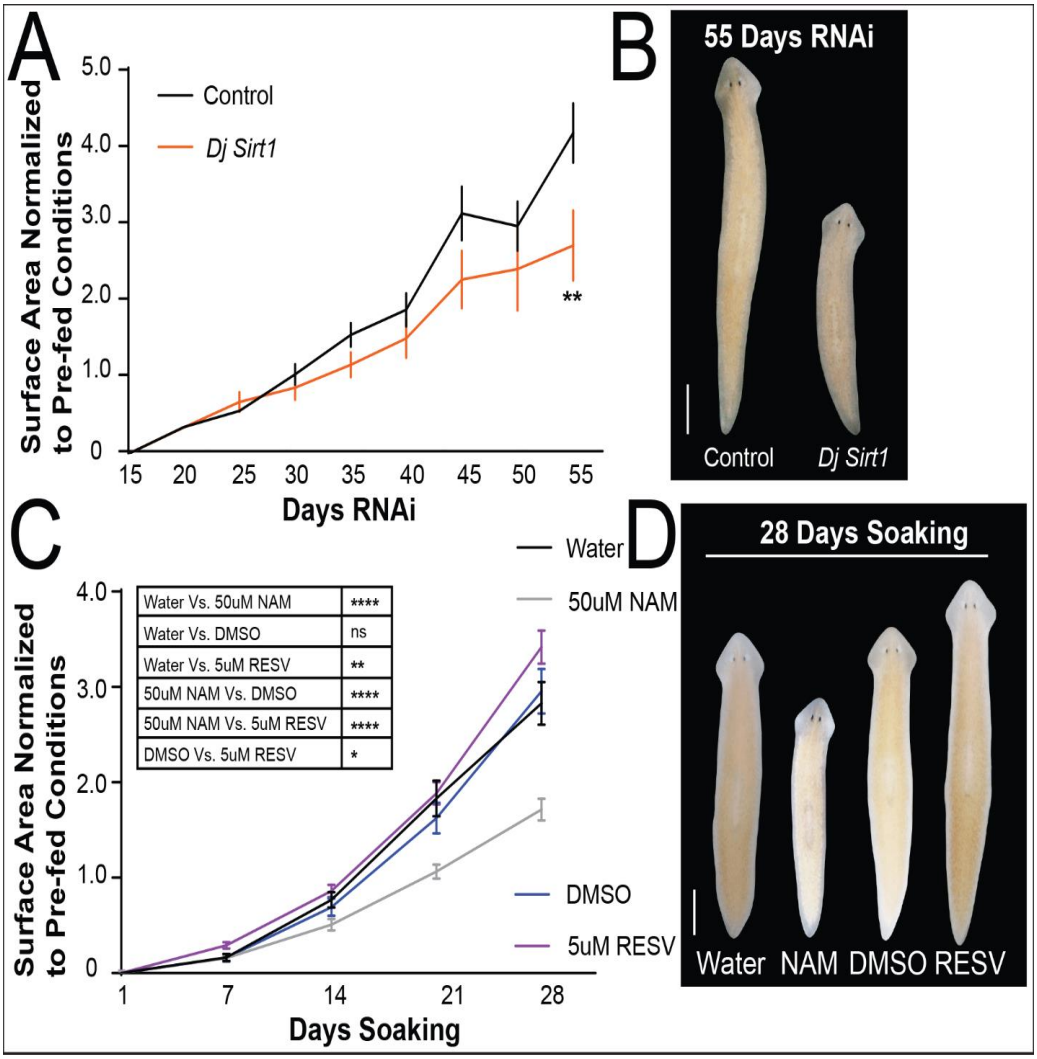

Figure 14. Sirtuin-1 function is conserved among the planarian model *Dugesia japonica*. **A)** Changes in surface area over the RNAi growth schedule (Figure 4E). Changes in the surface area is represented as fold change, normalized to pre-fed conditions, 15 days after the first injection. Data was obtained with an N=10 from 1 individual experiments; **p<0.01; one-way ANOVA. **B)** Representative images of control and *Dj-Sirt-1 (RNAi)* animals 55 days after the 1stinjection. Scale bar = 1mm. **C)** Changes in surface area over the pharmacological growth schedule (Figure 5D). Changes in the surface area is represented as fold change, normalized to pre-fed conditions, 5 days after the first soaking. Data was obtained with an N=20 from 2 individual experiments; *p<0.05, **p<0.01, ****p<0.0001; two-way ANOVA. Displayed statistics was provided for only 28

days post 1st soaking. **D)** Representative images of control (Water and DMSO), NAM, and RESV soaked animals 28 days after the 1stsoaking. Scale bar = 1mm.

4. Discussion

Nutrients play a vital role in the ability to expend energy and allow for cells to divide. Nutrition is one of the biggest influences on body growth, most importantly during development[44–47]. Some organisms, mostly invertebrates have the ability to alter body size throughout their lives[276]. The planarian model provides a robust example of how nutrients influence the total number of cells in the body, regulating organismal growth fairly quickly in the adult body[235,266]. However, the underlying molecular mechanisms for how nutrients are sensed and incorporated into body mass in planarians has not been well established. IIS regulates body size in several models, including planarians. Metabolic post-translational modification through enzymes called Sirtuins regulate IIS[152,163–166]. Homozygous Sirtuin-1 null mice were shown to be smaller in size compared to wild type littermates, which was shown to occur as a result of disrupted IIS[153–155]. Unfortunately, the ability to study Sirtuin-1 in the context of the entire adult body has been troublesome in that Sirtuin-1 is linked to lifespan, and loss of Sirtuin-1 leads to premature death in several species[113,114,153–155,167–169]. Disruption of Sirtuin1 in the planarian model does not appear to reduce life span and allows us to study long term effects of Sirtuin-1 functionality in the adult body. This is critical because Sirtuins regulate a diverse panel of metabolic functions, however within the context of the entire body, not much is known about how Sirtuins function.

The extended number of Sirtuins homologs in *Schmidtea mediterranea* offers the possibility to analyze evolutionary aspects of this conserved signaling pathway in metazoans. Unlike other invertebrate model organisms (e.g. *C. elegans*, *D. melanogaster*), we demonstrate that the number of Sirtuins in planarians is almost equivalent to the number of human Sirtuins. Furthermore, the Sirtuin-1 domain in *Schmidtea mediterranea* shows a similar degree of conservation (~60%) with classical studied Sirtuin models, *C. elegans*, and *D. melanogaster* that together have contributed to expand our understanding of Sirtuin-1 signaling[91]. It is expected that further analysis using *Schmidtea mediterranea,* a member of the Lophotrocozoa clade will complement and provide unique insights about the evolution of Sirtuin-1 signaling in metazoans.

In this study, we examined how nutrients influence growth under the regulation of Sirtuin-1. We found that Sirtuins are evolutionarily conserved in the planarian model *Schmidtea mediterranea* and *Japonica Dugesia.* We have shown that Sirtuin-1 function can be easily manipulated pharmacologically with RESV and NAM, two well established Sirtuin targeting drugs. We demonstrated that Sirtuin-1 regulates organismal growth by affecting feeding behavior, which is might result from changes in neural gene expression upon stimulation of sensing food. At the cellular level, *Smed-Sirt-1* signaling is critical to maintain the balance between cell division and cell death during planarian growth. We also reveal that *Smed-Sirt-1* has a critical

role in adult stem cell differentiation and the maintenance of intestine. All of this can be summarized in Figure 15. Altogether, we introduce the planarian *Schmidtea mediterranea* as a tractable model to analyze behavioral and molecular mechanisms integrating Sirtuin-1 signaling with the presence of nutrients.

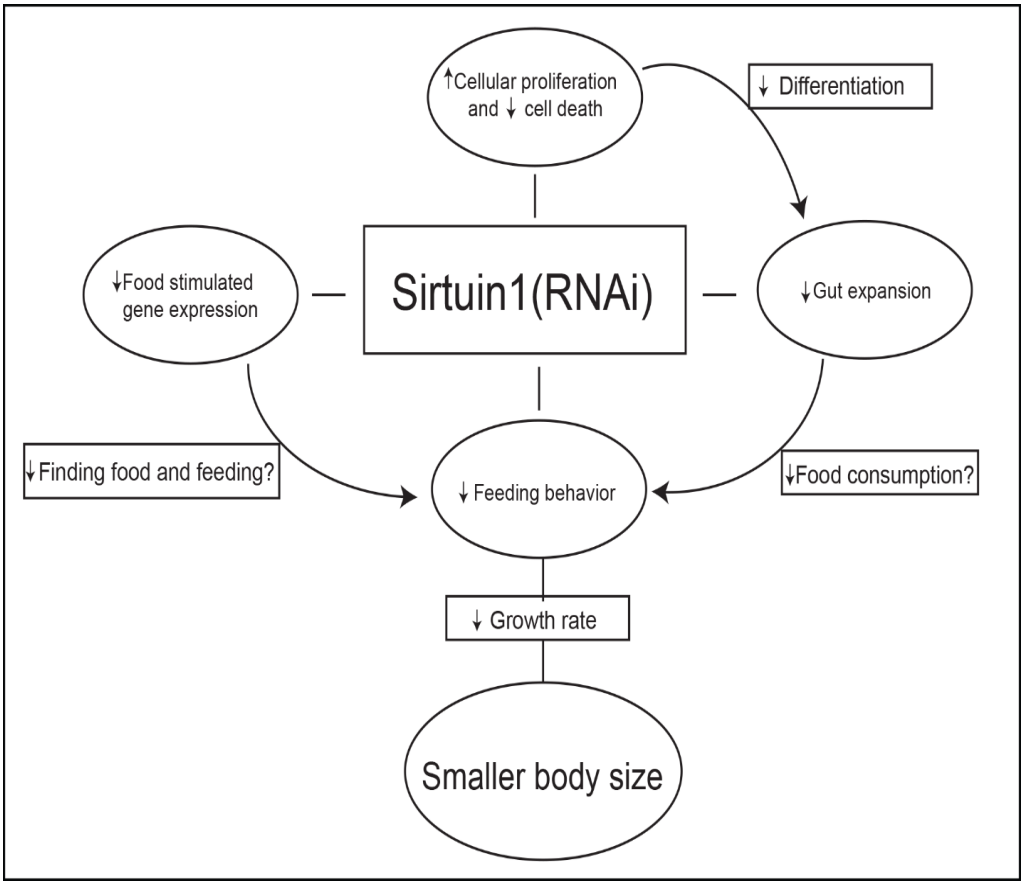

Figure 15. Graphical representation of Sirtuin1 function in the planarian *Schmidtea mediterranea*. Our findings indicate that Sirtuin1 animals are smaller in size over a period of growth. However, these animals show increases in cellular proliferation and decreases in cell death. We suspect that decreases in differentiation markers for the gut lead to disrupted gut formation, which might lead to decreased food consumption. Decreases in gene expression for neuropeptides upon stimulation of liver water might influence the amount of time to find food and begin feeding. Thus this feeding behavior might be responsible for decreased growth.

4.1. Sirtuin1 a metabolic sensor, regulating tissue renewal of the gut in planarian

We provide alternative opportunities to analyze Sirtuin-1 function in the context of tissue renewal. For example, our findings reveal that inhibition of *Smed-Sirt-1* signaling lead to an imbalance between cell division and cell death during tissue turnover. There is very limited information available about how Sirtuin-1 affects the fate and the flux of cells involving progenitors and differentiated cells during the constant renewal of adult tissues. The

underlying mechanisms for the cellular imbalances are not clear; but based in our results, we speculate that continuous neoblast proliferation may be promoted by the deficient differentiation of cells toward the gut lineage. Sirtuin1 has shown to have a role on stem cell differentiation[277–282], such as adult intestinal stem cells, which contribute to the intestinal epithelium of the gut in mice[102,283]

Several differentiation markers have been identified in planarian, including lineages of different cell types[191,196,272–274,284–286]. We found *Smed-Sirt-1(RNAi)* reduces the expression of the gut differentiation marker, glutathione S-transferase 1 (*GST1)*, which was accompanied by fewer intestinal branches. These effects in intestinal morphology appear independent of *EGFR-1* and its ligand *nrg-1* that are critical for gut branching [274]. Nonetheless, our findings suggest defective gut morphology in *Smed-Sirt-1(RNAi)* animals may be associated with the reduction in expression of two putative cytoskeletal regulators, *Tpm-1* and *Rho-A. Tpm-1* and *Rho-A* are known to regulate branching formation in intact and regenerating animals [273]. These finding together imply that *Smed-Sirt-1* may regulate gut branching formation not only through differentiation but also through cytoskeletal regulation.

The planarian gastrointestinal system plays an important role in breaking down and digesting food, while distributing nutrients throughout the body[287]. In many models, resident adult stem cells constantly replace epithelial lining[102,288–292]. In the planarian, neoblasts in the mesenchyme commit to intestinal cell fates where they then cross a layer of the enteric muscles and basement membrane, and integrate into the gastrodermal epithelium, functioning as part of the gut. The formation of new branches occurs by remodeling of pre-existing gut tissue[182]. Additionally, the number of intestinal branches remains proportional to the size of the animal. Smaller planarians have less branching in comparison to larger planarians[182].We speculate that expansion of the gut controlled in part by *Smed-Sirt-1* may interfere with total food consumption, limiting growing capacity.

4.2. Sirtuin1 influences feeding behavior in the planarian model

The function of Sirtuins in planarians can be analyzed at the organismal, cellular, and at the molecular level. For example, an advantage of studying effects in the complexity of the adult body includes comprehensive analysis integrating behavioral, neural, and metabolic inputs. This is evident by the behavioral effects associated with food consumption and the resulting decrease in body size after disrupting *Smed-Sirt-1* function. The underlying mechanisms regulating food consumption in planarians remain largely unknown. Studies in different organisms consistently show feedback between the nervous and digestive system influence food intake. For example, in humans and other vertebrates, orexigenic molecules such as ghrelin are secreted from the stomach and trigger hunger response through the arcuate

nucleus of the hypothalamus, stimulating neuropeptide Y(NPY) / agouti-related protein (AgRP) neuronal release of NPY and AgRP. [293,294].

In the planarian *Dugesia japonica,* NPY and other neuropeptides regulate feeding rate. The *Schmidtea mediterranea* model contains 11 NPYs. Approximately half of the *Schmidtea mediterranea* NPYs resemble vertebrate NPYs, while the other half resembles invertebrate NPF, displayed by either a tyrosine or phenylalnine in the C-terminus respectively [265]. Recent studies also revealed the transcription factor friend leukemia integration 1 transcription factor (*FLI-1*) as a potential regulator of the planarian chemosensory response [217]. The newly developed protocols to evaluate feeding stimulation in this study showed that the expression of *NPY* homologs, *FLI-1*, and components of the IIS were activated upon feeding. We found that *Smed-Sirt-1* regulates a handful of these genes. Although, these results validate the efficacy of our feeding stimulation assay, further biochemical and genetic studies will be required to determine the epistatic regulation of these components and how *Smed-Sirt-1* and the neurohumoral response are integrated to regulate the hunger response.

4.3. IIS signaling components might influence limited growth in Sirtuin1 RNAi animals

In invertebrates, IIS through ILPs plays major roles in regulating growth occurring mostly during development[17,241,242]. IIS and its downstream components AKT and mTOR are the only well-defined regulators of growth in the planarian model[16,170,238]. In the present study we identified Sirtuin-1 as a novel regulator of organismal growth in the planarian*, Schmidtea mediterranea* and *Japonica Dugesia*. These findings are consistent with impaired growth in Sirtuin1 null mice mediated by insulin growth factor signaling[153–155]. We also found that animals subjected to *Smed-Sirt-1(RNAi)* display an important reduction in insulin signaling components, particularly *IGFBP3*, *IGFBP5*, and *ALS*. IGFBP1 can antagonize actions of growth, as seen in mice overexpressing IGFBP1 or Sirtuin-1 null mice.[79,295–299,153,154]. In mice, the loss of ALS lead to a 20% reduction in body weight and 8% reduction in body length[300]. Similarly, humans with mutations in ALS have a reduction in birth weight and postnatal growth, followed by a delay in puberty[84]. In Drosophila, ALS plays a role not only in growth, but also in metabolism. It is possible that ALS acts as a metabolic sensor or regulator of growth in planarian under the control of *Smed-Sirt-1*, and loss of *Smed-Sirt-1* leads to impaired ALS production, disrupting growth in the early part of the phenotype. However, further analyses using planarian specific antibodies would provide a complementary view to the current gene expression studies. Predictions can be made on how proteins might be influenced based off changes in gene expression, however the activity of these proteins may require events, such as phosphorylation which cannot be detected with gene expression alone.

4.4. Final remarks and future direction

Our results demonstrate the possibility of modulating Sirtuin function in planarians by genetic and pharmacological approaches. Gain of function methods are limited in planarians, but the use of RESV treatment as enhancer of Sirtuin-1 function allowed us to overcome this hurdle. On the other hand, the specific effects achieved with the RNAi could be recapitulated with NAM treatment, which is commonly used to inhibit Sirtuin function in other experimental models[103,110,301,302]. Together, we introduce a simplified experimental platform amenable for *in vivo* systemic analysis of Sirtuin-1 function.

This work has highlighted the important of Sirtuin-1 as a regulator of organismal growth in the planarian model. Sirtuin-1 plays important roles in metabolic function, lifespan, and development in various organisms[155,306,307]. However, studying Sirtuin-1 function can be challenging in the adult body, as loss of Sirtuin-1 can decrease lifespan[113,153–155]. Using the planarian model to circumvent this limitation, our findings introduce novel opportunities to study systemic effects of Sirtuin-1 signaling integrating long-range intercellular communication (e.g. neural and stem cells) that affect the overall homeostasis and organismal behavior. Future studies would be guided toward dissecting the genetic regulatory networks modulating Sirtuin-1 signaling in the adult body.

The signals that regulate food seeking behavior are mostly unknown in the planarian model. Our approach in constructing new assays to test this behavior has provided additional knowledge, contributing towards the overall understanding of feeding behavior in the planarian field. However, our results provide candidates that have not been validated in regards to the planarian model *Schmidtea mediterranea*. The stimulation assay identified seven candidate genes that influence feeding behavior and are regulated by *Smed-Sirt-1.* Further work would decipher the accuracy of our stimulation assay by performing RNAi on these candidate genes. After knocking down these genes, we would determine if the RNAi animals take longer to find food and begin feeding, or if food consumption is decreased, using the assays created in this study. Due to the increased gene expression of these candidate genes upon the stimulation assay, we anticipate that RNAi animals will either have a difficult time locating food or consume less food than control animals. Based off these results, candidates that are shown to regulate feeding behavior will be analyzed for Sirtuin-1 specificity using RESV. The stimulation assay would be repeated using RESV in place of *Smed-Sirt-1 (RNAi)*. If gene expression of the suspected candidate gene is increased upon stimulation this would help identify the molecular mechanism underlying feeding behavior in *Smed-Sirt-1(RNAi)* animals.

IIS in planarians and other models regulates organismal growth in response to nutrients. Whether IIS in planarians acts as a metabolic

regulator, a growth factor regulator, or as both remains unknown. We identified evolutionary conservation of IGFBPs and ALS, allowing us to speculate that IIS might act in part as a regulator of growth factor signaling. Performing RNAi on IGFBPs and ALS in planarian would identify how IIS functions in the planarian model. We would anticipate that RNAi of IGFBPs and ALS would disrupt growth in an IIS dependent manner, and animals would grow at a slower rate than control animals[16]. In Drosophila, loss of ALS under nutrient stress leads to decreased adult weight, while under normal conditions, the opposite effect is seen[81]. *Smed-Sirt-1(RNAi)* animals showed decreased ALS expression under starved conditions (early time point) and increased ALS expression upon the presence of feeding (late time point). Using RESV, we would expect opposite trends of *Smed-Sirt-1(RNAi)*, which could provide a Sirtuin-1 specific target of growth in the planarian model.

The gut is pivotal to the planarians ability to grow. The size and branching of the gut changes depending on the amount of nutrients being consumed. The gut also plays a huge role in breaking down food which will be converted into usable energy. We found that *Smed-Sirt-1(RNAi)* animals have diminished gut branching which results from reduced differentiation of gut progenitors. While the morphology of the gut is more than likely to impair food consumption and hence growth of the organism, we have yet to explore functionality of the gut. Phagocytic enterocytes allow for intracellular digestion through engulfment of food particles entering the gut. These cells can be tracked using a fluorescently labeled dextrans dye which can allow for the quantification of phagocytes, and provide some information about the quantity of food being processed by the gut[273]. Secretory cells surrounding the intestinal lumen, contain digestive proteases that breakdown food particles[182]. Measuring digestive proteases using rhodamine-labeled BSA/SA could tell us if *Smed-Sirt-1* is hindering the amount proteases being produced, which could reduce the amount of nutrients being absorbed[308].

As mentioned previously, *Smed-Sirt-1* could be influencing the amount of nutrients being absorbed. In addition to measuring digestion, metabolic input is a variable that might influence growth rate. To test this, animals could be placed on either a high calorie diet or enhanced feeding schedule. We would anticipate that this would cause animals to grow at an accelerated rate. Changes in metabolic input might bridge the gap in growth between *Smed-Sirt-1(RNAi)* and control animals, as a higher volume of nutrients might alter their metabolic levels. As a consequence of higher metabolic inputs, animals will fission when reaching certain increased sizes, which provides limits to this feeding regimen. Little is known about how this process occurs or how to control it, which could be problematic in quantifying changes in body size[174–178]. The metabolic rate of the animals can also be measured based off of oxygen consumption[309]. This would allow us to determine if *Smed-Sirt-1(RNAi)* animals have an altered metabolic rate and are unable to obtain

significant amounts of energy compared to control animals. Lastly, a recent advancement in the planarian field has shown that planarians have lipid stores in the gut. We could determine if *Smed-Sirt-1* plays a role in storing lipids which might result in changes of body size. We would expect that due to the nature of *Smed-Sirt-1* reducing growth, these smaller sized animals might have a reduction in lipid content, as high lipid content is usually associated with larger body mass. Using lipid droplet dye LD540, we can visualize and quantify the presence of lipids in both *Smed-Sirt-1(RNAi)* and control animals[235].

In this study we explored the function of Sirtuin-1 in the context of the adult body, something that remains challenging in other models. Metabolic networks are fairly well established in vertebrate models, yet very little is known about metabolic regulation in the planarian *Schmidtea mediterranea.* We introduce *Smed-Sirt*-1 as a novel metabolic regulator in the planarian model that act as a regulator of growth. Our experiments also provide several new assays for studying feeding behavior, which is mostly unexplored in the planarian. While tissue renewal has mostly been in context with regeneration in planarians, our findings demonstrate the complexity of gut tissue renewal outside of regeneration. Lastly, Sirtuin-1 specific pharmacological compounds can be easily administered to planarians, therefore we suggest the planarian as an attractive model for testing Sirtuin-1 specific drugs.

5. References

1. Okazaki, K. & Holtzer, H. Myogenesis: fusion, myosin synthesis, and the mitotic cycle. *Proc. Natl. Acad. Sci. U. S. A.* **56**, 1484–1490 (1966).
2. Lacroix, B. & Maddox, A. S. Cytokinesis, ploidy and aneuploidy. *J. Pathol.* **226**, 338–351 (2012).
3. Thomas, G. & Hall, M. N. TOR signalling and control of cell growth. *Curr. Opin. Cell Biol.* **9**, 782–787 (1997).
4. Vanhaesebroeck, B., Leevers, S. J., Panayotou, G. & Waterfield, M. D. Phosphoinositide 3-kinases: A conserved family of signal transducers. *Trends Biochem. Sci.* **22**, 267–272 (1997).
5. Downward, J. Mechanisms and consequences of activation of protein kinase B/Akt. *Curr. Opin. Cell Biol.* **10**, 262–267 (1998).
6. Bhaskar, P. T. & Hay, N. The Two TORCs and Akt. *Dev. Cell* **12**, 487–502 (2007).
7. Huang, K. & Fingar, D. C. Growing knowledge of the mTOR signaling network. *Semin. Cell Dev. Biol.* **36**, 79–90 (2014).
8. Sarbassov, D. D., Ali, S. M. & Sabatini, D. M. Growing roles for the mTOR pathway. *Curr. Opin. Cell Biol.* **17**, 596–603 (2005).
9. Kim, S.-E. *et al.* Drosophila PI3 kinase and Akt involved in insulin-stimulated proliferation and ERK pathway activation in Schneider cells. *Cell. Signal.* **16**, 1309–1317 (2004).
10. Chen, C., Jack, J. & Garofalo, R. S. The Drosophila insulin receptor is required for normal growth. *Endocrinology* **137**, 846–856 (1996).

11. Leevers, S. J., Weinkove, D., MacDougall, L. K., Hafen, E. & Waterfield, M. D. The Drosophila phosphoinositide 3-kinase Dp110 promotes cell growth. *EMBO J.* **15**, 6584–6594 (1996).

12. Weinkove, D., Neufeld, T. P., Twardzik, T., Waterfield, M. D. & Leevers, S. J. Regulation of imaginal disc cell size, cell number and organ size by Drosophila class I(A) phosphoinositide 3-kinase and its adaptor. *Curr. Biol. CB* **9**, 1019–1029 (1999).

13. Thomas, G. An encore for ribosome biogenesis in the control of cell proliferation. *Nat. Cell Biol.* **2**, E71-72 (2000).

14. Montagne, J. *et al.* Drosophila S6 kinase: a regulator of cell size. *Science* **285**, 2126–2129 (1999).

15. Liu, J. P., Baker, J., Perkins, A. S., Robertson, E. J. & Efstratiadis, A. Mice carrying null mutations of the genes encoding insulin-like growth factor I (Igf-1) and type 1 IGF receptor (Igf1r). *Cell* **75**, 59–72 (1993).

16. Miller, C. M. & Newmark, P. A. An insulin-like peptide regulates size and adult stem cells in planarians. *Int. J. Dev. Biol.* **56**, 75–82 (2012).

17. Dabour, N. *et al.* Cricket body size is altered by systemic RNAi against insulin signaling components and epidermal growth factor receptor. *Dev. Growth Differ.* **53**, 857–869 (2011).

18. Purves, D., Snider, W. D. & Voyvodic, J. T. Trophic regulation of nerve cell morphology and innervation in the autonomic nervous system. *Nature* **336**, 123–128 (1988).

19. Conlon, I. & Raff, M. Size Control in Animal Development. *Cell* **96**, 235–244 (1999).

20. Sherr, C. J. G1 phase progression: cycling on cue. *Cell* **79**, 551–555 (1994).

21. Morgan, D. O. Principles of CDK regulation. *Nature* **374**, 131–134 (1995).

22. Brooks, R. F. & Riddle, P. N. The 3T3 cell cycle at low proliferation rates. *J. Cell Sci.* **90 (Pt 4)**, 601–612 (1988).

23. Gao, F. B. & Raff, M. Cell size control and a cell-intrinsic maturation program in proliferating oligodendrocyte precursor cells. *J. Cell Biol.* **138**, 1367–1377 (1997).

24. Calver, A. R. *et al.* Oligodendrocyte population dynamics and the role of PDGF in vivo. *Neuron* **20**, 869–882 (1998).

25. Martin, G. R. The roles of FGFs in the early development of vertebrate limbs. *Genes Dev.* **12**, 1571–1586 (1998).

26. Pardee, A. B. A restriction point for control of normal animal cell proliferation. *Proc. Natl. Acad. Sci. U. S. A.* **71**, 1286–1290 (1974).

27. Sherr, C. J. & Roberts, J. M. Inhibitors of mammalian G1 cyclin-dependent kinases. *Genes Dev.* **9**, 1149–1163 (1995).

28. Goss, R. *The physiology of growth*. (1978).

29. McPherron, A. C., Lawler, A. M. & Lee, S. J. Regulation of skeletal muscle mass in mice by a new TGF-beta superfamily member. *Nature* **387**, 83–90 (1997).

30. Willems, A. R. *et al.* Cdc53 Targets Phosphorylated G1 Cyclins for Degradation by the Ubiquitin Proteolytic Pathway. *Cell* **86**, 453–463 (1996).

31. Kipreos, E. T., Lander, L. E., Wing, J. P., He, W. W. & Hedgecock, E. M. cul-1 is required for cell cycle exit in C. elegans and identifies a novel gene family. *Cell* **85**, 829–839 (1996).

32. Casaccia-Bonnefil, P. *et al.* Oligodendrocyte precursor differentiation is perturbed in the absence of the cyclin-dependent kinase inhibitor p27Kip1. *Genes Dev.* **11**, 2335–2346 (1997).

33. Fero, M. L. *et al.* A syndrome of multiorgan hyperplasia with features of gigantism, tumorigenesis, and female sterility in p27(Kip1)-deficient mice. *Cell* **85**, 733–744 (1996).

34. Kiyokawa, H. *et al.* Enhanced Growth of Mice Lacking the Cyclin-Dependent Kinase Inhibitor Function of p27Kip1. *Cell* **85**, 721–732 (1996).

35. Nakayama, K. *et al.* Mice lacking p27(Kip1) display increased body size, multiple organ hyperplasia, retinal dysplasia, and pituitary tumors. *Cell* **85**, 707–720 (1996).

36. Raff, M. C. Social controls on cell survival and cell death. *Nature* **356**, 397–400 (1992).

37. Tsujimoto, Y., Finger, L. R., Yunis, J., Nowell, P. C. & Croce, C. M. Cloning of the chromosome breakpoint of neoplastic B cells with the t(14;18) chromosome translocation. *Science* **226**, 1097–1099 (1984).

38. Nicholson, D. W. & Thornberry, N. A. Caspases: killer proteases. *Trends Biochem. Sci.* **22**, 299–306 (1997).

39. Barres, B. A. & Raff, M. C. Control of oligodendrocyte number in the developing rat optic nerve. *Neuron* **12**, 935–942 (1994).

40. Ryoo, H. D. & Steller, H. Hippo and its mission for growth control. *Nat. Cell Biol.* **5**, 853–855 (2003).

41. Huang, J., Wu, S., Barrera, J., Matthews, K. & Pan, D. The Hippo Signaling Pathway Coordinately Regulates Cell Proliferation and Apoptosis by Inactivating Yorkie, the Drosophila Homolog of YAP. *Cell* **122**, 421–434 (2005).

42. Martinou, J. C. *et al.* Overexpression of BCL-2 in transgenic mice protects neurons from naturally occurring cell death and experimental ischemia. *Neuron* **13**, 1017–1030 (1994).

43. Bosch, T. C. & David, C. N. Growth regulation in Hydra: relationship between epithelial cell cycle length and growth rate. *Dev. Biol.* **104**, 161–171 (1984).

44. Perkins, J. M., Subramanian, S. V., Davey Smith, G. & Özaltin, E. Adult height, nutrition, and population health. *Nutr. Rev.* **74**, 149–165 (2016).

45. Redmer, D. A., Wallace, J. M. & Reynolds, L. P. Effect of nutrient intake during pregnancy on fetal and placental growth and vascular development. *Domest. Anim. Endocrinol.* **27**, 199–217 (2004).

46. Mirth, C. K. & Shingleton, A. W. Integrating Body and Organ Size in Drosophila: Recent Advances and Outstanding Problems. *Front. Endocrinol.* **3**, (2012).

47. Hietakangas, V. & Cohen, S. M. Regulation of tissue growth through nutrient sensing. *Annu. Rev. Genet.* **43**, 389–410 (2009).

48. Layalle, S., Arquier, N. & Léopold, P. The TOR pathway couples nutrition and developmental timing in Drosophila. *Dev. Cell* **15**, 568–577 (2008).

49. Dewey, K. G. & Cohen, R. J. Does birth spacing affect maternal or child nutritional status? A systematic literature review. *Matern. Child. Nutr.* **3**, 151–173 (2007).

50. *MYCOTOXIN CONTROL IN LOW- AND MIDDLE-INCOME COUNTRIES*. (International Agency for Research on Cancer, 2015).

51. Aponte, Y., Atasoy, D. & Sternson, S. M. AGRP neurons are sufficient to orchestrate feeding behavior rapidly and without training. *Nat. Neurosci.* **14**, 351–355 (2011).

52. Balthasar, N. *et al.* Divergence of Melanocortin Pathways in the Control of Food Intake and Energy Expenditure. *Cell* **123**, 493–505 (2005).

53. Sohn, J.-W. Network of hypothalamic neurons that control appetite. *BMB Rep.* **48**, 229–233 (2015).

54. Kojima, M. *et al.* Ghrelin is a growth-hormone-releasing acylated peptide from stomach. *Nature* **402**, 656–660 (1999).

55. Cummings, D. E. *et al.* A preprandial rise in plasma ghrelin levels suggests a role in meal initiation in humans. *Diabetes* **50**, 1714–1719 (2001).

56. Kohno, D., Gao, H.-Z., Muroya, S., Kikuyama, S. & Yada, T. Ghrelin Directly Interacts With Neuropeptide-Y-Containing Neurons in the Rat Arcuate Nucleus: Ca2+ Signaling via Protein Kinase A and N-Type Channel-Dependent Mechanisms and Cross-Talk With Leptin and Orexin. *Diabetes* **52**, 948–956 (2003).

57. Wren, A. M. *et al.* The novel hypothalamic peptide ghrelin stimulates food intake and growth hormone secretion. *Endocrinology* **141**, 4325–4328 (2000).

58. Chen, H. Y. *et al.* Orexigenic Action of Peripheral Ghrelin Is Mediated by Neuropeptide Y and Agouti-Related Protein. *Endocrinology* **145**, 2607–2612 (2004).

59. Li, X., Qu, M.-J., Zhang, Y., Li, J.-W. & Liu, T.-X. Expression of Neuropeptide F Gene and Its Regulation of Feeding Behavior in the Pea Aphid, Acyrthosiphon pisum. *Front. Physiol.* **9**, 87 (2018).

60. Lin-Su, K. & Wajnrajch, M. P. Growth Hormone Releasing Hormone (GHRH) and the GHRH Receptor. *Rev. Endocr. Metab. Disord.* **3**, 313–323 (2002).

61. Møller, N. & Jørgensen, J. O. L. Effects of Growth Hormone on Glucose, Lipid, and Protein Metabolism in Human Subjects. *Endocr. Rev.* **30**, 152–177 (2009).

62. Lin, S., Li, C., Li, C. & Zhang, X. Growth Hormone Receptor Mutations Related to Individual Dwarfism. *Int. J. Mol. Sci.* **19**, (2018).

63. Heyner, S. & Garside, W. T. Biological actions of IGFs in mammalian development. *BioEssays News Rev. Mol. Cell. Dev. Biol.* **16**, 55–57 (1994).

64. Fernandez, A. M. & Torres-Alemán, I. The many faces of insulin-like peptide signalling in the brain. *Nat. Rev. Neurosci.* **13**, 225–239 (2012).

65. Cross, D. A., Alessi, D. R., Cohen, P., Andjelkovich, M. & Hemmings, B. A. Inhibition of glycogen synthase kinase-3 by insulin mediated by protein kinase B. *Nature* **378**, 785–789 (1995).

66. Rutter, G. A. Nutrient-secretion coupling in the pancreatic islet beta-cell: recent advances. *Mol. Aspects Med.* **22**, 247–284 (2001).

67. Lizcano, J. M. & Alessi, D. R. The insulin signalling pathway. *Curr. Biol. CB* **12**, R236-238 (2002).

68. Asnaghi, L., Bruno, P., Priulla, M. & Nicolin, A. mTOR: a protein kinase switching between life and death. *Pharmacol. Res.* **50**, 545–549 (2004).

69. Ogawa, W., Matozaki, T. & Kasuga, M. Role of binding proteins to IRS-1 in insulin signalling. *Mol. Cell. Biochem.* **182**, 13–22 (1998).

70. Houston, M. S. The Astounding Insulin-like Growth Factor System. *Trends Endocrinol. Metab.* **11**, 159–161 (2000).

71. Foulstone, E. *et al.* Insulin-like growth factor ligands, receptors, and binding proteins in cancer. *J. Pathol.* **205**, 145–153 (2005).

72. Ghosh, P., Dahms, N. M. & Kornfeld, S. Mannose 6-phosphate receptors: new twists in the tale. *Nat. Rev. Mol. Cell Biol.* **4**, 202–212 (2003).

73. Pandini, G. *et al.* Insulin/Insulin-like Growth Factor I Hybrid Receptors Have Different Biological Characteristics Depending on the Insulin Receptor Isoform Involved. *J. Biol. Chem.* **277**, 39684–39695 (2002).

74. Chen, J., Nagle, A. M., Wang, Y.-F., Boone, D. N. & Lee, A. V. Controlled dimerization of insulin-like growth factor-1 and insulin receptors reveals shared and distinct activities of holo and hybrid receptors. *J. Biol. Chem.* **293**, 3700–3709 (2018).

75. Brogiolo, W. *et al.* An evolutionarily conserved function of the Drosophila insulin receptor and insulin-like peptides in growth control. *Curr. Biol. CB* **11**, 213–221 (2001).

76. Hwangbo, D. S. *et al.* Drosophila dFOXO controls lifespan and regulates insulin signalling in brain and fat body. *Nature* **429**, 562–566 (2004).

77. Murphy, C. T. *et al.* Genes that act downstream of DAF-16 to influence the lifespan of Caenorhabditis elegans. *Nature* **424**, 277–283 (2003).

78. Hwa, V., Oh, Y. & Rosenfeld, R. G. The Insulin-Like Growth Factor-Binding Protein (IGFBP) Superfamily [1]. *Endocr. Rev.* **20**, 761–787 (1999).

79. Firth, S. M. & Baxter, R. C. Cellular actions of the insulin-like growth factor binding proteins. *Endocr. Rev.* **23**, 824–854 (2002).

80. Allard, J. B. & Duan, C. IGF-Binding Proteins: Why Do They Exist and Why Are There So Many? *Front. Endocrinol.* **9**, 117 (2018).

81. Arquier, N. *et al.* Drosophila ALS regulates growth and metabolism through functional interaction with insulin-like peptides. *Cell Metab.* **7**, 333–338 (2008).

82. Rajaram, S., Baylink, D. J. & Mohan, S. Insulin-Like Growth Factor-Binding Proteins in Serum and Other Biological Fluids: Regulation and Functions*. *Endocr. Rev.* **18**, 801–831 (1997).

83. Zapf, J., Hauri, C., Waldvogel, M. & Froesch, E. R. Acute metabolic effects and half-lives of intravenously administered insulinlike growth factors I and II in normal and hypophysectomized rats. *J. Clin. Invest.* **77**, 1768–1775 (1986).

84. Domené, H. M. *et al.* Human acid-labile subunit deficiency: clinical, endocrine and metabolic consequences. *Horm. Res.* **72**, 129–141 (2009).

85. Shore, D., Squire, M. & Nasmyth, K. A. Characterization of two genes required for the position-effect control of yeast mating-type genes. *EMBO J.* **3**, 2817–2823 (1984).

86. Rine, J. & Herskowitz, I. Four genes responsible for a position effect on expression from HML and HMR in Saccharomyces cerevisiae. *Genetics* **116**, 9–22 (1987).

87. Wu, M.-Y. & Wu, R.-C. A Sensitive and Flexible Assay for Determining Histone Deacetylase 1 (HDAC1) Activity. in *Histone Deacetylases* (ed. Sarkar, S.) vol. 1436 3–13 (Springer New York, 2016).

88. Liszt, G., Ford, E., Kurtev, M. & Guarente, L. Mouse Sir2 homolog SIRT6 is a nuclear ADP-ribosyltransferase. *J. Biol. Chem.* **280**, 21313–21320 (2005).

89. Cheng, H.-L. *et al.* Developmental defects and p53 hyperacetylation in Sir2 homolog (SIRT1)-deficient mice. *Proc. Natl. Acad. Sci.* **100**, 10794–10799 (2003).

90. Fang, Y., Tang, S. & Li, X. Sirtuins in Metabolic and Epigenetic Regulation of Stem Cells. *Trends Endocrinol. Metab.* **30**, 177–188 (2019).

91. Frye, R. A. Phylogenetic classification of prokaryotic and eukaryotic Sir2-like proteins. *Biochem. Biophys. Res. Commun.* **273**, 793–798 (2000).

92. Vassilopoulos, A., Fritz, K. S., Petersen, D. R. & Gius, D. The human sirtuin family: Evolutionary divergences and functions. *Hum. Genomics* **5**, 485 (2011).

93. Finkel, T., Deng, C.-X. & Mostoslavsky, R. Recent progress in the biology and physiology of sirtuins. *Nature* **460**, 587–591 (2009).

94. Tanno, M., Sakamoto, J., Miura, T., Shimamoto, K. & Horio, Y. Nucleocytoplasmic shuttling of the NAD+-dependent histone deacetylase SIRT1. *J. Biol. Chem.* **282**, 6823–6832 (2007).

95. Mostoslavsky, R. *et al.* Genomic instability and aging-like phenotype in the absence of mammalian SIRT6. *Cell* **124**, 315–329 (2006).

96. Ford, E. *et al.* Mammalian Sir2 homolog SIRT7 is an activator of RNA polymerase I transcription. *Genes Dev.* **20**, 1075–1080 (2006).

97. van de Ven, R. A. H., Santos, D. & Haigis, M. C. Mitochondrial Sirtuins and Molecular Mechanisms of Aging. *Trends Mol. Med.* **23**, 320–331 (2017).

98. Min, Z., Gao, J. & Yu, Y. The Roles of Mitochondrial SIRT4 in Cellular Metabolism. *Front. Endocrinol.* **9**, 783 (2019).

99. Yaku, K., Okabe, K. & Nakagawa, T. NAD metabolism: Implications in aging and longevity. *Ageing Res. Rev.* **47**, 1–17 (2018).

100. Strømland, Ø. *et al.* Keeping the balance in NAD metabolism. *Biochem. Soc. Trans.* **47**, 119–130 (2019).

101. Liu, L. *et al.* Quantitative Analysis of NAD Synthesis-Breakdown Fluxes. *Cell Metab.* **27**, 1067-1080.e5 (2018).

102. Igarashi, M. *et al.* NAD $^{+}$ supplementation rejuvenates aged gut adult stem cells. *Aging Cell* **18**, e12935 (2019).

103. Bitterman, K. J., Anderson, R. M., Cohen, H. Y., Latorre-Esteves, M. & Sinclair, D. A. Inhibition of Silencing and Accelerated Aging by Nicotinamide, a Putative Negative Regulator of Yeast Sir2 and Human SIRT1. *J. Biol. Chem.* **277**, 45099–45107 (2002).

104. Malavasi, F. *et al.* The hidden life of NAD+-consuming ectoenzymes in the endocrine system. *J. Mol. Endocrinol.* **45**, 183–191 (2010).

105. Cantó, C., Menzies, K. J. & Auwerx, J. NAD+ Metabolism and the Control of Energy Homeostasis: A Balancing Act between Mitochondria and the Nucleus. *Cell Metab.* **22**, 31–53 (2015).

106. Okabe, K., Yaku, K., Tobe, K. & Nakagawa, T. Implications of altered NAD metabolism in metabolic disorders. *J. Biomed. Sci.* **26**, 34 (2019).

107. Bonkowski, M. S. & Sinclair, D. A. Slowing ageing by design: the rise of NAD+ and sirtuin-activating compounds. *Nat. Rev. Mol. Cell Biol.* **17**, 679–690 (2016).

108. Elvehjem, C. A., Madden, R. J., Strong, F. M. & Wolley, D. W. The isolation and identification of the anti-black tongue factor. 1937. *J. Biol. Chem.* **277**, e22 (2002).

109. Fischer, F. *et al.* Sirt5 Deacylation Activities Show Differential Sensitivities to Nicotinamide Inhibition. *PLoS ONE* **7**, e45098 (2012).

110. Avalos, J. L., Bever, K. M. & Wolberger, C. Mechanism of sirtuin inhibition by nicotinamide: altering the NAD(+) cosubstrate specificity of a Sir2 enzyme. *Mol. Cell* **17**, 855–868 (2005).

111. Rahnasto-Rilla, M., Lahtela-Kakkonen, M. & Moaddel, R. Sirtuin 6 (SIRT6) Activity Assays. in *Histone Deacetylases* (ed. Sarkar, S.) vol. 1436 259–269 (Springer New York, 2016).

112. McBurney, M. W., Clark-Knowles, K. V., Caron, A. Z. & Gray, D. A. SIRT1 is a Highly Networked Protein That Mediates the Adaptation to Chronic Physiological Stress. *Genes Cancer* **4**, 125–134 (2013).

113. Dang, W. The controversial world of sirtuins. *Drug Discov. Today Technol.* **12**, e9–e17 (2014).

114. Sun, Y. & Dang, W. The Controversy Around Sirtuins and Their Functions in Aging. in *Molecular Basis of Nutrition and Aging* 227–241 (Elsevier, 2016). doi:10.1016/B978-0-12-801816-3.00017-0.

115. Barber, M. F. *et al.* SIRT7 links H3K18 deacetylation to maintenance of oncogenic transformation. *Nature* **487**, 114–118 (2012).

116. Kim, J. K. *et al.* Sirtuin7 oncogenic potential in human hepatocellular carcinoma and its regulation by the tumor suppressors MiR-125a-5p and MiR-125b. *Hepatology* **57**, 1055–1067 (2013).

117. Zhao, L. & Wang, W. miR-125b suppresses the proliferation of hepatocellular carcinoma cells by targeting Sirtuin7. *Int. J. Clin. Exp. Med.* **8**, 18469–18475 (2015).

118. Vakhrusheva, O. *et al.* Sirt7 Increases Stress Resistance of Cardiomyocytes and Prevents Apoptosis and Inflammatory Cardiomyopathy in Mice. *Circ. Res.* **102**, 703–710 (2008).

119. Seman, M., Adriouch, S., Haag, F. & Koch-Nolte, F. Ecto-ADP-ribosyltransferases (ARTs): emerging actors in cell communication and signaling. *Curr. Med. Chem.* **11**, 857–872 (2004).

120. Mao, Z. *et al.* SIRT6 Promotes DNA Repair Under Stress by Activating PARP1. *Science* **332**, 1443–1446 (2011).

121. Jiang, H. *et al.* SIRT6 regulates TNF-α secretion through hydrolysis of long-chain fatty acyl lysine. *Nature* **496**, 110–113 (2013).

122. Zhong, L. *et al.* The histone deacetylase Sirt6 regulates glucose homeostasis via Hif1alpha. *Cell* **140**, 280–293 (2010).

123. Kumar, S. & Lombard, D. B. Generation and Purification of Catalytically Active Recombinant Sirtuin5 (SIRT5) Protein. in *Histone*

Deacetylases (ed. Sarkar, S.) vol. 1436 241–257 (Springer New York, 2016).

124. Du, J. *et al.* Sirt5 Is a NAD-Dependent Protein Lysine Demalonylase and Desuccinylase. *Science* **334**, 806–809 (2011).

125. Peng, C. *et al.* The first identification of lysine malonylation substrates and its regulatory enzyme. *Mol. Cell. Proteomics MCP* **10**, M111.012658 (2011).

126. Tan, M. *et al.* Lysine Glutarylation Is a Protein Posttranslational Modification Regulated by SIRT5. *Cell Metab.* **19**, 605–617 (2014).

127. Nakagawa, T., Lomb, D. J., Haigis, M. C. & Guarente, L. SIRT5 Deacetylates Carbamoyl Phosphate Synthetase 1 and Regulates the Urea Cycle. *Cell* **137**, 560–570 (2009).

128. Lin, Z.-F. *et al.* SIRT5 desuccinylates and activates SOD1 to eliminate ROS. *Biochem. Biophys. Res. Commun.* **441**, 191–195 (2013).

129. Liu, B. *et al.* SIRT5: A Safeguard Against Oxidative Stress-Induced Apoptosis in Cardiomyocytes. *Cell. Physiol. Biochem.* **32**, 1050–1059 (2013).

130. Mathias, R. A., Greco, T. M. & Cristea, I. M. Identification of Sirtuin4 (SIRT4) Protein Interactions: Uncovering Candidate Acyl-Modified Mitochondrial Substrates and Enzymatic Regulators. in *Histone Deacetylases* (ed. Sarkar, S.) vol. 1436 213–239 (Springer New York, 2016).

131. Kumar, S. & Lombard, D. B. For Certain, SIRT4 Activities! *Trends Biochem. Sci.* **42**, 499–501 (2017).

132. Haigis, M. C. *et al.* SIRT4 Inhibits Glutamate Dehydrogenase and Opposes the Effects of Calorie Restriction in Pancreatic β Cells. *Cell* **126**, 941–954 (2006).

133. Ahuja, N. *et al.* Regulation of Insulin Secretion by SIRT4, a Mitochondrial ADP-ribosyltransferase. *J. Biol. Chem.* **282**, 33583–33592 (2007).

134. Anderson, K. A. *et al.* SIRT4 Is a Lysine Deacylase that Controls Leucine Metabolism and Insulin Secretion. *Cell Metab.* **25**, 838-855.e15 (2017).

135. Laurent, G. *et al.* SIRT4 Coordinates the Balance between Lipid Synthesis and Catabolism by Repressing Malonyl CoA Decarboxylase. *Mol. Cell* **50**, 686–698 (2013).

136. Nasrin, N. *et al.* SIRT4 regulates fatty acid oxidation and mitochondrial gene expression in liver and muscle cells. *J. Biol. Chem.* **285**, 31995–32002 (2010).

137. Man, A. W. C., Bai, B. & Wang, Y. Cloning and Characterization of Sirtuin3 (SIRT3). in *Histone Deacetylases* (ed. Sarkar, S.) vol. 1436 201–211 (Springer New York, 2016).

138. Ansari, A. *et al.* Function of the SIRT3 mitochondrial deacetylase in cellular physiology, cancer, and neurodegenerative disease. *Aging Cell* **16**, 4–16 (2017).

139. Ozden, O. *et al.* SIRT3 deacetylates and increases pyruvate dehydrogenase activity in cancer cells. *Free Radic. Biol. Med.* **76**, 163–172 (2014).

140. Carrico, C., Meyer, J. G., He, W., Gibson, B. W. & Verdin, E. The Mitochondrial Acylome Emerges: Proteomics, Regulation by Sirtuins, and Metabolic and Disease Implications. *Cell Metab.* **27**, 497–512 (2018).

141. Jing, E. *et al.* Sirtuin-3 (Sirt3) regulates skeletal muscle metabolism and insulin signaling via altered mitochondrial oxidation and reactive oxygen species production. *Proc. Natl. Acad. Sci.* **108**, 14608–14613 (2011).

142. Cheng, Y. *et al.* Interaction of Sirt3 with OGG1 contributes to repair of mitochondrial DNA and protects from apoptotic cell death under oxidative stress. *Cell Death Dis.* **4**, e731–e731 (2013).

143. North, B. J. & Verdin, E. Interphase nucleo-cytoplasmic shuttling and localization of SIRT2 during mitosis. *PloS One* **2**, e784 (2007).

144. Vaquero, A. *et al.* SirT2 is a histone deacetylase with preference for histone H4 Lys 16 during mitosis. *Genes Dev.* **20**, 1256–1261 (2006).

145. Ji, S., Doucette, J. R. & Nazarali, A. J. Sirt2 is a novel in vivo downstream target of Nkx2.2 and enhances oligodendroglial cell differentiation. *J. Mol. Cell Biol.* **3**, 351–359 (2011).

146. Li, W. *et al.* Sirtuin 2, a Mammalian Homolog of Yeast Silent Information Regulator-2 Longevity Regulator, Is an Oligodendroglial Protein That Decelerates Cell Differentiation through Deacetylating -Tubulin. *J. Neurosci.* **27**, 2606–2616 (2007).

147. Jing, E., Gesta, S. & Kahn, C. R. SIRT2 Regulates Adipocyte Differentiation through FoxO1 Acetylation/Deacetylation. *Cell Metab.* **6**, 105–114 (2007).

148. Wang, F. & Tong, Q. SIRT2 Suppresses Adipocyte Differentiation by Deacetylating FOXO1 and Enhancing FOXO1's Repressive Interaction with PPARγ. *Mol. Biol. Cell* **20**, 801–808 (2009).

149. Ramakrishnan, G. *et al.* Sirt2 Deacetylase Is a Novel AKT Binding Partner Critical for AKT Activation by Insulin. *J. Biol. Chem.* **289**, 6054–6066 (2014).

150. Gomes, A. R. *et al.* Sirtuin1 (SIRT1) in the Acetylation of Downstream Target Proteins. in *Histone Deacetylases* (ed. Sarkar, S.) vol. 1436 169–188 (Springer New York, 2016).

151. Tang, S. *et al.* Methionine metabolism is essential for SIRT1-regulated mouse embryonic stem cell maintenance and embryonic development. *EMBO J.* **36**, 3175–3193 (2017).

152. Bordone, L. *et al.* Sirt1 Regulates Insulin Secretion by Repressing UCP2 in Pancreatic β Cells. *PLoS Biol.* **4**, e31 (2005).

153. Li, H. *et al.* SirT1 modulates the estrogen-insulin-like growth factor-1 signaling for postnatal development of mammary gland in mice. *Breast Cancer Res. BCR* **9**, R1 (2007).

154. Lemieux, M. E. *et al.* The Sirt1 deacetylase modulates the insulin-like growth factor signaling pathway in mammals. *Mech. Ageing Dev.* **126**, 1097–1105 (2005).

155. McBurney, M. W. *et al.* The mammalian SIR2alpha protein has a role in embryogenesis and gametogenesis. *Mol. Cell. Biol.* **23**, 38–54 (2003).

156. Dietrich, M. O. *et al.* Agrp Neurons Mediate Sirt1's Action on the Melanocortin System and Energy Balance: Roles for Sirt1 in Neuronal Firing and Synaptic Plasticity. *J. Neurosci.* **30**, 11815–11825 (2010).

157. Martins, L. *et al.* Hypothalamic mTOR Signaling Mediates the Orexigenic Action of Ghrelin. *PLoS ONE* **7**, e46923 (2012).

158. Fujitsuka, N. *et al.* Increased ghrelin signaling prolongs survival in mouse models of human aging through activation of sirtuin1. *Mol. Psychiatry* **21**, 1613–1623 (2016).

159. Velasquez, D. A. *et al.* The Central Sirtuin 1/p53 Pathway Is Essential for the Orexigenic Action of Ghrelin. *Diabetes* **60**, 1177–1185 (2011).

160. Giblin, W. & Lombard, D. B. Sirtuins, Healthspan, and Longevity in Mammals. in *Handbook of the Biology of Aging* 83–132 (Elsevier, 2016). doi:10.1016/B978-0-12-411596-5.00003-4.

161. Howitz, K. T. *et al.* Small molecule activators of sirtuins extend Saccharomyces cerevisiae lifespan. *Nature* **425**, 191–196 (2003).

162. Baur, J. A. Resveratrol, sirtuins, and the promise of a DR mimetic. *Mech. Ageing Dev.* **131**, 261–269 (2010).

163. Movahed, A. *et al.* Antihyperglycemic effects of short term resveratrol supplementation in type 2 diabetic patients. *Evid.-Based Complement. Altern. Med. ECAM* **2013**, 851267 (2013).

164. Bhatt, J. K., Thomas, S. & Nanjan, M. J. Resveratrol supplementation improves glycemic control in type 2 diabetes mellitus. *Nutr. Res. N. Y. N* **32**, 537–541 (2012).

165. Brasnyó, P. *et al.* Resveratrol improves insulin sensitivity, reduces oxidative stress and activates the Akt pathway in type 2 diabetic patients. *Br. J. Nutr.* **106**, 383–389 (2011).

166. Liu, K., Zhou, R., Wang, B. & Mi, M.-T. Effect of resveratrol on glucose control and insulin sensitivity: a meta-analysis of 11 randomized controlled trials. *Am. J. Clin. Nutr.* **99**, 1510–1519 (2014).

167. Kaeberlein, M., McVey, M. & Guarente, L. The SIR2/3/4 complex and SIR2 alone promote longevity in Saccharomyces cerevisiae by two different mechanisms. *Genes Dev.* **13**, 2570–2580 (1999).

168. Aström, S. U., Cline, T. W. & Rine, J. The Drosophila melanogaster sir2+ gene is nonessential and has only minor effects on position-effect variegation. *Genetics* **163**, 931–937 (2003).

169. Viswanathan, M., Kim, S. K., Berdichevsky, A. & Guarente, L. A Role for SIR-2.1 Regulation of ER Stress Response Genes in Determining C. elegans Life Span. *Dev. Cell* **9**, 605–615 (2005).

170. Peiris, T. H. *et al.* TOR signaling regulates planarian stem cells and controls localized and organismal growth. *J. Cell Sci.* **125**, 1657–1665 (2012).

171. Newmark, P. A. & Sánchez Alvarado, A. Not your father's planarian: a classic model enters the era of functional genomics. *Nat. Rev. Genet.* **3**, 210–219 (2002).

172. Reddien, P. W. & Alvarado, A. S. FUNDAMENTALS OF PLANARIAN REGENERATION. *Annu. Rev. Cell Dev. Biol.* **20**, 725–757 (2004).

173. Riutort, M., Álvarez-Presas, M., Lázaro, E., Sol, E. & Paps, J. Evolutionary history of the Tricladida and the Platyhelminthes: an up-to-

date phylogenetic and systematic account. *Int. J. Dev. Biol.* **56**, 5–17 (2012).

174. Baguñà, J. *et al.* From morphology and karyology to molecules. New methods for taxonomical identification of asexual populations of freshwater planarians. A tribute to Professor Mario Benazzi. *Ital. J. Zool.* **66**, 207–214 (1999).

175. Felix, D. A., Gutiérrez-Gutiérrez, Ó., Espada, L., Thems, A. & González-Estévez, C. It is not all about regeneration: Planarians striking power to stand starvation. *Semin. Cell Dev. Biol.* **87**, 169–181 (2019).

176. Sakurai, T. *et al.* The planarian P2X homolog in the regulation of asexual reproduction. *Int. J. Dev. Biol.* **56**, 173–182 (2012).

177. Best, J. B., Abelein, M., Kreutzer, E. & Pigon, A. Cephalic mechanism for social control of fissioning in planarians: III. Central nervous system centers of facilitation and inhibition. *J. Comp. Physiol. Psychol.* **89**, 923–932 (1975).

178. Best, J. B., Goodman, A. B. & Pigon, A. Fissioning in Planarians: Control by the Brain. *Science* **164**, 565–566 (1969).

179. Agata, K. *et al.* Structure of the planarian central nervous system (CNS) revealed by neuronal cell markers. *Zoolog. Sci.* **15**, 433–440 (1998).

180. Rink, J. C., Vu, H. T.-K. & Sánchez Alvarado, A. The maintenance and regeneration of the planarian excretory system are regulated by EGFR signaling. *Dev. Camb. Engl.* **138**, 3769–3780 (2011).

181. Currie, K. W. & Pearson, B. J. Transcription factors lhx1/5-1 and pitx are required for the maintenance and regeneration of serotonergic neurons in planarians. *Development* **140**, 3577–3588 (2013).

182. Forsthoefel, D. J., Park, A. E. & Newmark, P. A. Stem cell-based growth, regeneration, and remodeling of the planarian intestine. *Dev. Biol.* **356**, 445–459 (2011).

183. Roberts-Galbraith, R. H. & Newmark, P. A. On the organ trail: insights into organ regeneration in the planarian. *Curr. Opin. Genet. Dev.* **32**, 37–46 (2015).

184. Pellettieri, J. & Sánchez Alvarado, A. Cell turnover and adult tissue homeostasis: from humans to planarians. *Annu. Rev. Genet.* **41**, 83–105 (2007).

185. Reddien, P. W., Bermange, A. L., Murfitt, K. J., Jennings, J. R. & Sánchez Alvarado, A. Identification of Genes Needed for Regeneration, Stem Cell Function, and Tissue Homeostasis by Systematic Gene Perturbation in Planaria. *Dev. Cell* **8**, 635–649 (2005).

186. Peiris, T. H. & Oviedo, N. J. Gap junction proteins: Master regulators of the planarian stem cell response to tissue maintenance and injury. *Biochim. Biophys. Acta BBA - Biomembr.* **1828**, 109–117 (2013).

187. Pellettieri, J. *et al.* Cell death and tissue remodeling in planarian regeneration. *Dev. Biol.* **338**, 76–85 (2010).

188. Eisenhoffer, G. T., Kang, H. & Alvarado, A. S. Molecular Analysis of Stem Cells and Their Descendants during Cell Turnover and Regeneration in the Planarian Schmidtea mediterranea. *Cell Stem Cell* **3**, 327–339 (2008).

189. Thiruvalluvan, M., Barghouth, P. G., Tsur, A., Broday, L. & Oviedo, N. J. SUMOylation controls stem cell proliferation and regional cell death

through Hedgehog signaling in planarians. *Cell. Mol. Life Sci.* **75**, 1285–1301 (2018).

190. de Sousa, N., Rodríguez-Esteban, G., Rojo-Laguna, J. I., Saló, E. & Adell, T. Hippo signaling controls cell cycle and restricts cell plasticity in planarians. *PLOS Biol.* **16**, e2002399 (2018).

191. Zeng, A. *et al.* Prospectively Isolated Tetraspanin + Neoblasts Are Adult Pluripotent Stem Cells Underlying Planaria Regeneration. *Cell* **173**, 1593-1608.e20 (2018).

192. Wagner, D. E., Wang, I. E. & Reddien, P. W. Clonogenic neoblasts are pluripotent adult stem cells that underlie planarian regeneration. *Science* **332**, 811–816 (2011).

193. Morgan, T. H. Regeneration in Planarians. (1900).

194. Morgan, T. H. Experimental Studies of the Regeneration of Planaria muculata. (1898).

195. Wenemoser, D. & Reddien, P. W. Planarian regeneration involves distinct stem cell responses to wounds and tissue absence. *Dev. Biol.* **344**, 979–991 (2010).

196. Tasaki, J. *et al.* ERK signaling controls blastema cell differentiation during planarian regeneration. *Dev. Camb. Engl.* **138**, 2417–2427 (2011).

197. Elliott, S. A. & Sánchez Alvarado, A. The history and enduring contributions of planarians to the study of animal regeneration. *Wiley Interdiscip. Rev. Dev. Biol.* **2**, 301–326 (2013).

198. Petersen, C. P. & Reddien, P. W. Polarized notum Activation at Wounds Inhibits Wnt Function to Promote Planarian Head Regeneration. *Science* **332**, 852–855 (2011).

199. Salo, E. *et al.* Planarian regeneration: achievements and future directions after 20 years of research. *Int. J. Dev. Biol.* **53**, 1317–1327 (2009).

200. Sandmann, T., Vogg, M. C., Owlarn, S., Boutros, M. & Bartscherer, K. The head-regeneration transcriptome of the planarian Schmidtea mediterranea. *Genome Biol.* **12**, R76 (2011).

201. Rink, J. C. Stem cell systems and regeneration in planaria. *Dev. Genes Evol.* **223**, 67–84 (2013).

202. Kato, K., Orii, H., Watanabe, K. & Agata, K. The role of dorsoventral interaction in the onset of planarian regeneration. *Dev. Camb. Engl.* **126**, 1031–1040 (1999).

203. Oviedo, N. J. *et al.* Long-range neural and gap junction protein-mediated cues control polarity during planarian regeneration. *Dev. Biol.* **339**, 188–199 (2010).

204. Oviedo, N. J. & Levin, M. smedinx-11 is a planarian stem cell gap junction gene required for regeneration and homeostasis. *Development* **134**, 3121–3131 (2007).

205. Roberts-Galbraith, R. H. & Newmark, P. A. Follistatin antagonizes activin signaling and acts with notum to direct planarian head regeneration. *Proc. Natl. Acad. Sci. U. S. A.* **110**, 1363–1368 (2013).

206. Gurley, K. A., Rink, J. C. & Alvarado, A. S. Beta-Catenin Defines Head Versus Tail Identity During Planarian Regeneration and Homeostasis. *Science* **319**, 323–327 (2008).

207. Molina, M. D. *et al.* Noggin and Noggin-Like Genes Control Dorsoventral Axis Regeneration in Planarians. *Curr. Biol.* **21**, 300–305 (2011).

208. Scimone, M. L., Lapan, S. W. & Reddien, P. W. A forkhead Transcription Factor Is Wound-Induced at the Planarian Midline and Required for Anterior Pole Regeneration. *PLoS Genet.* **10**, e1003999 (2014).

209. Witchley, J. N., Mayer, M., Wagner, D. E., Owen, J. H. & Reddien, P. W. Muscle Cells Provide Instructions for Planarian Regeneration. *Cell Rep.* **4**, 633–641 (2013).

210. Chen, C.-C. G., Wang, I. E. & Reddien, P. W. pbx is required for pole and eye regeneration in planarians. *Development* **140**, 719–729 (2013).

211. Lapan, S. W. & Reddien, P. W. Transcriptome Analysis of the Planarian Eye Identifies ovo as a Specific Regulator of Eye Regeneration. *Cell Rep.* **2**, 294–307 (2012).

212. Handberg-Thorsager, M. & Saló, E. The planarian nanos-like gene Smednos is expressed in germline and eye precursor cells during development and regeneration. *Dev. Genes Evol.* **217**, 403–411 (2007).

213. Cowles, M. W., Omuro, K. C., Stanley, B. N., Quintanilla, C. G. & Zayas, R. M. COE Loss-of-Function Analysis Reveals a Genetic Program Underlying Maintenance and Regeneration of the Nervous System in Planarians. *PLoS Genet.* **10**, e1004746 (2014).

214. Cebrià, F., Guo, T., Jopek, J. & Newmark, P. A. Regeneration and maintenance of the planarian midline is regulated by a slit orthologue. *Dev. Biol.* **307**, 394–406 (2007).

215. Kobayashi, C., Watanabe, K. & Agata, K. The process of pharynx regeneration in planarians. *Dev. Biol.* **211**, 27–38 (1999).

216. Felix, D. A. & Aboobaker, A. A. The TALE Class Homeobox Gene Smed-prep Defines the Anterior Compartment for Head Regeneration. *PLoS Genet.* **6**, e1000915 (2010).

217. Roberts-Galbraith, R. H., Brubacher, J. L. & Newmark, P. A. A functional genomics screen in planarians reveals regulators of whole-brain regeneration. *eLife* **5**, (2016).

218. Reddien, P. W., Oviedo, N. J., Jennings, J. R., Jenkin, J. C. & Sánchez Alvarado, A. SMEDWI-2 is a PIWI-like protein that regulates planarian stem cells. *Science* **310**, 1327–1330 (2005).

219. Higuchi, S. *et al.* Characterization and categorization of fluorescence activated cell sorted planarian stem cells by ultrastructural analysis: Heterogeneity of planarian stem cells. *Dev. Growth Differ.* **49**, 571–581 (2007).

220. Hayashi, T., Asami, M., Higuchi, S., Shibata, N. & Agata, K. Isolation of planarian X-ray-sensitive stem cells by fluorescence-activated cell sorting. *Dev. Growth Differ.* **48**, 371–380 (2006).

221. Palakodeti, D., Smielewska, M., Lu, Y.-C., Yeo, G. W. & Graveley, B. R. The PIWI proteins SMEDWI-2 and SMEDWI-3 are required for stem cell function and piRNA expression in planarians. *RNA N. Y. N* **14**, 1174–1186 (2008).

222. Robb, S. M. C., Gotting, K., Ross, E. & Sánchez Alvarado, A. SmedGD 2.0: The *Schmidtea mediterranea* genome database: The Planarian Genome Database. *genesis* **53**, 535–546 (2015).

223. Cantarel, B. L. *et al.* MAKER: An easy-to-use annotation pipeline designed for emerging model organism genomes. *Genome Res.* **18**, 188–196 (2007).

224. Alvarado, A. S. The Schmidtea mediterranea database as a molecular resource for studying platyhelminthes, stem cells and regeneration. *Development* **129**, 5659–5665 (2002).

225. Brandl, H. *et al.* PlanMine – a mineable resource of planarian biology and biodiversity. *Nucleic Acids Res.* **44**, D764–D773 (2016).

226. Wurtzel, O. *et al.* A Generic and Cell-Type-Specific Wound Response Precedes Regeneration in Planarians. *Dev. Cell* **35**, 632–645 (2015).

227. Fincher, C. T., Wurtzel, O., de Hoog, T., Kravarik, K. M. & Reddien, P. W. Cell type transcriptome atlas for the planarian *Schmidtea mediterranea*. *Science* **360**, eaaq1736 (2018).

228. Rozanski, A. *et al.* PlanMine 3.0—improvements to a mineable resource of flatworm biology and biodiversity. *Nucleic Acids Res.* **47**, D812–D820 (2019).

229. Swapna, L. S., Molinaro, A. M., Lindsay-Mosher, N., Pearson, B. J. & Parkinson, J. Comparative transcriptomic analyses and single-cell RNA sequencing of the freshwater planarian Schmidtea mediterranea identify major cell types and pathway conservation. *Genome Biol.* **19**, 124 (2018).

230. van Wolfswinkel, J. C., Wagner, D. E. & Reddien, P. W. Single-Cell Analysis Reveals Functionally Distinct Classes within the Planarian Stem Cell Compartment. *Cell Stem Cell* **15**, 326–339 (2014).

231. Oviedo, N. J., Newmark, P. A. & Sánchez Alvarado, A. Allometric scaling and proportion regulation in the freshwater planarian Schmidtea mediterranea. *Dev. Dyn. Off. Publ. Am. Assoc. Anat.* **226**, 326–333 (2003).

232. Baguñà, J. *et al.* Growth, Degrowth and Regeneration as Developmental Phenomena in Adult Freshwater Planarians. in *Experimental Embryology in Aquatic Plants and Animals* (ed. Marthy, H.-J.) 129–162 (Springer US, 1990). doi:10.1007/978-1-4615-3830-1_7.

233. Takeda, H., Nishimura, K. & Agata, K. Planarians maintain a constant ratio of different cell types during changes in body size by using the stem cell system. *Zoolog. Sci.* **26**, 805–813 (2009).

234. Baguna, J. & Romero, R. Quantitative analysis of cell types during growth, degrowth and regeneration in the planarians Dugesia mediterranea and Dugesia tigrina. *Hydrobiologia* **84**, 181–194 (1981).

235. Thommen, A. *et al.* Body size-dependent energy storage causes Kleiber's law scaling of the metabolic rate in planarians. *eLife* **8**, (2019).

236. Shimoyama, S., Inoue, T., Kashima, M. & Agata, K. Multiple Neuropeptide-Coding Genes Involved in Planarian Pharynx Extension. *Zoolog. Sci.* **33**, 311–319 (2016).

237. Tu, K. C., Pearson, B. J. & Sánchez Alvarado, A. TORC1 is required to balance cell proliferation and cell death in planarians. *Dev. Biol.* **365**, 458–469 (2012).

238. Peiris, T. H., Ramirez, D., Barghouth, P. G. & Oviedo, N. J. The Akt signaling pathway is required for tissue maintenance and regeneration in planarians. *BMC Dev. Biol.* **16**, 7 (2016).

239. Nässel, D. R., Liu, Y. & Luo, J. Insulin/IGF signaling and its regulation in Drosophila. *Gen. Comp. Endocrinol.* **221**, 255–266 (2015).

240. Rulifson, E. J., Kim, S. K. & Nusse, R. Ablation of insulin-producing neurons in flies: growth and diabetic phenotypes. *Science* **296**, 1118–1120 (2002).

241. Murphy, C. T. & Hu, P. J. Insulin/insulin-like growth factor signaling in C. elegans. *WormBook Online Rev. C Elegans Biol.* 1–43 (2013) doi:10.1895/wormbook.1.164.1.

242. Vallejo, D. M., Juarez-Carreño, S., Bolivar, J., Morante, J. & Dominguez, M. A brain circuit that synchronizes growth and maturation revealed through Dilp8 binding to Lgr3. *Science* **350**, aac6767 (2015).

243. Russell, R. C., Fang, C. & Guan, K.-L. An emerging role for TOR signaling in mammalian tissue and stem cell physiology. *Development* **138**, 3343–3356 (2011).

244. Tan, T. C. J. *et al.* Telomere maintenance and telomerase activity are differentially regulated in asexual and sexual worms. *Proc. Natl. Acad. Sci.* **109**, 4209–4214 (2012).

245. Iglesias, M. *et al.* Downregulation of mTOR Signaling Increases Stem Cell Population Telomere Length during Starvation of Immortal Planarians. *Stem Cell Rep.* **13**, 405–418 (2019).

246. Pearson, B. J. *et al.* Formaldehyde-based whole-mount in situ hybridization method for planarians. *Dev. Dyn.* **238**, 443–450 (2009).

247. King, R. S. & Newmark, P. A. In situ hybridization protocol for enhanced detection of gene expression in the planarian Schmidtea mediterranea. *BMC Dev. Biol.* **13**, 8 (2013).

248. Brown, D. D. R. & Pearson, B. J. One FISH, dFISH, Three FISH: Sensitive Methods of Whole-Mount Fluorescent In Situ Hybridization in Freshwater Planarians. in *In Situ Hybridization Methods* (ed. Hauptmann, G.) vol. 99 127–150 (Springer New York, 2015).

249. Newmark, P. A. & Sánchez Alvarado, A. Bromodeoxyuridine specifically labels the regenerative stem cells of planarians. *Dev. Biol.* **220**, 142–153 (2000).

250. Robb, S. M. C. & Alvarado, A. S. Identification of immunological reagents for use in the study of freshwater planarians by means of whole-mount immunofluorescence and confocal microscopy. *genesis* **32**, 293–298 (2002).

251. Ross, K. G. *et al.* Novel monoclonal antibodies to study tissue regeneration in planarians. *BMC Dev. Biol.* **15**, 2 (2015).

252. Hans, F. & Dimitrov, S. Histone H3 phosphorylation and cell division. *Oncogene* **20**, 3021–3027 (2001).

253. Rawls, S. M., Patil, T., Yuvasheva, E. & Raffa, R. B. First evidence that drugs of abuse produce behavioral sensitization and cross sensitization in planarians. *Behav. Pharmacol.* **21**, 301–313 (2010).

254. Newmark, P. A., Reddien, P. W., Cebrià, F. & Sánchez Alvarado, A. Ingestion of bacterially expressed double-stranded RNA inhibits gene expression in planarians. *Proc. Natl. Acad. Sci. U. S. A.* **100 Suppl 1**, 11861–11865 (2003).

255. Rouhana, L. *et al.* RNA interference by feeding in vitro-synthesized double-stranded RNA to planarians: Methodology and dynamics: Planarian

RNAi by Feeding in Vitro-Synthesized dsRNA. *Dev. Dyn.* **242**, 718–730 (2013).

256. Orii, H., Mochii, M. & Watanabe, K. A simple 'soaking method' for RNA interference in the planarian Dugesia japonica. *Dev. Genes Evol.* **213**, 138–141 (2003).

257. Sánchez Alvarado, A. & Newmark, P. A. Double-stranded RNA specifically disrupts gene expression during planarian regeneration. *Proc. Natl. Acad. Sci. U. S. A.* **96**, 5049–5054 (1999).

258. Oviedo, N. J., Nicolas, C. L., Adams, D. S. & Levin, M. Establishing and maintaining a colony of planarians. *CSH Protoc.* **2008**, pdb.prot5053 (2008).

259. Oviedo, N. J., Nicolas, C. L., Adams, D. S. & Levin, M. Gene knockdown in planarians using RNA interference. *CSH Protoc.* **2008**, pdb.prot5054 (2008).

260. Peiris, T. H. *et al.* Regional signals in the planarian body guide stem cell fate in the presence of genomic instability. *Development* **143**, 1697–1709 (2016).

261. Satoh, A., Stein, L. & Imai, S. The Role of Mammalian Sirtuins in the Regulation of Metabolism, Aging, and Longevity. in *Histone Deacetylases: the Biology and Clinical Implication* (eds. Yao, T.-P. & Seto, E.) vol. 206 125–162 (Springer Berlin Heidelberg, 2011).

262. Stückemann, T. *et al.* Antagonistic Self-Organizing Patterning Systems Control Maintenance and Regeneration of the Anteroposterior Axis in Planarians. *Dev. Cell* **40**, 248-263.e4 (2017).

263. Aditi, K., Shakarad, M. N. & Agrawal, N. Altered lipid metabolism in Drosophila model of Huntington's disease. *Sci. Rep.* **6**, 31411 (2016).

264. Debban, C. L. & Dyer, K. A. No evidence for behavioural adaptations to nematode parasitism by the fly Drosophila putrida. *J. Evol. Biol.* **26**, 1646–1654 (2013).

265. Collins, J. J. *et al.* Genome-Wide Analyses Reveal a Role for Peptide Hormones in Planarian Germline Development. *PLoS Biol.* **8**, e1000509 (2010).

266. Baguna, J. & Romero, R. Quantitative analysis of cell types during growth, degrowth and regeneration in the planarians Dugesia mediterranea and Dugesia tigrina. *Hydrobiologia* **84**, 181–194 (1981).

267. Kang, H. & Sánchez Alvarado, A. Flow cytometry methods for the study of cell-cycle parameters of planarian stem cells. *Dev. Dyn. Off. Publ. Am. Assoc. Anat.* **238**, 1111–1117 (2009).

268. Baguñà, J. Dramatic mitotic response in planarians after feeding, and a hypothesis for the control mechanism. *J. Exp. Zool.* **190**, 117–122 (1974).

269. Mizushima, N., Yoshimori, T. & Ohsumi, Y. The role of Atg proteins in autophagosome formation. *Annu. Rev. Cell Dev. Biol.* **27**, 107–132 (2011).

270. Levine, B. & Kroemer, G. Biological Functions of Autophagy Genes: A Disease Perspective. *Cell* **176**, 11–42 (2019).

271. González-Estévez, C., Felix, D. A., Aboobaker, A. A. & Saló, E. Gtdap-1 promotes autophagy and is required for planarian remodeling during regeneration and starvation. *Proc. Natl. Acad. Sci. U. S. A.* **104**, 13373–13378 (2007).

272. Zhu, S. J., Hallows, S. E., Currie, K. W., Xu, C. & Pearson, B. J. A mex3 homolog is required for differentiation during planarian stem cell lineage development. *eLife* **4**, e07025 (2015).

273. Forsthoefel, D. J. *et al.* An RNAi Screen Reveals Intestinal Regulators of Branching Morphogenesis, Differentiation, and Stem Cell Proliferation in Planarians. *Dev. Cell* **23**, 691–704 (2012).

274. Barberán, S., Fraguas, S. & Cebrià, F. The EGFR signaling pathway controls gut progenitor differentiation during planarian regeneration and homeostasis. *Development* **143**, 2089–2102 (2016).

275. González-Estévez, C. *et al.* SMG-1 and mTORC1 act antagonistically to regulate response to injury and growth in planarians. *PLoS Genet.* **8**, e1002619 (2012).

276. Sebans, K. P. The Ecology of Intermediate Growth in Animals. *Annual Review of Ecology and Systemics* **18**, 371–407 (1987).

277. Prozorovski, T. *et al.* Sirt1 contributes critically to the redox-dependent fate of neural progenitors. *Nat. Cell Biol.* **10**, 385–394 (2008).

278. Arul Nambi Rajan, K. *et al.* Sirtuin1 is required for proper trophoblast differentiation and placental development in mice. *Placenta* **62**, 1–8 (2018).

279. Calvanese, V. *et al.* Sirtuin 1 regulation of developmental genes during differentiation of stem cells. *Proc. Natl. Acad. Sci.* **107**, 13736–13741 (2010).

280. Saunders, L. R. *et al.* miRNAs regulate SIRT1 expression during mouse embryonic stem cell differentiation and in adult mouse tissues. *Aging* **2**, 415–431 (2010).

281. Hisahara, S. *et al.* Histone deacetylase SIRT1 modulates neuronal differentiation by its nuclear translocation. *Proc. Natl. Acad. Sci. U. S. A.* **105**, 15599–15604 (2008).

282. Ou, X. *et al.* SIRT1 deficiency compromises mouse embryonic stem cell hematopoietic differentiation, and embryonic and adult hematopoiesis in the mouse. *Blood* **117**, 440–450 (2011).

283. Igarashi, M. & Guarente, L. mTORC1 and SIRT1 Cooperate to Foster Expansion of Gut Adult Stem Cells during Calorie Restriction. *Cell* **166**, 436–450 (2016).

284. Fraguas, S., Barberán, S. & Cebrià, F. EGFR signaling regulates cell proliferation, differentiation and morphogenesis during planarian regeneration and homeostasis. *Dev. Biol.* **354**, 87–101 (2011).

285. Tu, K. C. *et al.* Egr-5 is a post-mitotic regulator of planarian epidermal differentiation. *eLife* **4**, e10501 (2015).

286. Zhu, S. J. & Pearson, B. J. Smed-myb-1 Specifies Early Temporal Identity during Planarian Epidermal Differentiation. *Cell Rep.* **25**, 38-46.e3 (2018).

287. Brøndsted, H. V. *Planarian Regeneration*. (Pergamon, 1969).

288. Casali, A. & Batlle, E. Intestinal stem cells in mammals and Drosophila. *Cell Stem Cell* **4**, 124–127 (2009).

289. Faro, A., Boj, S. F. & Clevers, H. Fishing for intestinal cancer models: unraveling gastrointestinal homeostasis and tumorigenesis in zebrafish. *Zebrafish* **6**, 361–376 (2009).

290. Illa-Bochaca, I. & Montuenga, L. M. The regenerative nidi of the locust midgut as a model to study epithelial cell differentiation from stem cells. *J. Exp. Biol.* **209**, 2215–2223 (2006).

291. Ishizuya-Oka, A. Regeneration of the amphibian intestinal epithelium under the control of stem cell niche. *Dev. Growth Differ.* **49**, 99–107 (2007).

292. van der Flier, L. G. & Clevers, H. Stem cells, self-renewal, and differentiation in the intestinal epithelium. *Annu. Rev. Physiol.* **71**, 241–260 (2009).

293. Klok, M. D., Jakobsdottir, S. & Drent, M. L. The role of leptin and ghrelin in the regulation of food intake and body weight in humans: a review. *Obes. Rev. Off. J. Int. Assoc. Study Obes.* **8**, 21–34 (2007).

294. Inui, A. *et al.* Ghrelin, appetite, and gastric motility: the emerging role of the stomach as an endocrine organ. *FASEB J. Off. Publ. Fed. Am. Soc. Exp. Biol.* **18**, 439–456 (2004).

295. Kajimura, S., Aida, K. & Duan, C. Understanding Hypoxia-Induced Gene Expression in Early Development: In Vitro and In Vivo Analysis of Hypoxia-Inducible Factor 1-Regulated Zebra Fish Insulin-Like Growth Factor Binding Protein 1 Gene Expression. *Mol. Cell. Biol.* **26**, 1142–1155 (2006).

296. Clemmons, D. R. Use of mutagenesis to probe IGF-binding protein structure/function relationships. *Endocr. Rev.* **22**, 800–817 (2001).

297. Crossey, P. A., Pillai, C. C. & Miell, J. P. Altered placental development and intrauterine growth restriction in IGF binding protein-1 transgenic mice. *J. Clin. Invest.* **110**, 411–418 (2002).

298. Gay, E. *et al.* Liver-specific expression of human insulin-like growth factor binding protein-1 in transgenic mice: repercussions on reproduction, ante- and perinatal mortality and postnatal growth. *Endocrinology* **138**, 2937–2947 (1997).

299. Rajkumar, K., Barron, D., Lewitt, M. S. & Murphy, L. J. Growth retardation and hyperglycemia in insulin-like growth factor binding protein-1 transgenic mice. *Endocrinology* **136**, 4029–4034 (1995).

300. Yakar, S. *et al.* Serum complexes of insulin-like growth factor-1 modulate skeletal integrity and carbohydrate metabolism. *FASEB J.* **23**, 709–719 (2009).

301. Green, K. N. *et al.* Nicotinamide restores cognition in Alzheimer's disease transgenic mice via a mechanism involving sirtuin inhibition and selective reduction of Thr231-phosphotau. *J. Neurosci. Off. J. Soc. Neurosci.* **28**, 11500–11510 (2008).

302. Sauve, A. A. & Schramm, V. L. Sir2 regulation by nicotinamide results from switching between base exchange and deacetylation chemistry. *Biochemistry* **42**, 9249–9256 (2003).

303. Knop, F. K. *et al.* Thirty days of resveratrol supplementation does not affect postprandial incretin hormone responses, but suppresses postprandial glucagon in obese subjects. *Diabet. Med. J. Br. Diabet. Assoc.* **30**, 1214–1218 (2013).

304. Nguyen, A. V. *et al.* Results of a phase I pilot clinical trial examining the effect of plant-derived resveratrol and grape powder on Wnt pathway target gene expression in colonic mucosa and colon cancer. *Cancer Manag. Res.* **1**, 25–37 (2009).

305. Sanchez-Fidalgo, S., Villegas, I., Sanchez-Hidalgo, M. & de la Lastra, C. A. Sirtuin modulators: mechanisms and potential clinical implications. *Curr. Med. Chem.* **19**, 2414–2441 (2012).

306. DeBerardinis, R. J., Lum, J. J., Hatzivassiliou, G. & Thompson, C. B. The biology of cancer: metabolic reprogramming fuels cell growth and proliferation. *Cell Metab.* **7**, 11–20 (2008).

307. Houtkooper, R. H., Pirinen, E. & Auwerx, J. Sirtuins as regulators of metabolism and healthspan. *Nat. Rev. Mol. Cell Biol.* **13**, 225–238 (2012).

308. Goupil, L. S. *et al.* Cysteine and Aspartyl Proteases Contribute to Protein Digestion in the Gut of Freshwater Planaria. *PLoS Negl. Trop. Dis.* **10**, e0004893 (2016).

309. Osuma, E. A., Riggs, D. W., Gibb, A. A. & Hill, B. G. High throughput measurement of metabolism in planarians reveals activation of glycolysis during regeneration. *Regeneration* **5**, 78–86 (2018).

5. Appendix

6.1. RNA extractions

1) Place all samples into 2mL screw cap tubes.
2) For each sample, extract all the water out first using a transfer pipette, then use a plastic pipette tip.
3) Add 1mL of trizol into each sample.
4) Add a small amount of plastic beads to the tubes.
5) Homogenize each sample using Nobiles homogenization device (program1-1min).
6) Spin samples to force beads and tissue to the bottom of tubes.
8) Let the samples sit for 5 mins @RT.
9) Add 266uL of chloroform per sample inside the fume hood.
10) Shake samples by hand vigorously (~15 secs) and let them sit @RT for 3 mins.
11) Spin samples for 15 mins 11000 rpm @4C.
12) Extract the clear layer into new RNase DNase free tubes.
13) Add 666.66uL of isopropanol.
14) Mix by inversion & let the samples sit for 10 mins @RT.
15) Spin samples for 10 mins 11000 rpm @4C.
16) Take out the supernatant & wash samples with 1mL of 75% EtOH (use 75% EtOH in -20C).
17) Spin samples for 5 mins 7500 rpm @4C.
18) Take out supernatant using a pipette (spin again to remove all EtOH) & air-dry it for about 2 mins.
19) Add 15uL of RNase free water to sample and incubate samples on ice for a few mins. The tissue eventually dissolves in the water (pipetting or shaking the samples at this point might result in breaking RNA components). Gentle is good.
20) Use nano drop to measure RNA concentration. Add more RNase free water to dilute the sample.
21) stored samples in -80C

Nano dropped DNA	ng/uL	260/230	260/280	1 ug (uL)

6.2. Verso cDNA synthesis

-Using RNase free PCR tubes add the following:

dNTP Mix	2uL
5x cDNA synthesis Buffer	4uL
RT Enhancer	1uL
Anchored oligo dTs	1uL
Verso Enzyme mix	1uL

Nano dropped DNA	ng/uL	1 ug (uL)	11uL total vol w/H2O
	X	Y=1000/X	11-Y

1. Master mix was made for samples, 9uL of master mix was added to each tube.
2. Incubated for 30 mins @ 42C followed by 2 mins @95C using the PCR machine.
3. Samples placed on ice, then stored @ -20C.

6.3. PCR and gel electrophoresis

1) While PCR is running, create 50ml of 1.0% agarose gel with 1x TBE (0.5g agarose in 50ml fresh 1xTBE).
2) Heat the gel in the microwave (1min).
3) Once all agarose is dissolved, remove from microwave and add 2µl of EtBr.
4) Pour gel w/ EtBr into cassette with comb; let agarose settle while PCR is running.
5) Once settled, fill to the fill line with 1x TBE.
6) Load wells with 2µl of Ladder and 7µl of (5µLPCR product: 2µl of 6xloading dye).
7) Run at 125V for 30 mins with the negative pole on the well side.
8) Once complete, image the gel using a UV Light.

Tube #	1X
Water	20.6
PCR Buffer+ MgCl2	2.5
DNTPs	0.5
Taq Polymerase	0.5
F primer	0.3125
R primer	0.3125

6.4. Topo cloning

-Combine the following in a tube:

Amplified DNA (fresh pcr products)	2uL
Salts [NaCl (1.2M), $MgCl_2$ (0.06M)]	1uL
Sterile Water	2uL
Topo-activated TA Vector (10ng/uL)	1uL

1. Gently mix and incubate @ RT for 30 mins.
2. Transfer reaction to ice.

3. Transform and Mini-prep.

6.5. Transformation

1. Combine one half of a tube of NEB5alpha bacteria (25 uL) with 2uL of cloning mix**.
2. Incubate tubes on ice for 30 mins.
3. Place tubes in 42C water bath and incubate for 45 secs.
4. Immediately return tubes to ice for 2 mins.
5. Add 250uL of S.O.C. media to tubes and rocked for 1 hr 225 rpm @ 37C.
6. Using sterile technique, add 300uL of the sample to Cabenicillin(Topo/pBlueScript) agar plates and spread evenly.
7. Let places sit face up for 30 mins, then incubate overnight @ 37C.
8. Pick a single colony with a pipette tip and place into 5mL 2XYT media with 10uL Carbenicillin (100ug/mL).
9. Incubate tube overnight (16-20 hrs) 225 rpm @ 37C.

** For sub-cloning of pBlueScript, use 5uL of ligation reaction.

6.6. Mini-prep

1. Overnight culture tubes were spun for 5 mins 5000rpm @ 4C.
2. Liquid was decanted and 250uL of P1 Buffer was added to tubes resuspending the pellet.
3. Resuspended solution was then transferred into a 2mL tube.
4. 250uL of P2 was added to the tubes, and then tubes were inverted 4-6 times.
5. Tubes were carefully opened to avoid mucus from spilling everywhere. 350uL of N3 Buffer was then added to the tubes, which were then spun for 10 mins 13000 rpm @ RT.
6. Switched gloves to avoid contamination.
7. Liquid was then decanted into a QIA Prep spin column.
8. Tubes were spun for 1 min 13000 rpm @ RT.
9. Flow through liquid was removed with a pipette and then 500uL PB Buffer was added to the columns.
10. Columns were spun for 1 min 13000 rpm @ RT.
11. Flow through liquid was removed with a pipette and then 750uL PE w/ethanol was added to the columns.
12. Columns were spun for 1 min 13000 rpm @ RT, liquid was removed and then spun again for 1 min 13000 rpm @ RT.
13. Columns were placed into a 1.5mL tube and then 50uL Nano pure water was added to columns, after 2 min columns were spun for 1 min 13000 rpm @ RT, repeated with elution liquid.
14. DNA was nano dropped.

Nano dropped DNA	ng/uL	260/230	260/280

6.7. Restriction digest

1. Empty pBlueScript plasmid& Topo Plasmid were digested for 2 hrs @ 37C.
2. 25uL digest w/10uL dye were run on a 2.0% agarose gel (1g Agarose: 50mL 1X TBE) for 1 hr.

Not1	0.5
Pst1	1.0
DNA (1ug)	2.1
NEB 2.1 Buffer	2.5
H20(up to 25uL)	18.9

6.8. Gel extraction

1. Run samples on 2% agarose gel.
2. Check with chemidoc for correct bands.
3. Place gel on UV box and slice out bands with a razor blade.
4. Weigh agarose fragments (100mg = 100uL vol).
5. Volume of gel(C) gets 3X volume(D) of QG buffer.
6. Incubated for 15 mins @ 50C or until slice is gone.
7. Add (B) volume of Isopropanol to the sample and mix by inversion.
8. Add up to 750uL of mixture to a spin column.
9. Spin column for 1 min @ 13,000 rpm and decant liquid (repeat if liquid remains).
10. Add 500uL QG buffer, spin for 1 min @ 13,000 rpm to remove agarose.
11. Wash with 750uL PE buffer w/ Ethanol and spin for 1 min @ 13,000 rpm.
12. Decant liquid and spin again for 2 mins @ 13,000 rpm.
13. Place column in a clean 1.5 mL tube.
14. Add 25uL H2O to the column, let it sit for 2 mins, spin for 1 min @ 13,000 rpm, repeat with eluted liquid.
15. nanodrop sample and record concentration.

Sample	A=Weight (g)	B=Weight (mg)	C=Volume (uL)	D=3x Volume (uL)
1	X	(X) x 1000	(X) x 1000	3 x ((X) x 1000)

Nano dropped DNA	ng/uL

6.9. Plasmid ligation

5X Rapid Ligation Buffer	4uL
Digested DNA (from gel extraction)	75ng
Empty Digested Vector (pBlueScript)	25ng
T4 DNA Ligase	5U (1uL)
Ultrapure Water	Up to 20uL

- Gently mix and incubate @ 22C for 5 mins.

6.10. Double stranded RNA (dsRNA) synthesis

	T3 Rxn	T7 Rxn
PCR Product(T3T7)	4uL	4uL
5X Transcription Buffer	4uL	4uL
*5X rNTP's	4uL	4uL
Rnasin (40U/uL)	1uL	1uL
T3 Polymerase	0.4uL	
T7 Polymerase		1uL
DTT (100mM)	2uL	2uL
Nuclease free H_2O	4.6uL	4uL

Total Volume	20uL	20uL

1. Incubation T3/T7 reactions @ 37C for 2 hrs.
2. Treat with DNase 1uL for 15 mins @ 37C.
3. Take out 1uL of each reaction and add to 2uL of 6X loading dye, keep @ -20C.
4. Make pool with RNA sense & antisense.
5. Add 380 uL of stop solution*, mix and leave for 10 mins @ RT.
6. Add 200 uL of phenol-chloroform mix and vortex vigorously & centrifuge for 2 mins 14000 rpm @ 4C.
7. Transfer upper phase to a fresh tube.
8. Add 200 uL of chloroform mix and vortex vigorously & centrifuge for 2 mins 14000 rpm @ 4C.
9. Transfer upper phase to a fresh tube.
10. Incubate for 10 mins @ 72C.
11. Turn off the power on Thermo-mixer and let incubate for 1 hr.
12. Add 1 mL 100% EtOH (-20C stock only for RNA) & centrifuge for 15 mins 14000 rpm @ 4C.
13. Take out carefully EtOH.
14. Rinse with 1 mL 80% EtOH (-20C stock only for RNA) & centrifuge for 10 mins 14000 rpm @ 4C.
15. Take out 80% EtOH & centrifuge for 30 secs 14000 rpm @ 4C.
16. Air dry pellet ~1-2 mins in fume hood.
17. Resuspend in 10 uL of Nuclease free water.
18. Run 1% of agarose gel with 1 uL of ssRNA (kept previously @ –20C) & 0.5 uL of dsRNA with 2 uL of 6X loading dye.

6.11. Riboprobe synthesis

	T3	T7
PCR Product(T3T7)	4 uL	4 uL
5X Transcription Buffer	5 uL	5 uL
10X DIG RNA Mix	2.5 uL	2.5 uL
Rnasin(40U/uL)	1.5 uL	1.5 uL
T3 Polymerase	1.0 uL	
T7 Polymerase		1.0 uL
Nuclease free H_2O	11 uL	11 uL
Total Volume	25 uL	25 uL

1. Incubate T3/T7 reactions in 37C water bath for 1 hr.
2. Add an additional 1uL of either T3 or T7 polymerase and incubate for an additional hr in the 37C water bath.

3. Add 1uL Dnase and incubate for 15 mins in the 37C water bath.
4. Add 2.7uL of 5M LiCl and 54uL of 100%EtOH (-20C) to each tube.
5. Immediately place tubes in -80C freezer for 15 mins.
6. Spin tubes for 20 mins 14,000rpm @ 4C.
7. Remove as much supernatant as possible without disrupting the pellet (can air dry for 1-2 mins).
8. Resuspend the pellet in 50uL of deionized formamide (1-2 mins @ RT, pipette up and down).
9. Run 2uL of each reaction with 2uL of 6X loading dye on a 1% Agarose gel.

6.12. Whole mount *in situ* hybridization (WISH)

Day 1

1. Remove NAC Fixed animals from -20C and allow to reach RT before proceeding. If NAC Fixed animals are bleaching, remove bleach and replace with 100% MeOH.
2. Replace 100% MeOH w/ 1:1 100% MeOH: 0.3% PBSTx and incubate samples for 5 mins.
3. Replace 1:1 100% MeOH: 0.3% PBSTx w/ 0.3% PBSTx and incubate samples for 5 mins.
4. Transfer animals from vials to baskets in 24 well plates and treated with:
5. Proteinase K solution for 10 mins.
6. 4% formalin for 10 mins.
7. 0.3% PBSTx 2x (quick rinses).
8. 1:1 Wash Hybe: 0.3% PBSTx for 15 mins.
9. Pre-hybridize for 2 hrs @ 56C in rotator.
10. Prepare probes in ultrahybe, vortex and heat them @ 72C for 5 mins before proceeding to next step.
11. Riboprobe mix for at least 16 hrs @ 56C in rotator.

Day 2

1. Remove riboprobes and perform the following with preheated solutions @ 56C in rotator:
2. 100% Wash Hybe for 20 mins.
3. 2X SSC + 0.1% Tx 3x 20 mins.
4. 0.2X SSC + 0.1% Tx 3x 20 mins.
5. Remove plate from incubator and allow to cool to RT before proceeding to the next step.
6. MABT 2 x 10 mins.
7. MABTB 1 hr.
8. Anti-DIG AP 1:2000 in MABTB and incubate samples overnight @ 4C.

Day 3

1. Remove antibody and perform the following:
2. MABT 6 x 20 mins.
3. AP Buffer 2x 5 mins.
4. AP Buffer (5% PVA) 5mins.
5. NBT/BCIP tablet in 10% PVA until staining has reached appropriate levels (1-5 hrs).
6. 0.3% PBSTx 2x (quick rinses).
7. 4% Paraformaldehyde 30 mins.
8. 0.3% PBSTx 2x (quick rinses).
9. If desired, use 100% EtOH for 10 mins to get rid of background.
10. 0.3% PBSTx 2x (quick rinses).
11. Animals were removed from baskets and placed onto slides. 0.3% PBSTx was removed and Gelvatol mounting media was added prior to the addition of coverslips.

6.13. Fluorescent *in situ* hybridization (FISH)

Day 1

1. Remove NAC Fixed animals from -20C and allow to reach RT before proceeding.
2. Replace 100% MeOH w/ 1:1 100% MeOH: 0.1% PBSTx and incubate samples for 5 mins.
3. Replace 1:1 100% MeOH: 0.1% PBSTx w/ 0.1% PBSTx and incubate samples for 5 mins.
4. Transfer animals from vials to baskets in 24 well plates and treated with:
5. 1XSSC for 10 mins.
6. Bleach under light for 1 hr 15 mins.
7. 1XSSC for 10 mins.
8. 0.1% PBSTx for 5 mins.
9. 0.1% PBSTx for 10 mins.
10. Proteinase K solution for 10 mins.
11. 4% formalin for 10 mins.
12. 0.1% PBSTx for 5 mins.
13. 0.1% PBSTx for 10 mins.
14. 1:1 Wash Hybe: 0.1% PBSTx for 10 mins.
15. Pre Hybe for 2 hrs @ 56C in rotator.
16. Prepare probes in Hybe, vortex and heat them @ 72C for 5 mins before proceeding to next step.
17. Riboprobe mix for at least 16 hrs @ 56C in rotator.

Day 2

1. Remove riboprobes and perform the following with preheated solutions @ 56C in rotator:
2. Pre Hybe 2x 30 mins.

3. Pre Hybe: 2X SSC + 0.1% Tx [1:1] 2x 30 mins.
4. 2X SSC + 0.1% Tx 2x 30 mins.
5. 0.2X SSC + 0.1% Tx 2x 30 mins.
6. Remove plate from incubator and allow to cool to RT before proceeding to the next step.
7. 0.1% PBSTx 2 x 10 mins.
8. Blocking solution 1 hr.
9. Anti-DIG POD 1:2000 in Blocking solution and incubate samples overnight @ 4C.

Day 3

1. Remove antibody and perform the following:
2. 0.1% PBSTx 7x 15 mins.
3. FITC Tyramide solution 12 mins.
4. 0.1% PBSTx 2x (quick rinses).
5. 0.1% PBSTx 7x 15 mins.
6. Animals were removed from baskets and placed onto slides. 0.1% PBSTx was removed and Gelvatol mounting media was added prior to the addition of coverslips.

6.14. Immunohistochemistry (IHC)

Day 1

1. Remove formamide fixed animals from -20C and allow to reach RT before proceeding. If formamide fixed animals are bleaching, remove bleach and replace with 0.05% PBSTx (Skip Steps 2&3).
2. Replace 100% MeOH w/ 1:1 100% MeOH: 0.05% PBSTx and incubate for 5 mins.
3. Replace 1:1 100% MeOH: 0.05% PBSTx w/ 0.05% PBSTx and incubate for 5 mins.
4. Transfer animals from vials into a 24 well plate.
5. Replace 0.05% PBSTx w/ PBSTxB and incubate for 4 hrs.
6. Replace PBSTxB w/ Anti-phosphorylated histone H3 (Ser10) H3P 1:500 in PBSTxB and incubate overnight @ 4C.

Day 2

1. Remove and collect antibody.
2. Wash 2x w/ 0.05% PBSTx (quick washes).
3. Wash 6x 40 mins with 0.05% PBSTx.
4. Wash 3x 40 mins with 0.05% PBSTxB.
5. Replace PBSTxB w/ HRP Anti-Rabbit 1:500 in PBSTxB and incubate overnight @ 4C.

Day 3

1. Remove and collect antibody.
2. Wash 2x w/ 0.05% PBSTx (quick washes).
3. Wash 6x 40 mins with 0.05% PBSTx.
4. Replace 0.05% PBSTx with 300uL FITC PBSTI for 20 mins.
5. Add an additional 300uL of FITC PBSTI containing (0.0015% H_2O_2) for 40 mins.
6. Remove FITC PBSTI and wash 2x w/ 0.05% PBSTx (quick washes).
7. Wash 6x 40 mins with 0.05% PBSTx.
8. Animals were removed from wells and placed onto slides. 0.05% PBSTx was removed and Gelvatol mounting media was added.
9. Surface area images of animals were taken prior to the addition of coverslips.
10. Gelvatol coated slides set overnight and fluorescent images were taken the following day.

6.15. qPCR

1. Templates designed using triplicates for all samples with a standard curve using 0.25,0.5,1.0 uL of cDNA. Each experimental condition has its own standard curve and experimental conditions. Standard curve used TATA Binding Protein Domain Primers as an internal control. All primers were used at a concentration of 40pM.
2. Master Mix was made and placed on ice (cover-light sensitive).
3. cDNA and Primers(Experimental) were added prior to the addition of master mix. All liquids were added to the first of triplicate wells, mixed, and dispersed (20uL/well).
4. Once plate has been completed, adhesive film was placed on top of plate.
5. Plates were spun down for 5 min 1500rpm @ 4C.
6. Plates were run on the Step One Plus qPCR instrument.

Master Mix

Experimental Primers	Amount (uL)	Sample +1
SYBR Green	10	(Sample)x(10) +10
Water	8.2	(Sample)x(8.2) +8.2
Curve 0.25uL cDNA		
SYBR Green	10	(Sample)x(10) +10
Water	8.95	(Sample)x(8.95) +8.95
F Primer	0.4	(Sample)x(0.4) +0.4
R Primer	0.4	(Sample)x(0.4) +0.4
Curve 0.5uL cDNA		
SYBR Green	10	(Sample)x(10) +10
Water	8.7	(Sample)x(8.7) +8.7
F Primer	0.4	(Sample)x(0.4) +0.4
R Primer	0.4	(Sample)x(0.4) +0.4

Curve 1.0uL cDNA		
SYBR Green	10	(Sample)x(10) +10
Water	8.2	(Sample)x(8.2) +8.2
F Primer	0.4	(Sample)x(0.4) +0.4
R Primer	0.4	(Sample)x(0.4) +0.4

cDNA, Experimental primers, Master Mix

Sample	cDNA	F Primer	R Primer	Master Mix
Experimental	3.5	1.6	1.6	56
Curve 0.25uL cDNA	0.875			60.5
Curve 0.5uL cDNA	1.75			60
Curve 1.0uL cDNA	3.5			59

6.16. Protein extractions

1. Prepare 1X RIPA Buffer and place on ice.
2. 15-30 animals were placed into 1.5mL tubes with ~300uL of water. Tubes were placed in ice. Water was quickly removed and 150-200uL of 1X RIPA was added to each tube, one by one. *If samples are for storage and not immediate use, place tubes into dry ice and move to -80C. Using a motorized pestle, samples were homogenized ~20-30 secs on ice. Each sample was further incubated on ice for an additional 40 mins.
3. Spin down the extracts for 20 mins 14,000rpm @ 4C.
4. Transfer all Supernatant into new tube. Avoid sucking up debris with supernatant. Pipette supernatant up and down to get a homogeneous solution.
5. Set up Bradford assay:
   -Standards 0-10ug/uL BSA made in 15mL conical tubes and frozen into 150uL aliquots in PCR tubes.
   -Extracts were run in triplicates: 95uL Water +5uL Extract, vortexed quickly.
   In a flat bottom 96 well plate, 20uL of standard and extracts added in triplicates. Set pipette to 20uL, push down to second stop and suck up liquid. Into each well only go to first stop. Once all standards and extracts have been added to wells, using a multichannel pipet, add 200uL of Bradford assay to each well, re-suspending extract in Bradford. Using a plate reader take readings at 595nm wavelength. Prior to starting, set up program to use standard concentrations 0-10ug/uL and using a linear equation for graphing standards.
6. Once desired protein has been calculated, immediately add water and 6xLamily buffer to samples, heat to 94C for 10 mins. Samples may either

be cooled down to RT before loading or placed immediately into freezer -20C.
7. Clean 96 well plate immediately, spray with EtOH and rinse with DI Water.

6.17. Casting acrylamide gels

1. Set up glass gel casing and place into green holder.
2. Place unit inside fume hood and begin preparing gel mixture in a 15mL conical tube.
3. After adding Components for gel, vortex tube ~5-10 secs.
4. Using a Transfer Pipette add mixture between the glass. Fill glass until it reaches the bottom of the top green clamp of the case holder.
5. Add ~500uL of Isopropanol to remove air bubbles and let gel set for 20 mins.
6. dump excess Isopropanol into sink and make stack solution.
7. Add stack solution avoiding air bubbles until liquid has reached the top.
8. Carefully place comb into the stack and allow it to set for ~5-10 mins.
9. place excess solution into plastic weigh boat and allow to air dry before disposing.
10. Wash gel with DI water and then transfer into a zip lock bag with fresh 1X running buffer. Store gels for no less than 6hrs and no more than 1 week @ 4C.

Materials	12% (5.5mL)	12% (11mL)	15% (5.5mL)	15% (11mL)	Stack (2mL)	Stack (3mL)
H2O	908uL x2	908uL x4	632uL x2	843uL x3	700uL x2	700uL x3
30% Acrylamide mix	2.2mL	4.4mL	2.75mL	5.5mL	330uL	500uL
1.5M Tris(pH8.8)	688uL x2	917uL x3	688uL x2	917uL x3	-	-
1.0M Tris(pH6.8)	-	-	-	-	250uL	380uL
10%SDS	55uL	110uL	55uL	110uL	20uL	30uL
10% APS	55uL	110uL	55uL	110uL	20uL	30uL
TEMED	5uL	10uL	5uL	10uL	5uL	10uL

6.18. Western blots

1. For fresh protein extracts, add required Protein to 6X Lamily Buffer and heat samples @ 94C for 10 mins. For previously frozen extracts, heat samples @ 94C for 5 mins.
2. Place samples @ RT and Spin down once cooled.
3. Wash Gels with DI Water especially inside the wells to remove debris.

4. Set up the gel box, inside of gels (lower glass) faces inside of the chamber. Place gels inside and fill with fresh 1X Running Buffer.
5. Load samples into gel (10-50ug) and 2uL Marker. Run gel at 120V for 1-2 hrs.
6. Membrane was activated, 1 min 100% MeOH, 1min 1X PBS, 1X Transfer buffer.
7. Membrane sandwich was put together so that low MW proteins were facing the crease. Black panel (sponge, filter paper, gel, membrane, filter paper, sponge) was placed next to the black portion of the cassette.
8. Fresh 1X Transfer Buffer and an ice pack were placed inside transfer box.
9. Transfer was done in the 4C cold room 2 hrs 55V.
10. Membrane was cut down to the size of the gel. A cut was made on the top right corner (top left- protein side up).
11. Membrane was transferred into dark container filled with 7mL of 1X TBS-T.
12. Membrane was blocked for 1 hr a@ RT in 5% BSA TBS-T.
13. Block was removed and primary was added to rock @ 4C O/N, 14-16 hrs.
14. Primary was retrieved and membrane was washed 4X with TBS-T, 5 mins each.
15. Secondary was added for 1 hr @ RT with TBS-T/SDS 5%Non-fat dry milk.
16. Secondary was dumped and replaced with TBS-T. 4X washed TBST, 5 mins each, followed by 2X, 1X PBS washes, 5 mins each.
17. For HRP Substrate blot was placed between plastic layers, on Red Chemi filter (NEW Chemi doc) tray. All surrounding liquid was removed. 250-400uL of HRP Substrate was placed on protein side of blot and top plastic was placed on top of blot. Blot was immediately imaged (Chemiluminescence) with high resolution rapid auto exposure.
18. For Fluorescent LiCOR secondary antibodies, set parameters for imaging:
19. Channel 680- intensity 5, Channel 800- intensity 7, Resolution 21um.

6.19. TUNEL fixation

1. Kill worms with 10% NAC for 5 mins rocking @ RT.
2. Remove NAC and Fix for 20 mins with 4% Formalin rocking @ RT.
3. Remove 4% Formalin and wash with 1X PBS.
4. Remove 1X PBS and add 1X PBS/SDS for 20 mins rocking @ RT.
5. Remove 1XPBS/SDS and wash with 1X PBS (several times).
6. Bleach animals in 6%H2O2 in 1X PBS 3-5 hrs under light.

6.20. Terminal deoxynucleotidyl transferase (TdT) dUTP nick-end labeling (TUNEL)

1. Remove bleach and wash animals 2X, 5 mins with 1X PBS.
2. Incubate animals in a 96well plate with 20uL of TUNEL Mix for 4 hrs @37C with film covering wells.

3. Remove TUNEL Mix and wash animals with 1X PBS.
4. Remove 1X PBS and add Stop Solution 1 min.
5. Remove Stop Solution and wash with 1X PBS.
6. Incubate with Rhodamine Antibody Solution for 5 hrs @ RT.
7. Remove Rhodamine Antibody Solution and wash 12 X 20 mins with 1X PBS.
8. Animals were removed from wells and placed onto slides. 1X PBS was removed and Gelvatol mounting media was added prior to the addition of coverslips.

6.21. Formamide fixation

1. Animals (5-10) per vial were placed into ice.
2. Animals were killed in 5.7% HCl for 7 mins on ice.
3. HCl was removed and animals were washed 2x 5mins w/ cold 0.05% PBSTx on ice.
4. 0.05% PBSTx was removed and replaced with ice cold formamide fix.
5. Vials containing formamide fix were rocking at RT for 20-30 mins.
6. Formamide fix was removed and replaced with bleaching solution.
7. Animals were bleached overnight under light.
8. Bleach was removed and replaced with 0.05% PBSTx.
9. *For long term storage, bleaching solution was replaced with 50% MeOH;0.05%PBSTx for 5 mins, followed by 100% MeOH for 5 mins. Animals were stored in 100% MeOH @ -20C.

6.22. NAC fixation

1. Picked n worms and n controls worms, placed into 20 ml scintillation vial.
2. Remove all planarian water and add 5% NAC solution. Rotate vials @ RT for 5-10 mins.
3. Remove NAC solution and add 4% formalin. Rotate vials @ RT for 20-30 mins.
4. Remove formalin and rinse 1x with .3% PBSTxs.
5. Add 37C preheated reduction solution and leave vials in 37C water bath for 10 mins, rotating occasionally.
6. Remove the reduction solution and rinse 1x with .3% PBSTx.
7. Add 50% MeOH/50% PBSTx solution. Rotate @ RT for 7 mins.
8. Replace 50% MeOH/50% PBSTx solution with 100% MeOH. Rotate @ RT for 7 mins.
9. Rinse 1x with 100% MeOH and store vials in -20C for at least 1 hr or long term.

10. Replace 100% MeOH with Bleaching solution and place under light overnight.
11. Replace bleaching solution with 100% MeOH and store vials in -20C.

6.23. Dye feeding assay

1. Surface Area measurements were taken for all animals prior feeding.
2. Animals were fed liver paste containing 0.2% Erioglaucine disodium salt dye overnight.
3. Prior to homogenization, dishes containing animals were cleaned and animals were placed into 2mL centrifuge tubes with 1.5mL of 1X PBS and a small amount of glass beads.
4. Samples were homogenized using a Bead Ruptor homogenizer (Omni international, 19-040) for 30 secs.
5. Samples were centrifuged for 1 minute 14000 rpm @ RT.
6. 1mL of supernatant was used to measure activity @ a 620nm absorbance.

*Food consumption was measured by taking the absorbance reading for the sample and dividing it by the surface area (mm^2) of the individual animals in each group. These values were normalized and measured in fold change between groups.

6.24. Behavioral feeding assay

1. A custom made dish containing 10 lanes approximately 1cm by 10cm were filled half way with planarian water.
2. In the middle of each lane 2 drops of liver paste, 10μL each was placed. Filming began prior to the addition of animals using.
3. Individual animals were placed into each end of the lane for all lanes, 2 animals total per lane. Lanes 1-5 contained the control group and lanes 6-10 contained the experimental group.
4. Animals were fed for 1 hr and then removed from lanes.

*The amount of time to begin feeding was quantified as the time in seconds, which the animal extended their pharynx out onto liver and subtracting it from the time the animal was placed into the lane.

6.25. Liver stimulation assay

1. Homogenized liver paste (50uL) was added to 50mL of planarian water and repeatedly vortexed.
2. The water settled for 10 mins @ RT. Using a serological pipette, 40mL of the 0.1% liver water was taken, avoiding anything that sank to the bottom of the tube and was transferred to clean dishes.

3. Animals that underwent stimulation were carefully transferred to these dishes containing 0.1% liver water for 30 mins. Non-stimulated, control animals were transferred to clean dishes containing 40mL of planarian water.
4. Following this incubation period, animals were removed and placed into 1mL TRIzol for RNA Extractions.